AD_____
(Leave blank)

Award Number:
W81XWH-08-1-0219

TITLE:
Inhibition of Ovarian Cancer by microRNA-mediated Regulation of Telomerase

PRINCIPAL INVESTIGATOR:
Brittney-Shea Herbert, Ph.D.

CONTRACTING ORGANIZATION:
Trustees of Indiana University
Indianapolis, IN 46202-5167

REPORT DATE:
May 2009

TYPE OF REPORT:
Annual

PREPARED FOR: U.S. Army Medical Research and Materiel Command
Fort Detrick, Maryland 21702-5012

DISTRIBUTION STATEMENT:

√ Approved for public release; distribution unlimited

# REPORT DOCUMENTATION PAGE

*Form Approved*
*OMB No. 0704-0188*



| **1. REPORT DATE** *(DD-MM-YYYY)* | **2. REPORT TYPE** | **3. DATES COVERED** *(From - To)* |
|---|---|---|
| 05-31-2009 | Annual | 1 May 2008- 30 April 2009 |

**4. TITLE AND SUBTITLE**
Inhibition of Ovarian Cancer by microRNA-mediated Regulation of Telomerase

**5a. CONTRACT NUMBER**

**5b. GRANT NUMBER**
W81XWH-08-1-0219

**5c. PROGRAM ELEMENT NUMBER**

**6. AUTHOR(S)**
Brittney-Shea Herbert, Ph.D.

Email: brittney-shea.herbert@utsouthwestern.edu

**5d. PROJECT NUMBER**

**5e. TASK NUMBER**

**5f. WORK UNIT NUMBER**

**7. PERFORMING ORGANIZATION NAME(S) AND ADDRESS(ES)**

Trustees of Indiana
University
Indianapolis IN 46202-5167

**8. PERFORMING ORGANIZATION REPORT NUMBER**

**9. SPONSORING / MONITORING AGENCY NAME(S) AND ADDRESS(ES)**
U.S. Army Medical Research and Materiel
Command
Fort Detrick, Maryland 21702-5012

**10. SPONSOR/MONITOR'S ACRONYM(S)**

**11. SPONSOR/MONITOR'S REPORT NUMBER(S)**

**12. DISTRIBUTION / AVAILABILITY STATEMENT**

Approved for public release; distribution unlimited

**13. SUPPLEMENTARY NOTES**

**14. ABSTRACT**
A hallmark of ovarian cancer is its limitless proliferative potential which is governed in part by elevated levels of human telomerase (hTERT) or telomerase activity. However, how telomerase can be regulated in normal cells, and how this regulation can be lost during cancer progression, is not completely understood. microRNAs (miRNAs) are evolutionarily conserved, small, non-coding, single-stranded, ~19–23 nucleotide RNA molecules that are estimated to negatively regulate protein encoding genes including those related to cancer development. The objective of this proposal is to determine whether telomerase (hTERT) is negatively regulated by microRNAs in normal ovarian surface epithelial cells and whether the expression of these microRNAs is lost during ovarian cancer progression. Using bioinformatics and databases of microRNAs, we identified putative microRNAs for hTERT. We correlated these microRNAs with their expression in normal ("up") and cancerous ("down") ovarian tissue. This correlation led to a microRNA short-list of potential hits to test for their effect on telomerase activity in ovarian cancer cells. Current studies include validating this list and the long-term effects on cancer cell growth. Telomerase inhibition by microRNAs can thus lead to new therapy as well as understanding how ovarian cancer progresses (from normal, early, then to late stage).

**15. SUBJECT TERMS**
microRNA, telomerase, tumor progression, ovarian cancer

| **16. SECURITY CLASSIFICATION OF:** | | | **17. LIMITATION OF ABSTRACT** | **18. NUMBER OF PAGES** | **19a. NAME OF RESPONSIBLE PERSON** |
|---|---|---|---|---|---|
| **a. REPORT** | **b. ABSTRACT** | **c. THIS PAGE** | | | USAMRMC |
| U | U | U | UU | 51 | **19b. TELEPHONE NUMBER** *(include area code)* |

## Table of Contents

## INTRODUCTION

A hallmark of ovarian cancer is its limitless proliferative potential which is governed in part by elevated levels of human telomerase (hTERT) or telomerase activity [1]. Most normal cells do not have sufficient expression of active telomerase and are mortal, while over 90% of cancer cells express active telomerase. Therefore, the understanding of how telomerase can be regulated in normal cells, and how this regulation can be lost during cancer progression, has led to the search for suppressors of telomerase. However, the search for the natural, direct negative regulator of telomerase in normal cells continues and may hold the key to halting ovarian cancer cell progression. Recently discovered, microRNAs (miRNA or miR) are evolutionarily conserved, small, non-coding, single-stranded, ~19–23 nucleotide RNA molecules that are estimated to negatively regulate at least 30% of all protein encoding genes [2-3]. Recent evidence has shown that alteration of microRNA levels can lead to cellular transformation and cancer development [4-10]. Based on information from public microRNA databases, microRNAs are predicted to target different regions of the hTERT mRNA, suggesting that telomerase expression in ovarian epithelial cells may be regulated in part by microRNA-mediated repression of hTERT mRNA translation and ultimately protein expression. However, these predicted microRNAs have not been tested for their ability to negatively regulate hTERT mRNA. *Therefore, the proposed concept is that microRNAs play a role in telomerase regulation in normal ovarian surface epithelial cells and that hTERT microRNA expression is lost during ovarian cancer progression leading to active telomerase and sustained growth.* Telomerase inhibition by microRNA can thus lead to new therapy as well as understanding how ovarian cancer progresses (from normal, early, then to late stage).

## BODY

The objective of this proposal is to determine whether telomerase (hTERT) is negatively regulated by microRNAs in normal ovarian surface epithelial cells and whether the expression of these microRNAs is lost during ovarian cancer progression. In order to test the concept that microRNAs play a role in telomerase regulation in ovarian cells, the specific aims are: (1) To examine the expression of telomerase activity and the predicted hTERT microRNAs in normal and cancerous (of different stages and recurrence) ovarian cells and tissue using commercial microRNA isolation and detection kits; (2) To determine the effects of the predicted hTERT microRNAs on telomerase activity in ovarian cancer cells; and (3) To test the hypothesis that inactivation of telomerase by microRNAs inhibits the growth of ovarian cancer cells.

### Materials and Methods:

***Identification of predicted hTERT microRNAs using informatics and public databases.*** The microRNA databases PicTar (pictar.bio.nyu.edu), TargetScan (www.targetscan.com), RNA22 (http://cbcsrv.watson.ibm.com/rna22.html), miRBase (http://microrna.sanger.ac.uk/cgi-bin/targets/v1/search.pl), and mir2Disease (http://www.mir2disease.org/) were used to list predicted microRNAs, and their binding energy, to the 3'UTR region of hTERT mRNA [11-14].

***Ovarian tissue collection and cell culture.*** The ovarian cancer cell lines OVCAR3, SKOV3, and HeyC2 were cultured in McCoy's media containing 5% fetal bovine serum or RPMI media containing 10% cosmic calf serum plus 1% sodium pyruvate . The normal human ovarian surface epithelial (HOSE) cell line was cultured in a 1:1 Medium 199:MCDB media containing 10% fetal bovine serum . All cell lines were cultured at 37°C, in a 5% CO2 incubator. Normal

and cancerous ovarian tissues were received from the IU Lily Tissue Bank according to an IRB-approved exempt protocol.

***Determination of Telomerase Activity using the Telomeric Repeat Amplification Protocol (TRAP)***. The TRAP assay was performed with the TRAP-eze Telomerase Detection kit (Serologicals/Invitrogen) and established protocols [15; **Appendix**]. Following PCR, the TRAP reaction products were run on a 10% non-denaturing acrylamide gel. The gel was visualized on a PhosphorImager using ImageQuant software (Molecular Dynamics, Sunnyvale, CA). Telomerase activity was observed as a 6-bp telomerase-specific ladder (telomerase products) above the 36-bp internal standard (ITAS).

***Real-time RT-PCR (qRT-PCR) for hTERT expression.*** Total RNA was prepared from logarithmically growing cells, or tissue, using the RNeasy Mini Kit (Qiagen, Valencia, CA) according to manufacturer's instructions. cDNA (2 μg) was synthesized for each reaction using the High-Capacity cDNA Reverse Transcription kit (ABI, Foster City, CA) according to manufacturer's instructions. 10 ng cDNA was used for each 25 μL reaction, done in triplicate, using 12.5 μL DyNAMo SYBR Green kit, 0.05% Rox Dye, (New England BioLabs, Ipswich, MA), and 400 nM for each primer. Cycling conditions for the 7500 Real-Time PCR System (ABI) were as follows: 50 $^{o}$C for 2 min, 95 $^{o}$C for 10 min, then 40 cycles of 95 $^{o}$C for 15 sec and 60 $^{o}$C for 1 min; a dissociation curve cycle was performed for melting curve analysis. Primers used include hTERT TaqMan primers (ABI Hs00162669_m1) or β-actin primers designed using Primer Express Software version 3.0 (ABI) with the sequences 5'-GAT GAG ATT GGC ATG GCT TT-3' (forward) and 5'-CAC CTT CAC CGT TCC AGT TT-3' (reverse). The Ct was calculated by the 7500 System Software (ABI) and raw Ct values were exported to Excel for ΔΔCt analysis and fold-change.

***Isolation of RNA enriched with small RNAs using the mirVana RNA isolation kit (Applied Biosystems).*** Samples of 1 – 3 x $10^7$ cells (or <200 mg tissue) were collected, washed with cold PBS, and pelleted at low speed according to instructions. After removing the PBS wash, cells were lysed by adding 600μl of Lysis Binding Solution to the sample and by vortexing the lysate. The miRNA Homogenate Additive (60 μl) was added to the lysate and the mixture was incubated on ice for 10 minutes. Next, the Acid-Phenol:Chloroform solution (600μl) was added and the mixture was vortexed for 30 to 60 seconds. The samples were then centrifuged for 5 minutes at maximum speed at room temperature. The upper aqueous phase was recovered, without disrupting the lower organic phase, and transferred to a fresh tube. DEPC $H_2O$ was preheated to 95° C. 100% ethanol at room temperature (750μl) was added to the tube containing the aqueous phase. A Filter Cartridge was placed into one of the Collection Tubes and up to 750μl of the lysate/ ethanol mixture was added onto the Filter Cartridge. The collection tube was centrifuged for about 15 seconds at 10,000 RPM and the flow-through was discarded. The Filter Cartridge was then washed with 700μl miRNA Wash Solution I, centrifuged for 5 to 10 seconds, and the flow-through was discarded. The Filter Cartridge was then washed two times with 500μl Wash Solution II/III, centrifuged for 5 to 10 seconds, and the flow-through was discarded. The Filter Cartridge was then spun for 1 minute to remove the extra liquid. The Filter Cartridge was transfer into a fresh Collection Tube and 100μl of the preheated DPEC $H_2O$ was applied to the filter, and the Filter Cartridge was centrifuged at the maximum speed for 20 to 30 seconds to recover the RNA. The concentration of RNA was quantified by spectrophotometer at an

absorbance of $A_{260}$ and using a 5:95 TE dilution. The sample was snap frozen and stored at -20°C until ready to use.

***Isolation of the specific mature microRNA of interest using the ABI TaqMan® Reverse Transcriptase miRNA Assay kit (Applied Biosystems).*** A separate isolation procedure for each miRNA to be analyzed (as described below) was performed according to instructions. 10ng ( <5 µl) of the desired isolated RNA sample, which is enriched for small RNAs as described above, was used for each reverse transcriptase (RT) reaction to obtain the mature microRNA. First, DEPC $H_2O$ was added to obtain a total of 5µl per enriched RNA sample. The RT master mix was prepared with the following (per sample): 0.15µl of 100mM dNTPs with dTTP, 1.00µl MultiScribe™Reverse Transcriptase (50 U/µl), 1.5µl 10x Reverse Transcription Buffer, 0.19µl RNase Inhibitor (20U/µl), and 4.16µl DEPC $H_2O$. The RT reaction was prepared in a PCR reaction tube as a total volume of 15µl containing the following: 7µl RT master mix, 3µl RT miRNA primer (ABI miRNA assay kit) and 5µl enriched RNA sample. The sample tube was centrifuged and incubated on ice for 5 minutes. The samples were then placed in a thermocycler (MJ Research) and PCR was initiated with the following steps: 30 min at 16°C, 30 min at 42°C, 5 min at 85°C, ∞ at 4°C. Once completed, the final concentration of the isolated miRNA was assumed to be 10ng/15µl, according to the instructions.

***PCR Amplification of the isolated miRNA using Real Time Primers from the miRNA Assay kit (Applied Biosystems).*** Once mature microRNA has been isolated from test samples or tissue, analysis of the expression of a specific microRNA was determined by real-time RT-PCR with specific microRNA primer sets (Applied Biosystems, ABI). Four replicates of each 20µl Real Time reaction were performed for each microRNA expression analysis. The master mix for the RT-PCR reaction was prepared in a 1.5 ml RNase free microcentrifuge tube on ice with the following: 10.00µl TaqMan 2x Universal PCR Master Mix, No-AmpErase UNG, 7.67µl DEPC $H_2O$, 4.5µl of the appropriate 20x TaqMan miRNA assay Real Time primer, 6.0µl of the appropriate mature microRNA product from above. The master mix and microRNA was mixed well and centrifuged. 20 µl of the appropriate reaction mixture was dispensed into the four replicate, corresponding wells of the Real Time plate (which calculated to 1 ng microRNA per well). The plate was sealed with an optical adhesive cover and centrifuged briefly. The TaqMan Real Time Template Program was used on ABI 7500 machine with the following PCR settings: 10 min at 95°C, then 40 cycles of 15 seconds at 95°C, and 60 seconds at 60°C. Once the run was completed, the data was analyzed using the ΔΔCt method and fold-change. U6 microRNA was used as a standard miRNA control.

***Transfection of precursor microRNAs into cells (Applied Biosystems).*** Transfection of pre-microRNAs into cancer cells was performed according to the instructions of the ABI pre-miR miRNA precursor transfection kit. The experimental setup included duplicate wells in six-well plates of the culture media only control, OptiMEM transfection media only control, siPORT transfection reagent only control, a negative precursor control (ABI), and the specific miRNA precursor of interest (e.g., mir105, mir432, mir192, and mir299-3p; ABI cat nos. PM12838, PM10941, PM10456, and PM10448, respectively). Cells were collected, counted, then resuspended in 30mL OptiMEM at $10^5$ cells/mL and incubated at 37°C until ready for transfection. 9µl of the siPORT amine transfection reagent was diluted into 291µl OptiMEM media for each replicate and incubated for 10 minutes at room temperature. Next, 24µl of the

selected precursor miRNA or negative control precursor were diluted in 276µl OptiMEM media for each replicate. Then, 300µl of the siPORT mixture was added to the precursor mixtures and incubated for 10 minutes at room temperature. An additional 300µl OptiMEM was added to the siPORT mixture before adding 600µl of the mixture could be added to the appropriate wells. The cell suspensions were then added to the appropriate wells. The transfection proceeded for 24-48 hrs, then the transfection media was changed to culture media followed by a 24 hour recovery and growth. Cells were collected and pelleted for the TRAP assay or RNA isolation.

**Results:**

***Expression of hTERT and telomerase activity in normal and cancerous ovarian cells and tissue (Task 1 of SOW).*** Using TaqMan real-time RT-PCR assays on isolated total RNA, we analyzed telomerase (hTERT) expression in normal and cancerous ovarian cell lines and tissues (representing stages I-IV of the disease, or invasive). **Figure 1** represents a summary of the hTERT mRNA expression data. As hypothesized and previously reported [reviewed in ref. 1], ovarian cancer cells/tissue were positive for hTERT expression compared to normal ovarian cells or tissue (**Figure 1**).

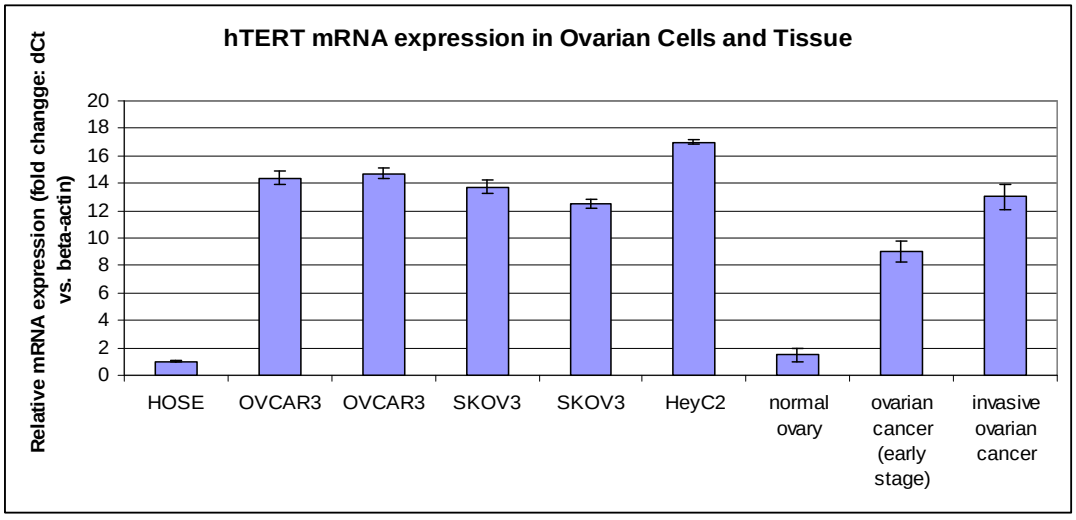


***Figure 1. Expression of hTERT mRNA in ovarian cancer cells/tissue and normal human ovarian surface epithelial (HOSE) cells/tissue.*** *Representative hTERT real-time RT-PCT data in three ovarian cancer cell lines* (OVCAR3, SKOV3, HeyC2), *HOSE cell line, normal ovarian tissue, ovarian cancer, and invasive ovarian cancer tissue. Cells were collected, total RNA isolated, and analyzed for hTERT expression using TaqMan primers and real-time PCR (Materials and Methods).*

Using the TRAP assay, we next analyzed telomerase activity levels in normal and cancerous ovarian cell lines. Corroborating the data in Figure 1, ovarian cancer cells were positive for telomerase activity compared to normal ovarian cells or tissue (**Figure 2**). Since HeyC2 ovarian cancer cells contained the highest amount of telomerase activity, we utilized the OVCAR3 and SKOV3 cells to initially test microRNA precursors for their effects on negatively regulating telomerase in these ovarian cancer cells.

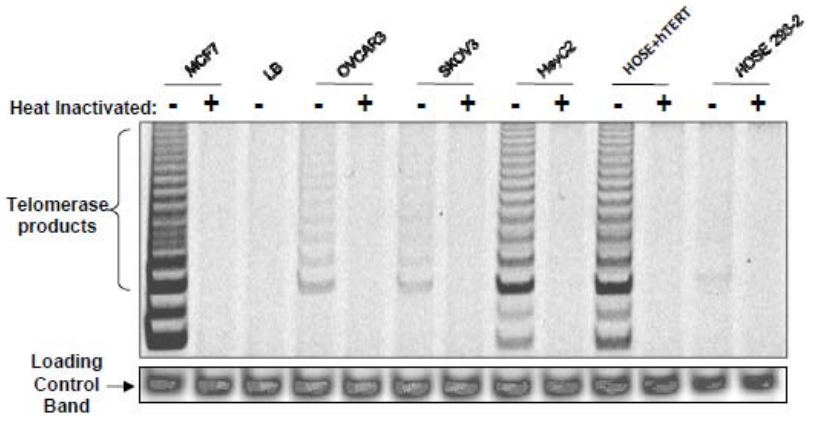


***Figure 2. Expression of telomerase activity in ovarian cancer cells, immortalized human ovarian surface epithelial (HOSE) cells and normal HOSE cells.*** *Representative telomerase activity data in three ovarian cancer cell lines* (OVCAR3, SKOV3, HeyC2)*, and HOSE cell lines. Cells were collected and analyzed for telomerase activity as previously described (Materials and Methods, ref. 15). Telomerase activity was represented as a ladder of telomerase products (brackets). To confirm telomerase activity and to check for PCR inhibitors, duplicate samples were heat inactivated (+). MCF7 breast cancer cells were used a positive control, lysis buffer (LB) only was used as a negative control, and a loading control band was used from a separate set of primers for the PCR step only. Since HeyC2 ovarian cancer cells contained the highest amount of telomerase activity, we utilized the OVCAR3 and SKOV3 cells to initially test microRNA precursors for their effects on negatively regulating telomerase in these ovarian cancer cells.*

***Expression of the predicted hTERT microRNAs in normal and cancerous ovarian and tissue (Task 1 of SOW).*** The microRNA databases were utilized to list predicted microRNAs that target the 3' UTR region of hTERT mRNA [11-13]. The lists of predicted hTERT microRNAs and their binding energies from each database are included in the **Appendix**. Next, the expression of hTERT microRNAs in normal and cancerous ovarian cell lines and tissues were characterized using microRNA isolation kits and real-time RT-PCR for specific microRNA primer sets (Applied Biosystems). Since the initiation of this proposal, a new public database was created for the documentation and use of microarray expression analysis data on microRNA expression in specific diseases (mir2Disease base, reference 14). In particular, microarray expression analyses of microRNAs in ovarian normal and cancer tissue revealed differential expression of certain microRNAs that were "up" in normal ovarian tissue and "down" in ovarian cancer tissue [16-18, **Appendix**]. Our goal was to characterize microRNAs that were present in normal cells and lost during cancer progression, which correlates to a negative regulation of hTERT and telomerase activity by microRNAs in normal cells/tissue. Using these analyses, we correlated the presence or absence of hTERT mRNA/telomerase activity with the expression of the predicted hTERT microRNAs in these ovarian tissues. This resulted in a compiled list of eight putative hTERT microRNAs that were present in normal ovarian tissue and lost or down-regulated in ovarian cancer tissue (**Table 1**). Validation of the expression of these microRNAs in cell lines confirmed a general trend that cancer cells grouped together in microRNA expression compared to a normal human ovarian surface epithelial cell expression (**Figure 3**). Interestingly, mir-432* and mir-105 displayed up-regulated expression in ovarian cancer cells compared to the normal ovarian cells, which is opposite from the tissue array data; therefore, this experiment will be repeated with fresh samples. MicroRNAs 518c and 518e were not expressed above threshold in either the normal or cancerous ovarian cell samples.

| microRNA | Sequence | SCORE* | PVALUE_OG* | TRANSCRIPT_ID | EXTERNAL_NAME |
|---|---|---|---|---|---|
| hsa-miR-9 | UCUUUGGUUAUCUAGCUGUAUGA | 16.7149 | 1.63E-02 | ENST00000310581 | TERT |
| hsa-miR-299-3p | UAUGUGGGAUGGUAAACCGCUU | 16.5813 | 1.49E-02 | ENST00000310581 | TERT |
| hsa-miR-432* | UCUUGGAGUAGGUCAUUGGGUGG | 15.4887 | 4.46E-02 | ENST00000310581 | TERT |
| hsa-miR-105 | UCAAAUGCUCAGACUCCUGUGGU | 15.4624 | 2.35E-03 | ENST00000310581 | TERT |
| hsa-miR-491 | AGUGGGGAACCCUUCCAUGAGGA | 15.3396 | 4.80E-03 | ENST00000310581 | TERT |
| hsa-miR-518c | CAAAGCGCUUCUCUUUAGAGUG | 14.5618 | 5.08E-03 | ENST00000310581 | TERT |
| hsa-miR-518e | AAAGCGCUUCCCUUCAGAGUGU | 14.4555 | 5.08E-03 | ENST00000310581 | TERT |
| hsa-miR-192 | CUGACCUAUGAAUUGACAGCC | 14.4205 | 8.48E-03 | ENST00000310581 | TERT |

***Table 1. List of putative hTERT microRNAs that were found to be present in normal ovarian tissue (telomerase negative) and down-regulated or lost in ovarian cancer tissue (telomerase positive). * The predicted microRNA should be prioritized based on column F and G (Score and p value). A higher score or lower p value indicates a higher binding affinity.***

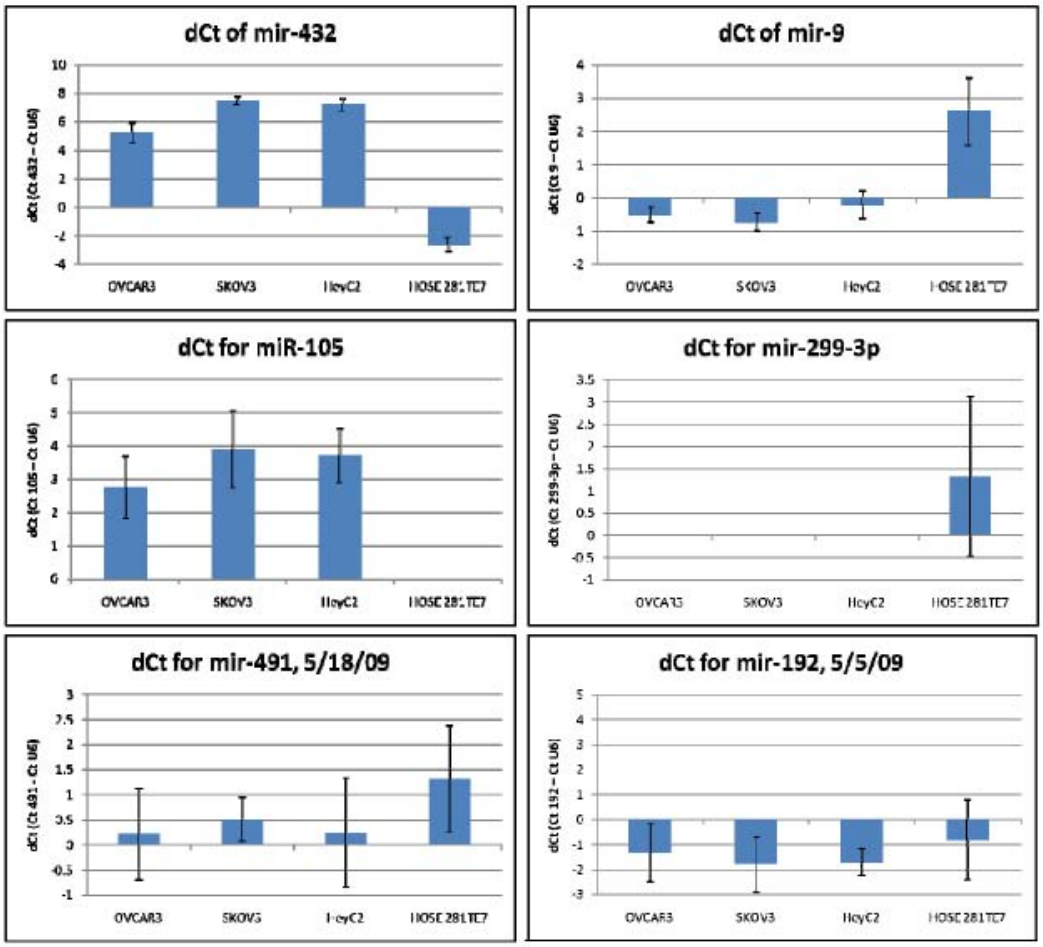


***Figure 3. Validation of the expression of putative hTERT microRNAs in normal ovarian cells (HOSE) and ovarian cancer cells (OVCAR3, SKOV3, HeyC2).*** *Specific microRNAs were isolated and analyzed by real-time RT-PCT following established protocols from Applied Biosystems. Data was determined using the Ct method (dCt) and fold-change (±SD) to a standard control microRNA (U6). A general trend was observed between microRNA expression and cancer status of cell lines. MicroRNAs 518c and 518e did not reach threshold and were negative for this experiment for both normal ovarian cells and ovarian cancer cells.*

***Effects of expressing hTERT microRNAs on telomerase activity in ovarian cancer cells (Tasks 2-3 of SOW).*** Of the eight putative hTERT microRNAs that were differentially expressed or present in normal versus cancerous ovarian cells, we, at the time of this report, have so far screened four of them for their ability to inhibit telomerase activity when their precursors are transfected into ovarian cancer cell lines that are known to contain active telomerase. Preliminary results in OVCAR3 ovarian cancer cells suggested that mir-432*, mir-299-3p, and miR-192 are negative regulators for telomerase activity as transfection of their precursors reduced telomerase activity by 30-50% in these cells (**Figures 4-6**). This experiment will be repeated for longer transfection periods in attempt to further reduce telomerase activity to zero.

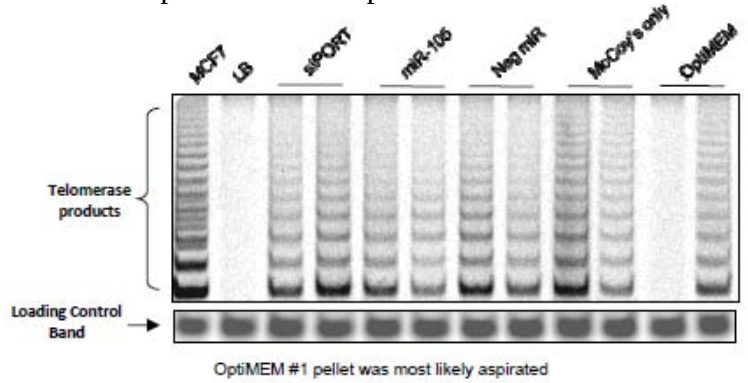


***Figure 4. Transfection of pre-miR-105 in OVCAR3 ovarian cancer cells does not negatively affect telomerase activity.*** *Representative telomerase activity data in duplicate samples of OVCAR3 ovarian cancer cells transfected with pre-miR-105 for 24 hr according to ABI precursor miR transfection protocol (Materials and Methods). Cells were collected and analyzed for telomerase activity as previously described (Materials and Methods, ref. 15). siPORT transfection reagent only (siPORT), negative pre-miRs (Neg miR), McCoy's culture media only (McCoy's only), and OptiMEM medial only were analyzed for their basal effects on telomerase activity. Telomerase activity was represented as a ladder of telomerase products (brackets). To confirm telomerase activity and to check for PCR inhibitors, duplicate samples were heat inactivated (+). MCF7 breast cancer cells were used a positive TRAP control, lysis buffer (LB) only was used as a negative TRAP control, and a loading control band was used from a separate set of primers for the PCR step only. No significant change in telomerase activity was observed after transfection of pre-miR-105.*

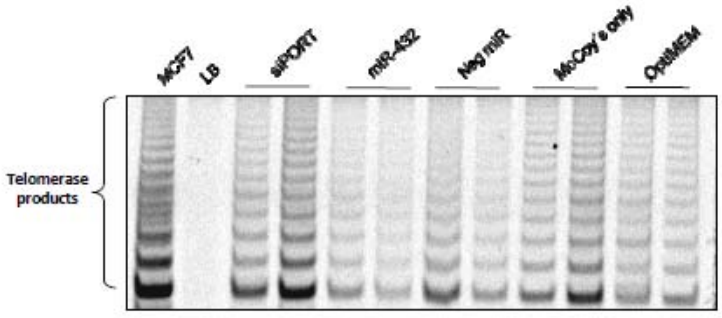


***Figure 5. Transfection of pre-miR-432* in OVCAR3 ovarian cancer cells does not negatively affect telomerase activity.*** *Representative telomerase activity data in duplicate samples of OVCAR3 ovarian cancer cells transfected with pre-miR-432* for 24 hr according to ABI precursor miR transfection protocol (Materials and Methods). Cells were collected and analyzed for telomerase activity as previously described (Materials and Methods, ref. 15). siPORT transfection reagent only (siPORT), negative pre-miRs (Neg miR), McCoy's culture media only (McCoy's only), and OptiMEM medial only were analyzed for their basal effects on telomerase activity. Telomerase activity was represented as a ladder of telomerase products (brackets). To confirm telomerase activity and to check for PCR inhibitors, duplicate samples were heat inactivated (+). MCF7 breast cancer cells were used a positive TRAP control, lysis buffer (LB) only was used as a negative TRAP control, and a loading control band was used from a separate set of primers for the PCR step only. A 30% change in telomerase activity was observed after transfection of pre-miR-432*.*

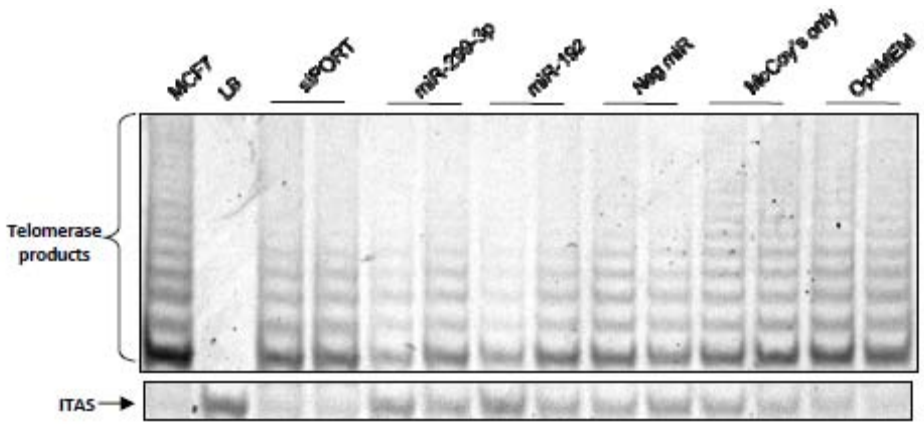


***Figure 6. Transfection of pre-miR-299-3p and pre-miR-192 in OVCAR3 ovarian cancer cells does not negatively affect telomerase activity.*** *Representative telomerase activity data in duplicate samples of OVCAR3 ovarian cancer cells transfected with* ***pre-miR-299-3p and pre-miR-192*** *for 24 hr according to ABI precursor miR transfection protocol (Materials and Methods). Cells were collected and analyzed for telomerase activity as previously described (Materials and Methods, ref. 15). siPORT transfection reagent only (siPORT), negative pre-miRs (Neg miR), McCoy's culture media only (McCoy's only), and OptiMEM medial only were analyzed for their basal effects on telomerase activity. Telomerase activity was represented as a ladder of telomerase products (brackets). To confirm telomerase activity and to check for PCR inhibitors, duplicate samples were heat inactivated (+). MCF7 breast cancer cells were used a positive TRAP control, lysis buffer (LB) only was used as a negative TRAP control, and a loading control band (ITAS) was used from a separate set of primers for the PCR step only. A 40-50% change in telomerase activity was observed after transfection of* ***pre-miR-299-3p and pre-miR-192****.*

A recent report by Mitomo et al. suggested that telomerase activity in cancer cells may be regulated in part by microRNA-138 [19]. Even though this microRNA was not identified in the original ovarian cell/tissue screens, we will include testing this microRNA for its ability to regulate telomerase activity in the next few months. All of these transfections will be repeated in the other ovarian cancer cell lines to obtain reliable, results. Future studies include validating confirmed, positive microRNA "hits" by knocking down the particular hTERT microRNA by microRNA-inhibitors in normal ovarian surface epithelial cells (initially negative for telomerase activity) and test for telomerase activity (Task 2b, SOW).

## KEY RESEARCH ACCOMPLISHMENTS

- Generated list of putative hTERT microRNAs using all available microRNA databases (RNA22, PicTar, Miranda, Sanger databases).
- Characterized the expression of putative hTERT microRNAs that were "up" in normal and "down" in cancerous ovarian cell lines and tissues; validated using miR2Disease base.
- Analyzed telomerase (hTERT) expression and activity in normal and cancerous ovarian cells (representing stages I-IV of the disease or recurrence) by real-time RT-PCR for hTERT mRNA as well as the telomerase activity (TRAP) assay
- Correlated the presence or absence of hTERT mRNA and telomerase activity with the expression of the hTERT microRNAs in these cell lines and tissues.
- Narrowed down the list of potential microRNAs for hTERT to 9 microRNAs to test for telomerase inhibition.

- Screened 4 out of the 9 short-list of hTERT microRNAs for their ability to inhibit telomerase activity (TRAP assay) when their precursors are transfected into ovarian cancer cell lines that are known to contain active telomerase.
- Identified three potential, positive "hits" for hTERT microRNAs to be validated.

**REPORTABLE OUTCOMES**

- Applied for DOD Ovarian Cancer Research Program Idea Award (pre-application) based on this work- not selected.
- Applied for Komen for the Cure Investigator-Initiated Award funding based on this work-not funded.
- Abstract presentation (in preparation): Skillman S, Fox M, Herbert B-S. Role of microRNAs in the Regulation of Telomerase in Ovarian Cancer. IUSM MSA Research Symposium, October 2009.

**CONCLUSION**

The study of microRNAs in cancer development and intervention, particularly in the field of ovarian cancer research, is novel and the concept of microRNA-mediated regulation of telomerase expression is untested. Telomerase reactivation is a common hallmark for cancer and represents a promising new target for biomarkers and intervention. Determining the regulation of the cancer hallmark telomerase in ovarian cancer progression is imperative for understanding how this disease begins and how telomerase can be controlled by re-expressing microRNAs for hTERT. Results obtained during this annual reporting period have suggested at least three putative microRNAs (mir-432*, mir-299-3p, and miR-192) that negatively regulate telomerase activity in ovarian cancer cells. Future research includes validating these microRNAs for effects on hTERT mRNA expression in normal and cancerous ovarian cells and testing for the long-term effects of microRNA transfection into ovarian cancer cell growth. Completion of this proposal will lead to development of mechanistic studies focusing on the contribution made by telomerase to ovarian cancer progression. Therefore, research completed in this proposal should help set the stage for new areas of investigation in ovarian cancer development, understanding microRNA mechanisms in ovarian cancer (e.g., Dicer, regulation of mircoRNAs), and the promising clinical potential of microRNAs as biomarkers for ovarian cancer. These studies should also provide the necessary and unique reagents to test a novel, nonviral gene therapy using hTERT microRNAs that can specifically target the cancer without harming normal cells.

**REFERENCES**


1. Cong YS, Wright WE, Shay JW, *Microbiol Mol Biol Rev.* **66,** 407 (2002).
2. Bartel DP, *Cell* **116,** 281 (2004).
3. Rana TM, *Nat Rev Mol Cell Biol* **8,** 23 (2007).
4. Calin GA, *et al., N. Engl. J. Med.* **353**,1793 (2005).
5. Croce CM, Calin GA, *Cell* **122,** 6 (2005).
6. Calin GA, Croce CM, *Nat Rev Cancer* **6,** 857 (2006).
7. He L, *et al., Nature* **435,** 828 (2005).
8. Iorio MV, *et al., Cancer Res.* **65,** 7065 (2005).
9. Liu CG, *et al., Proc Natl Acad Sci U S A* **101**, 9740 (2004).
10. Lu J, *et al., Nature* **435,** 834 (2005).
11. Krek A, *et al., Nat Genet* **37,** 495 (2005).
12. Lewis BP, *Cell* **115**,787 (2003).
13. Griffiths-Jones S, Grocock RJ, van Dongen S, Bateman A, Enright AJ, *Nucleic Acids Res.* **34**, D140 (2006).
14. Jiang Q, *et al., Nucleic Acids Res* **37,** D98 (2009).
15. Herbert BS, Hochreiter AE, Wright WE, Shay JW, *Nat. Protoc.* **1,** 1583 (2006).
16. Iorio MV, *et al., Cancer Res.* **67,** 8699 (2007).
17. Yang H, *et al., Cancer Res.* **68**, 425 (2008).
18. Zhang L, *et al., Proc Natl Acad Sci U S A* **105,** 7004 (2008).
19. Mitomo S, *Cancer Sci.* **99**, 280 (2008).


**APPENDIX**

- Publication describing the telomerase activity assay in detail: Herbert BS, Hochreiter AE, Wright WE, Shay JW, *Nat. Protoc.* **1,** 1583 (2006).
- Lists of predicted hTERT microRNAs from separate databases (PicTar, Miranda, miRBase, Sanger/RNA22 overlap)- 5 pages
- Microarray expression data on microRNAs in normal and ovarian cancer tissue (references 16-18):
    - Yang H, *et al., Cancer Res.* **68**, 425 (2008).
    - Zhang L, *et al., Proc Natl Acad Sci U S A* **105,** 7004 (2008).
    - Mitomo S, *Cancer Sci.* **99**, 280 (2008).

# Nonradioactive detection of telomerase activity using the telomeric repeat amplification protocol

Brittney-Shea Herbert[1], Amelia E Hochreiter[1], Woodring E Wright[2] & Jerry W Shay[2]

[1]Department of Medical and Molecular Genetics, Indiana University Cancer Center, Indiana University School of Medicine, Indianapolis, Indiana 46202-5251, USA. [2]Department of Cell Biology, University of Texas Southwestern Medical Center, Dallas, Texas 75390-9039, USA. Correspondence should be addressed to B.-S.H. (brherber@iupui.edu).

Published online 9 November 2006; doi:10.1038/nprot.2006.239



**The telomeric repeat amplification protocol (TRAP) is a two-step process for analyzing telomerase activity in cell or tissue extracts. Recent modifications of this sensitive assay include elimination of radioactivity by using a fluorescently labeled primer instead of a radiolabeled primer. In addition, the TRAP assay has been modified for real-time, quantitative PCR analysis. Here, we describe cost-effective procedures for detection of telomerase activity using a fluorescent-based assay as well as by using real-time PCR. These modified TRAP assays can be accomplished within 4 h (from lysis of samples to analysis of telomerase products).**

## INTRODUCTION

The discovery of telomerase[1] as a ribonucleoprotein complex that synthesizes telomeric repeats onto the 3′ end of chromosomes led to the development of an assay for the detection and measurement of its activity in cells and tissues. TRAP was developed as a PCR-based method to assess the level of telomerase activity in a given sample[2–4]. Briefly, a cell or tissue sample is lysed with a buffer containing detergent, and an aliquot of the lysate is mixed with a reaction solution containing elements for the two-step process of telomerase product formation and amplification. In the first step, the telomerase substrate and dNTPs within the reaction solution are used for the addition of telomeric repeats by telomerase if it is present within the sample lysate (represented as a ladder on acrylamide gels). In the second step, forward and reverse primers for these products are used for amplification. In addition amplification of an internal standard PCR control using separate forward and reverse primers is performed. Mismatches in the reverse ACX primer reduce primer–dimer artifacts while still being able to amplify telomerase addition products[2,5]. Improvement of the TRAP assay and lysis methods have allowed increased linearity and sensitivity[4–6]. For example, the incorporation of an internal standard PCR control with a separate set of primers allows the identification of false negatives. In addition, normalizing the intensity of the telomerase ladder to that of an internal standard PCR control permits the TRAP assay to become linear and allows accurate comparison between samples[4,5]. The NP-40-based lysis buffer, in addition to using whole-cell lysates, allows maximal detection of TRAP activity in a given sample as compared with the CHAPS-based lysis buffer[6]. The TRAP assay has been adapted to detect or quantitate telomerase activity in a diverse set of samples: tissue, normal and cancerous cells, proliferating or nonproliferating cells, as well as cells that have been treated with agents that may affect telomerase activity[7–10].

A variety of detection methods have been developed for TRAP[10,11]. Recently, nonradioactive detection methods have been developed for the TRAP assay to eliminate the handling of radioisotopes when labeling the telomerase substrate (TS) primer. For example, the TS primer can be designed to contain a Cy5 fluorescent label at the 5′ end of the oligonucleotide, which allows a sensitive, specific and nonradioactive approach (Cy5 fluorescent gel-based whole-cell TRAP (Cy5-TRAP)) for detecting telomerase activity in whole-cell lysates when telomerase products are analyzed on an acrylamide gel.

Real-time quantitative PCR analysis of telomerase activity has also been recently described by different groups[7,10–16]. This method allows a more rapid, high-throughput, quantitative analysis of telomerase activity in cell or tissue samples; therefore, this assay is optimal for clinical use[7,14]. For the real-time, quantitative TRAP (Q-TRAP) protocol described here, we reviewed various published protocols and considered the following criteria: simplicity, cost-effectiveness, reliability and reproducibility. Our protocol uses the SYBR Green method of detection[13,16], which is more cost-effective and easier to set up than the commercial TRAPeze® XL kit from Chemicon described previously[7]. However, the commercial TRAPeze® XL kit allows an internal standard control to normalize TRAP activity in the presence of PCR inhibitors. Although the SYBR Green method does not permit this, as SYBR Green and the sequence detection system cannot distinguish internal standard control products from telomerase products, the presence of PCR inhibitors in real-time PCR is obvious from the slope of the curves during real-time analysis. The use of the SYBR Green PCR master mix kit specifically designed for the ABI sequence detection system, as described in our analyses, simplifies the set-up and optimization and reduces potential troubleshooting problems. The addition of EGTA (as described in refs. 13,16) to the reaction mixture improves amplification cycle threshold ($C_t$) values. Analysis of Q-TRAP described in this protocol is based on standard real-time PCR analysis, which uses a relative standard curve method. The $C_t$ of an unknown sample is compared to a standard curve to quantify the relative amount of telomerase activity, which can then be normalized to the standard. Conventional TRAP assays are typically analyzed using cell equivalents from whole-cell lysates. For the Q-TRAP protocol, we added a precisely measured and consistent amount of cell protein lysate each time. We also analyzed samples with Q-TRAP using cell equivalents with similar results after normalizing for protein amounts (μg) per cell equivalents.

Finally, it is important to note that care must be taken not to contaminate reagents or samples with RNases or DNases during the TRAP assay. Furthermore, telomerase is heat sensitive; therefore, samples must be prepared and stored at cold temperatures (4 and

−80 °C), taking care not to heat the samples (as in tissue processing)[9]. When comparing the Cy5-TRAP and Q-TRAP methods, there are some quantitative and qualitative differences. The fraction of total telomerase liberated in a cell extract has been shown to be variable in different samples; hence, ideally, whole-cell lysates rather than cell extracts are used. However, tissues often contain "PCR inhibitors," much of which is removed by making extracts and spinning down the debris. Whole-cell lysates are preferred for Cy5-TRAP, whereas cell extracts are used for Q-TRAP to remove cellular debris for real-time SYBR Green PCR analysis; therefore, Q-TRAP may underestimate the amount of telomerase activity in samples with weak activity, as maximal activity has been shown to be in whole-cell lysates. On the other hand, the Q-TRAP method can eliminate human error during quantification because ABI software determines the $C_t$ values. However, the lack of a firm identification of telomerase extension products in Q-TRAP can be a limitation in accurately ruling out false positives. Therefore, it is recommended that one performs the Cy5-TRAP, which includes an internal control, to precede or confirm the Q-TRAP results. The Q-TRAP protocol can then be optimal for high-throughput, quantitative analysis of telomerase activity. Although prices vary by country, the relative costs of the different assays in the USA are about $0.53 per CY5-TRAP reaction, $1.13 per Q-TRAP reaction using the ABI SYBR Green PCR master mix and $3.79 per TRAPeze®XL kit reaction.

## MATERIALS

### REAGENTS

- Cell pellet from 25,000 to 100,000 cells
- RNase/DNase-free $H_2O$ (Ambion)
- BCA protein assay kit (Pierce)
- SYBR Green PCR master mix kit (Applied Biosystems, cat. no. 4309155; keep RNase-free)
- 10 mM EGTA (RNase/DNase-free)
- *Taq* DNA polymerase (New England Biologicals)
- Acrylamide (19:1 acrylamide:bis-acrylamide; Bio-Rad)
  **! CAUTION** (acrylamide is a neurotoxin and should be handled with gloves).
- 10× TBE
- TEMED (N,N,N′,N′-Tetramethylethylenediamine) (Bio-Rad)
- 10% (wt/vol) ammonium persulfate solution
- Ultrapure BSA (Ambion, cat. no. 2616)
- RNA-Zap to help eliminate RNases
- 50× dNTP mix (2.5 mM each of dATP, dTTP, dGTP and dCTP in RNase-free $H_2O$)
- 100 ng $\mu l^{-1}$ TS primer, HPLC-purified (5′-AATCCGTCGAGCAGAGTT)
- 100 ng $\mu l^{-1}$ Cy5-TS primer, HPLC-purified (5′-Cy5-AATCCGTCGAGCAGAGTT)
- 1 $\mu g\ \mu l^{-1}$ ACX primer, HPLC-purified (5′-GCGCGGCTTACCCTTACCCTTACCCTAACC-3′)
- 1 $\mu g\ \mu l^{-1}$ NT primer, HPLC-purified (5′-ATCGCTTCTCGGCCTTTT-3′)
- NP-40 lysis buffer (RNase/DNase-free): 10 mM Tris-HCl, pH 8.0; 1 mM $MgCl_2$; 1 mM EDTA; 1% (vol/vol) NP-40; 0.25 mM sodium deoxycholate; 10% (vol/vol) glycerol; 150 mM NaCl; 5 mM β-mercaptoethanol; 0.1 mM AEBSF (4-(2-Aminoethyl)benzenesulfonyl fluoride hydrochloride)
- 10× TRAP buffer (RNase/DNase-free): 200 mM Tris-HCl, pH 8.3; 15 mM $MgCl_2$; 630 mM KCl; 0.5% Tween 20; 10 mM EGTA
- Loading dye: 0.25% (wt/vol) bromophenol blue in 50% (vol/vol) glycerol/50 mM EDTA
- 50× TRAP primer mix recipe for Cy5-TRAP; see REAGENT SETUP

### EQUIPMENT

- DNase-, RNase-free microfuge tubes
- DNase-, RNase-free filter pipette tips
- 96-well PCR plates with optical lids
- Liquid nitrogen or snap-freeze box
- Tabletop centrifuge (up to 16,000*g* capability) at 4 °C (Eppendorf 5415R or equivalent)
- Thermocycler
- Power supplies and vertical gel apparatus
- PhosphorImager capable of reading Cy5 fluorescence
- ABI Prism 7000, 7700 Sequence Detector (PE Applied Biosystems) or equivalent

### REAGENT SETUP

**50× TRAP primer mix recipe for Cy5-TRAP** The primer mix includes the substrate for the 36-bp internal standard control (TSNT) and reverse primers (NT and ACX) for amplification of internal standard control (IC) and telomerase products. See **Box 1** for details on how to prepare this. The TSNT primer should be ordered either from a different company or at a different time from the NT and ACX primers to avoid any possibility of cross-contamination, as it functions in the reaction as a PCR substrate rather than a primer. **▲ CRITICAL** The stock TSNT primer should be prepared in a separate room from the other TRAP steps and with separate pipetmen[9]. The reason for separating PCR setup from PCR analysis in different rooms is that the PCR product is so abundant that minor aerosols can contaminate primers, etc. and cause problems. The TSNT primer is essentially a PCR product that is spiked into the reaction to compare its relative amplification by the TS and ACX primers; therefore, it needs to be prepared in a different room for exactly the same reasons as using a different room for PCR products.

## PROCEDURE

### Preparation of cell lysates ● TIMING 30 min

**1|** Harvest 25,000–100,000 cells into a DNase-, RNase-free 1.5-ml microfuge tube. Pellet cells by centrifugation in a tabletop centrifuge at 3,000*g* for 5 min at room temperature (18–25 °C). Carefully discard the supernatant. It is not necessary to wash the pellet, but ensure that all residual liquid is removed. Proceed to Step 2 if samples are ready for lysis.

## BOX 1 | PROTOCOL FOR MAKING UP THE 50× PRIMER MIX FOR CY5-TRAP

This recipe makes enough primer mix for 100 sample reactions.

1. In a separate room with separate pipetmen and tips from the other steps, dilute HPLC-purified TSNT oligonucleotide (5′-AATCCGTCGAGCAGAGTTAAAAGGCCGAGAAGCGAT-3′) to 100 μM with RNase-free $H_2O$. Perform serial dilutions (e.g., 1:100, 1:1,000 and 1:1,000) so that the final concentration of the TSNT stock is $1.0\times10^{-18}$ mol $\mu l^{-1}$.
2. Mix 10 μl each of the ACX and NT primers and 79.0 μl of RNase-free $H_2O$ together in an RNase-free tube (final concentration, 100 ng $\mu l^{-1}$).
3. Move to the area where the TSNT was prepared and add 1 μl of TSNT (final concentration, $0.01\times10^{-18}$ mol $\mu l^{-1}$) to the mix. Clean the outside of the tube with diluted bleach.
4. Aliquot the primer mix in a separate room and store at −20 °C.

■ **PAUSE POINT** In case it is required to collect samples for use over a period of time, snap-freeze the cell pellet in liquid nitrogen and store at −80 °C until ready for lysis.

**2|** Resuspend the cell pellet in ice-cold NP-40 lysis buffer at a concentration of 500–1,250 cells $\mu l^{-1}$ and incubate on ice for 30 min. We have observed that NP-40 lysis buffer is more efficient in extracting telomerase activity than the CHAPS-based lysis buffer[9].

▲ **CRITICAL STEP** Care must be taken not to contaminate any step in the TRAP assay with RNases.

**3|** Prepare lysates for the TRAP assay. This step can be performed using option A (Cy5 fluorescent gel-based TRAP on whole-cell lysates) or option B (real-time Q-TRAP on cell extracts).

**(A) Cy5 fluorescent gel-based whole-cell TRAP** ● **TIMING 3 h**

(i) Keep samples on ice.

■ **PAUSE POINT** Whole-cell lysates can be snap-frozen in liquid nitrogen and placed at −80 °C until ready for analysis.

(ii) Prepare samples so that the final volume is 2 µl. Keep all the samples on ice.

(iii) Choose a telomerase-positive sample for making a standard curve (e.g., this can be human MCF-7 breast carcinoma, H1299 lung carcinoma, HeLa cervical carcinoma or immortalized 293 human embryonic kidney cells). Prepare a dilution series of your standard sample (e.g., 1:10, 1:5 or 1:2 starting at 2,500 cell equivalents).

(iv) Prepare control samples: (a) 5 µl of lysate incubated with 1 µg of RNase at 37 °C for 20 min or heat-inactivated at 85 °C for 10 min before the telomerase assay; (b) a positive control lysate containing known telomerase activity as described above; and (c) a lysis buffer-only control should also be included to check for the presence of contamination in the lysis buffer. Keep all the samples on ice.

(v) Prepare the TRAP master mix and reaction mixture for the appropriate number of samples ($n$ + 2). The final volume of sample, primers, buffers and enzyme is 50 µl per sample. Prepare a master mix containing 1× TRAP buffer, 1× dNTP mix, 1× TRAP primer mix, 100 ng of Cy5-TS primer per sample, 20 µg $ml^{-1}$ BSA, RNase-free $H_2O$ (to bring the final volume to 48 µl per sample) and 2 U of *Taq* DNA polymerase. For example, for ten samples:

| Component | Volume |
|---|---|
| RNase-free $H_2O$ | 392 µl |
| 10× TRAP buffer | 50 µl |
| 50× dNTP mix | 10 µl |
| 50× TRAP primer mix | 10 µl |
| Cy-5 TS primer (100 ng $\mu l^{-1}$) | 10 µl |
| BSA (50 mg $ml^{-1}$) | 4 µl |
| *Taq* DNA polymerase (5 U $\mu l^{-1}$) | 4 µl |

(vi) Add 48 µl of the master mix to each sample (total volume 50 µl). Incubate the samples at 22–30 °C for 30 min for the extension of the substrate by telomerase.

(vii) Amplify the extension products by PCR: 95 °C for 5 min to inactivate telomerase, and 24 cycles at 95 °C for 30 s, 52 °C for 30 s and 72 °C for 30 s.

■ **PAUSE POINT** After PCR, samples can be kept at 4 °C for no more than 2 days or at −20 °C for a longer time (<1 month) until analysis on an acrylamide gel.

(viii) Following PCR, add 5 µl of loading dye to each TRAP reaction mixture and run 25 µl on a 10% nondenaturing acrylamide gel in 0.5× TBE (1.5 h, 17–20 V $cm^{-1}$). Fixing the gel is optional, but fixation prevents DNA diffusion and results in slightly sharper bands. Fix the gel by incubating in 0.5 M NaCl, 50% (vol/vol) ethanol and 40 mM sodium acetate (pH 4.2) for 15 min.

(ix) Visualize the gel using a PhosphorImager that is capable of reading Cy5 fluorescence, and determine the intensity of the telomerase products (6-bp ladder) and the 36-bp IC band with ImageQuant software (Molecular Dynamics). Calculate the relative telomerase activity (RTA) as the ratio of the intensity of the TRAP ladder to that of IC. Normalize the relative intensity of each sample to that of a positive control (i.e., percentage). For example, ((intensity of sample's TRAP ladder/intensity of sample's IC band)/(intensity of positive control's TRAP ladder/intensity of positive control's IC band))×100. **? TROUBLESHOOTING**

**(B) Real-time Q-TRAP** ● **TIMING 3 h**

(i) Centrifuge the sample lysates to remove cellular debris at 16,000*g* for 20 min at 4 °C using a tabletop microcentrifuge.

(ii) Keep the samples on ice. Collect 80% of the supernatant in a fresh DNase/RNase-free Eppendorf tube making sure that no traces of cell debris from the pellet are withdrawn.

■ **PAUSE POINT** Extracts can be snap-frozen in liquid nitrogen and placed at −80 °C until ready for analysis.

(iii) Quantify the total protein concentration of your samples using a BCA protein assay kit (Pierce) according to the manufacturer's protocols.

(iv) Prepare control samples: (a) 5 µl of extract incubated with 1 µg of RNase at 37 °C for 20 min or heat-inactivated at 85 °C for 10 min before the telomerase assay; (b) a positive control lysate containing known telomerase activity; and (c) a lysis buffer-only control to check for the presence of contamination. Keep all samples on ice.

(v) Choose a telomerase-positive sample for making the standard curve (e.g., this can be human MCF-7 breast carcinoma, H1299 lung carcinoma, HeLa cervical carcinoma or immortalized 293 human embryonic kidney cells).

(vi) Create a 1:10 or 1:5 dilution series of your standard to yield at least five separate curves that are spaced widely apart. Note that $>1$ µg protein lysate may interfere with the reaction and increase $C_t$ values.

(vii) Choose how much protein of your unknown/test samples you will analyze so that the $C_t$ values for these samples fall within the standard range. For example, 1–3 µg protein lysate is usually sufficient (however, the amount of protein from the unknown samples may need to be empirically determined as 1 µg protein lysate may contain only ~300–500 cell equivalents, which may be too low to detect TRAP products in samples with weak activity). Prepare each sample in triplicate as 2 µl final volume aliquots.

(viii) Prepare the TRAP master mix and reaction mixture for the appropriate number of samples ($n$ + 2). The final volume of the reaction mixture (sample, primers, buffers and enzymes) is 25 µl per sample. Prepare a master mix containing 1× SYBR Green Master Mix (includes *Taq* polymerase and a passive reference dye, ROX), 100 ng TS primer per sample, 100 ng ACX primer per sample, 1 mM EGTA and enough water to bring the final volume to 25 µl. For example, for ten samples:

| Component | Volume |
|---|---|
| RNase/DNase-free $H_2O$ | 60 µl |
| ABI SYBR Green PCR master mix | 125 µl |
| EGTA (10 mM) | 25 µl |
| ACX primer (100 ng $\mu l^{-1}$) | 10 µl |
| TS primer (100 ng $\mu l^{-1}$) | 10 µl |

(ix) Add 23 µl of Q-TRAP master mix to each sample well of a 96-well PCR plate that will be analyzed (it is helpful to prepare a template of a 96-well PCR plate in order to plan the location of samples for analysis).

(x) Add your sample volume (2 µl) to each well to bring the total volume to 25 µl per well.

(xi) Incubate the 96-well plate for 30 min at 22–30 °C in the dark for extension of the substrate by telomerase.

(xii) Take the plate to the ABI Prism Sequence Detector and cycle (under SYBR Green setting) using the standard protocol that comes with the kit: 95 °C for 10 min (to activate the hot start *Taq* polymerase in the master mix); 40 cycles at 95 °C for 15 s and at 60 °C for 60 s.

(xiii) After PCR, collect real-time data according to the sequence detector manual and analysis software program. Set the baseline and threshold to be 10 standard deviations (s.d.) above the background (10 s.d. = 1 power of 10).

(xiv) You can also run the real-time PCR products on a 10% nondenaturing acrylamide gel to confirm the presence/absence of telomerase products.

(xv) Plot a standard curve according to the guidelines for the sequence detector using your telomerase-positive sample dilution series. Take the $\log_{10}$ of your protein concentration values for each sample. Plot your standard curve's average $C_t$ values (± s.d.) on the $y$ axis and the $\log_{10}$ protein concentration on the $x$ axis. Add a linear trend line and record the equation on the graph. Ensure that $R^2$ is $>0.90$.

(xvi) Convert your unknown/test sample data into RTA units that are defined by your standard curve and linear equation. For each raw $C_t$ value, perform the following calculation: converted RTA of sample=$10((C_t \text{ sample} - Y_{int})/\text{slope})$. Calculate the average RTA (± s.d.) for each test sample. Normalize the RTA to that of a positive control (for example, percentage telomerase activity compared to a positive control).

**? TROUBLESHOOTING**

## ● TIMING

Steps 1 and 2: 30 min
Step 3A: 3 h
Step 3B: 3 h

## ? TROUBLESHOOTING

Troubleshooting advice can be found in **Table 1**.

**TABLE 1** | Troubleshooting table.

| Problem | Possible causes | Solution |
|---|---|---|
| No products/very high $C_t$ for any sample including the positive control. | RNase/DNase contamination. | Practice sterile technique and use only RNase/DNase-free reagents. |
| | PCR amplification not initiated. | Check thermocycler for proper temperature and cycling conditions. |
| | | *Taq* is a hot start enzyme and you must incubate samples at 95 °C for 10 min to activate it. |
| | | Make sure you correctly added primers and that your lysates are still active (keep them at −80°C and avoid freeze–thaw). |
| | | Check to see if the *Taq* is still active (keep all reagents on ice). |
| Products present/low $C_t$ in negative controls. | Lysis buffer contamination. | Collect fresh lysates using freshly prepared lysis buffer. |
| | Kit, water or primer stocks contaminated. | Run quality control to see where the contamination is and then replace with fresh reagent. |
| | Background. | Inevitably 40 cycles may pick up background noise; hence do not consider it contamination unless the $C_t$ is below 30–35 cycles. |
| | DNA-contaminated plates or tubes. | Use only RNase/DNase-free consumables. |
| Jagged amplification plots. | Unoptimized kit. | Optimize the protocol by adjusting [$MgCl_2$], [EGTA], [Primer], and/or add BSA or T4 protein. |
| | | Adjust thermocycler conditions. |
| | | Test another brand of SYBR Green Q-PCR kit; however, we have found that the ABI kit works best on ABI systems. |
| High background fluorescence. | Primer dimers and unoptimized thermocycler conditions. | Empirically adjust temperatures for annealing and cycle time. |



## ANTICIPATED RESULTS

As human telomerase is processive, varying numbers of hexameric repeats are added to it during the initial 30-min incubation in the presence of the TS primer. When subsequently amplified, a 6-bp DNA incremental ladder of telomerase products is visualized (**Fig. 1a,c**). This ladder is reflective of the amount of telomerase activity per cell equivalent or protein used in the assay. In addition, a 36-bp internal standard control band is seen on the acrylamide gel when using the Cy5-TRAP method. The RTA can then be expressed as the ratio of the intensity of the entire ladder to that of the IC band (**Fig. 1b,d**). When performing a dilution series on a sample, the RTA should behave in a linear manner (**Fig. 1b**; $R^2 > 0.90$). Dividing the intensity of the telomerase addition products by that of the internal standard permits the linear relationship to be maintained. Samples with high amounts of telomerase activity will appear to compete with the IC amplification as well as having extra bands between 36 and 50 bp (the first telomerase product) because the *Taq* polymerase becomes limiting (**Fig. 1c**). The amount of lysate should then be reduced so that it does not compete with the internal standard. The number of PCR cycles can also be adjusted to determine a more optimal end point of amplification. In addition, tissue samples often contain inhibitors of *Taq* polymerase, which will reduce the intensity of both the TRAP ladder and the

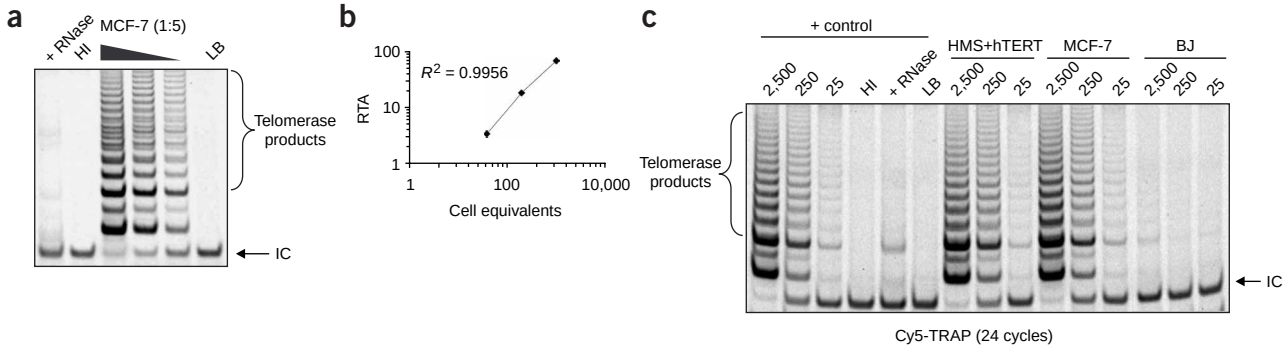


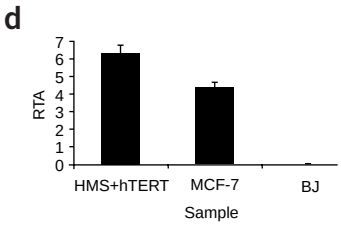


**Figure 1** | Analysis of telomerase activity using Cy5-TRAP. (**a**) Human cancer cell lysates (MCF-7 breast carcinoma cells) are shown to be positive for telomerase activity, as evidenced by the 6-bp incremental TRAP ladder. Lysis buffer (LB) only, RNase-treated (+RNase) and heat-inactivated (HI) MCF-7 cell lysates served as negative controls. Each TRAP reaction includes a 36-bp internal standard control (IC). Serial dilutions (1:5) of MCF-7 whole-cell lysates (1,000, 200 and 40 cell equivalents) result in a decreased intensity of the telomerase products TRAP ladder and return of the internal standard control band (IC). (**b**) Quantification of telomerase activity using Cy5-TRAP. The total peak intensity of the telomerase products TRAP ladder for each sample was divided by the intensity of the IC band. The RTA ± s.d. for each cell equivalent was plotted using a logarithmic scale. The serial dilution of MCF-7 whole-cell lysate exhibited a linear relationship for RTA ($R^2 > 0.90$). Note that each fivefold dilution in (**a**) only decreases the intensity of the actual TRAP ladder two- to threefold, and it is only by dividing the intensity of the actual TRAP ladder by the increasing intensity of the IC that one gains the linearity of response shown in (**b**). (**c**) Cy5-TRAP analysis of telomerase activity using 25, 250 and 2,500 cell equivalents from normal fibroblasts (BJ), a cancer cell line with endogenous telomerase activity (MCF-7) and human stromal cells with exogenous hTERT (HMS+hTERT). Positive telomerase activity is evidenced as the 6-bp incremental TRAP ladder of telomerase products. A serial dilution of whole-cell lysates from a positive control (MCF-7 cells) served as a positive control (+control). Lysis buffer (LB) only, RNase-treated (+RNase) and heat-inactivated (HI) MCF-7 cell lysates served as negative controls. Each TRAP reaction includes a 36-bp internal standard control (IC). (**d**) Relative amounts of telomerase activity (RTA±s.d.) for 250 cell equivalents from HMS + hTERT, MCF-7 and BJ whole-cell lysates analyzed by Cy5-TRAP. The ratio of the intensity of the sample's TRAP ladder (telomerase products, TP) to that of the internal control (IC) band was calculated after compensating for the background in the LB sample (i.e., $(TP - TP_{LB})/IC$).



internal control; therefore, these samples should be diluted with lysis buffer to achieve detectable telomerase products. Cy5-TRAP allows a relatively inexpensive method to detect reliably the presence or absence of a ladder that can be documented for figures as authentic telomerase addition products without major artifacts.

Q-TRAP follows traditional quantitative, real-time PCR experimental design, where the threshold of amplification can be determined ($C_t$). In this protocol, we describe the analysis of samples using known protein concentrations so that we can be confident about the amount of starting material for real-time PCR analysis with SYBR Green. We also performed this protocol using cell equivalent with similar results after normalizing for protein amounts (μg) per cell equivalents. Repeating the serial dilution series for a cell line as illustrated in **Figure 1**, the data screen that appears during real-time PCR (here with the ABI Prism 7000 sequence detector software) shows separate curves with increasing threshold cycles ($C_t$, *x* axis) for each sample (**Fig. 2a**). The green line represents the threshold that can be manipulated within the file so that it is ten s.d.s. above the baseline signal or background (the background lines of the curves can also be omitted as in these figures). Following the relative standard curve method for real-time data analysis (which should be included in the procedure handbook associated with the sequence detector), the $C_t$ values of the samples were plotted against log[protein] to calculate the linear equation (**Fig. 2b**). The $R^2$ should be $>0.90$. The *Y*-intercept and the slope values from the equation are used to quantify the RTA of unknown samples (RTA of unknown sample$= 10^{[(C_{t\,sample} - Y_{int})/slope]}$). Using the relative standard curve method, as described above, allows one to compare the RTA of one sample with thatof another sample performed in the same experiment, which is standard for analyzing real-time PCR products.

Analysis of telomerase activity of various samples should also reveal individual curves as shown in **Figure 2c** (the standard curves were omitted in this figure). The relative standard curve method as described above is used to quantify the RTA of different samples performed in the same experiment (**Fig. 2d**). Confirmation of real-time PCR analysis can be performed using an acrylamide gel, which is then stained with SYBR Green; however, this step is optional and can also reveal artifacts and spurious PCR products from the interaction of the ACX primer with the telomerase substrate, genomic DNA or PCR product contamination of reagents as the samples were collected after 40 cycles. These artifact signals are easily distinguishable from true telomerase products. An additional consideration is the functional linear range of the two assays. The single band in

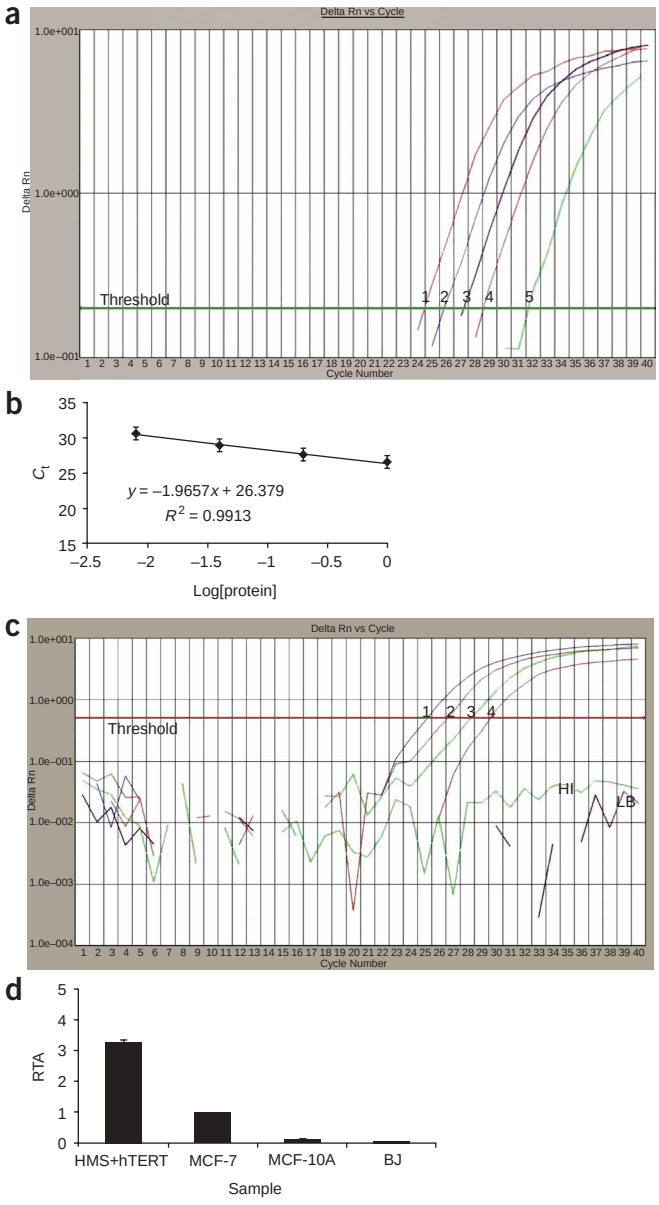


**Figure 2** | Real-time Q-TRAP analysis of telomerase activity: preparation of the standard curve. (**a**) The amount of cellular protein in MCF-7 breast carcinoma cell lysates was determined and then analyzed for telomerase activity using Q-TRAP and an ABI Prism 7000 Sequence Detector. Real-time amplification plots of serially diluted (1:5) MCF-7 breast carcinoma cell lysates (curves 1–5: 1.0, 0.2, 0.04, 0.008 and 0.0016 μg, respectively). The change in fluorescence of SYBR Green (Delta Rxn) was plotted against cycle number. $C_t$ represents the cycle at which fluorescence is first detected above the threshold (baseline signal plus 10 s.d.). Serial dilutions of protein extract result in increased $C_t$ values. (**b**) Determination of the standard curve and linear relationship for Q-TRAP. The $C_t$ values (±s.d.) of the standard control were plotted against log[protein] to calculate the linear equation. The *Y*-intercept and the slope values from the equation are used to quantify the RTA of unknown samples ($=10^{[(C_{t\ sample}-Y_{int})/slope]}$). (**c**) Real-time Q-TRAP analysis of telomerase activity in cell extracts. Various samples representing normal fibroblasts (BJ), a cancer cell line with high telomerase activity (MCF-7), an immortal cell line with low telomerase activity (MCF-10A) and human cells with exogenous hTERT (HMS + hTERT) were analyzed for telomerase activity using both the Cy5-TRAP and Q-TRAP protocols. Amplification plots of 1-μg protein extracts from human cells with exogenous hTERT (curve 1), a cancer cell line with high endogenous telomerase activity (curve 2), an immortal cell line with low telomerase activity (curve 3) and normal fibroblasts with no detectable hTERT mRNA (curve 4). HI, heat inactivated; LB, lysis buffer. (**d**) Samples were quantified as described in the protocol and plotted as RTA ± s.d. For Q-TRAP quantification, the RTA for an unknown sample was calculated based on the following standard curve and equation obtained for the same Q-TRAP assay: $y=-1.9657x + 26.379$; RTA$= 10^{[(C_{t\ sample}-Y_{int})/slope]}$.

the 2,500 BJ cell lane of **Figure 1c** is often seen in the lysis buffer control and thus represents an artifact; therefore, there is at least a 100-fold difference in telomerase activity between BJ and MCF-7 cells. Because cell extracts (rather than whole-cell lysates) and only 370 cell equivalents were analyzed by Q-PCR, BJ fibroblasts appear to only have an approximately tenfold rather than a 100-fold lower activity than MCF-7 cells. Q-PCR thus tends to overestimate the activity of very low-activity samples.

**ACKNOWLEDGMENTS** We thank P. Erickson and E. Badenhop for technical assistance. This work was supported by the Indiana University Cancer Center and the Indiana Genomics Initiative (INGEN). INGEN of Indiana University is supported in part by Lilly Endowment Inc.

**COMPETING INTERESTS STATEMENTS** The authors declare competing financial interests (see the HTML version of this article for details).

Published online at http://www.natureprotocols.com
Reprints and permissions information is available online at http://npg.nature.com/reprintsandpermissions

1. Greider, C.W. & Blackburn, E.H. Identification of a specific telomere terminal transferase activity in *Tetrahymena* extracts. *Cell* **43**, 405–413 (1985).
2. Kim, N.-W. *et al.* Specific association of human telomerase activity with immortal cells and cancer. *Science* **266**, 2011–2015 (1994).
3. Norton, J.C., Holt, S.E., Wright, W.E. & Shay, J.W. Enhanced detection of human telomerase activity. *DNA Cell Biol.* **17**, 217–219 (1998).
4. Wright, W.E., Shay, J.W. & Piatyszek, M.A. Modifications of a telomeric repeat amplification protocol (TRAP) result in increased reliability, linearity and sensitivity. *Nucleic Acids Res.* **23**, 3794–3795 (1995).
5. Kim, N.W. & Wu, F. Advances in quantification and characterization of telomerase activity by the telomeric repeat amplification protocol (TRAP). *Nucleic Acids Res.* **25**, 2595–2597 (1997).
6. Norton, J.C., Holt, S.E., Wright, W.E. & Shay, J.W. Enhanced detection of human telomerase activity. *DNA Cell Biol.* **17**, 217–219 (1998).
7. Elmore, L.W. *et al.* Real-time quantitative analysis of telomerase activity in breast tumor specimens using a highly specific and sensitive fluorescent-based assay. *Diagn. Mol. Pathol.* **11**, 177–185 (2002).
8. Gollahon, L.S. & Holt, S.E. Alternative methods of extracting telomerase activity from human tumor samples. *Cancer Lett.* **159**, 141–149 (2000).
9. Piatyszek, M.A. *et al.* Detection of telomerase activity in human cells and tumors by a telomeric repeat amplification protocol (TRAP). *Methods Cell Sci.* **17**, 1–15 (1995).
10. Saldanha, S.N., Andrews, L.G. & Tollefsbol, T.O. Analysis of telomerase activity and detection of its catalytic subunit, hTERT. *Anal. Biochem.* **315**, 1–21 (2003).
11. Fajkus, J. Detection of telomerase activity by the TRAP assay and its variants and alternatives. *Clin. Chim. Acta* **371**, 25–31 (2006).
12. Huang, Y.P., Liu, Z.S., Tang, H., Liu, M. & Li, X. Real-time telomeric repeat amplification protocol using the duplex scorpion and two reverse primers system:

the high sensitive and accurate method for quantification of telomerase activity. *Clin. Chim. Acta* **372**, 112–119 (2006).
13. Hou, M., Xu, D., Bjorkholm, M. & Gruber, A. Real-time quantitative telomeric repeat amplification protocol assay for the detection of telomerase activity. *Clin. Chem.* **47**, 519–524 (2001).
14. Jakupciak, J.P. Real-time telomerase activity measurements for detection of cancer. *Expert Rev. Mol. Diagn.* **5**, 745–753 (2005).
15. Jakupciak, J.P., Barker, P.E., Wang, W., Srivastava, S. & Atha, D.H. Preparation and characterization of candidate reference materials for telomerase assays. *Clin. Chem.* **51**, 1443–1450 (2005).
16. Wege, H., Chui, M.S., Le, H.T., Tran, J.M. & Zern, M.A. SYBR Green real-time telomeric repeat amplification protocol for the rapid quantification of telomerase activity. *Nucleic Acids Res. Methods Online* **31**, E3 (2003).

**hTERT microRNA predictions using PicTarDatabase**

*** The predicted microRNA should be prioritized based on column H (combined interaction energy). A lower energy (more negative) indicates a higher binding affinity.**

| ReSeq ID | Gene name | microRNA name | site position | seed type | microRNA-target hybridization energy | energy required to make the target site accessible | combined interaction energy* | site conservation | chromosome | seed start position | seed end position | strand | unique PITA site name |
|---|---|---|---|---|---|---|---|---|---|---|---|---|---|
| NM_198255 | TERT | hsa-miR-671 | 301 | 7:00:00 | -32.55 | -13.63 | -18.91 | 0.00025 | 5 | 1306542 | 1306549 | - | TERT\|hsa-miR-671\|1 |
| NM_198255 | TERT | hsa-miR-608 | 328 | 7:00:01 | -25.22 | -7.38 | -17.83 | 0.00025 | 5 | 1306515 | 1306522 | - | TERT\|hsa-miR-608\|3 |
| NM_198255 | TERT | hsa-miR-637 | 331 | 7:00:01 | -25.09 | -7.45 | -17.63 | 0.00037 | 5 | 1306512 | 1306519 | - | TERT\|hsa-miR-637\|1 |
| NM_198255 | TERT | hsa-miR-663 | 360 | 8:00:01 | -25 | -10.12 | -14.87 | 0.001 | 5 | 1306483 | 1306491 | - | TERT\|hsa-miR-663\|2 |
| NM_198255 | TERT | hsa-miR-608 | 350 | 7:00:01 | -20.41 | -6 | -14.4 | 0.00075 | 5 | 1306493 | 1306500 | - | TERT\|hsa-miR-608\|4 |
| NM_198255 | TERT | hsa-miR-608 | 306 | 7:00:01 | -27.4 | -13.55 | -13.84 | 0.00012 | 5 | 1306537 | 1306544 | - | TERT\|hsa-miR-608\|2 |
| NM_198255 | TERT | hsa-miR-150 | 522 | 6:00:00 | -23.11 | -10.4 | -12.7 | 0 | 5 | 1306321 | 1306327 | - | TERT\|hsa-miR-150\|1 |
| NM_198255 | TERT | hsa-miR-422b | 324 | 6:00:00 | -18.02 | -7.3 | -10.71 | 0 | 5 | 1306519 | 1306525 | - | TERT\|hsa-miR-422b\|1 |
| NM_198255 | TERT | hsa-miR-652 | 340 | 6:00:00 | -18.6 | -8.96 | -9.63 | 0 | 5 | 1306503 | 1306509 | - | TERT\|hsa-miR-652\|1 |
| NM_198255 | TERT | hsa-miR-491 | 310 | 7:00:00 | -23.3 | -13.97 | -9.32 | 0.00012 | 5 | 1306533 | 1306540 | - | TERT\|hsa-miR-491\|3 |
| NM_198255 | TERT | hsa-miR-422a | 324 | 6:00:00 | -16.32 | -7.3 | -9.01 | 0 | 5 | 1306519 | 1306525 | - | TERT\|hsa-miR-422a\|1 |
| NM_198255 | TERT | hsa-miR-663 | 355 | 7:00:01 | -17.1 | -8.37 | -8.72 | 0.0012 | 5 | 1306488 | 1306495 | - | TERT\|hsa-miR-663\|1 |
| NM_198255 | TERT | hsa-miR-150 | 507 | 7:00:01 | -22.86 | -15.41 | -7.44 | 0 | 5 | 1306336 | 1306343 | - | TERT\|hsa-miR-150\|3 |
| NM_198255 | TERT | hsa-miR-363* | 349 | 7:00:01 | -14.5 | -7.07 | -7.42 | 0.0005 | 5 | 1306494 | 1306501 | - | TERT\|hsa-miR-363*\|1 |
| NM_198255 | TERT | hsa-miR-516-5p | 333 | 6:00:00 | -14.19 | -7.37 | -6.81 | 0.00042 | 5 | 1306510 | 1306516 | - | TERT\|hsa-miR-516-5p\|2 |
| NM_198255 | TERT | hsa-miR-608 | 266 | 7:00:00 | -32.7 | -26.35 | -6.34 | 0 | 5 | 1306577 | 1306584 | - | TERT\|hsa-miR-608\|5 |
| NM_198255 | TERT | hsa-miR-608 | 379 | 7:00:00 | -23 | -17.22 | -5.77 | 0.00037 | 5 | 1306464 | 1306471 | - | TERT\|hsa-miR-608\|1 |
| NM_198255 | TERT | hsa-miR-548d | 547 | 6:00:00 | -12 | -6.26 | -5.73 | 0 | 5 | 1306296 | 1306302 | - | TERT\|hsa-miR-548d\|1 |
| NM_198255 | TERT | hsa-miR-548a | 554 | 8:00:01 | -11.86 | -6.15 | -5.7 | 0 | 5 | 1306289 | 1306297 | - | TERT\|hsa-miR-548a\|2 |
| NM_198255 | TERT | hsa-miR-594 | 393 | 8:00:01 | -24.6 | -18.9 | -5.69 | 0 | 5 | 1306450 | 1306458 | - | TERT\|hsa-miR-594\|1 |
| NM_198255 | TERT | hsa-miR-632 | 36 | 8:00:00 | -24 | -18.58 | -5.41 | 0 | 5 | 1306807 | 1306815 | - | TERT\|hsa-miR-632\|1 |
| NM_198255 | TERT | hsa-miR-363* | 327 | 7:00:01 | -12.3 | -7.49 | -4.8 | 0.00012 | 5 | 1306516 | 1306523 | - | TERT\|hsa-miR-363*\|2 |
| NM_198255 | TERT | hsa-miR-484 | 117 | 7:00:01 | -27.89 | -23.16 | -4.72 | 0.00037 | 5 | 1306726 | 1306733 | - | TERT\|hsa-miR-484\|1 |
| NM_198255 | TERT | hsa-miR-657 | 226 | 6:00:00 | -20.53 | -16.12 | -4.4 | 0 | 5 | 1306617 | 1306623 | - | TERT\|hsa-miR-657\|1 |
| NM_198255 | TERT | hsa-miR-299-3p | 312 | 7:00:00 | -18 | -13.79 | -4.2 | 0.00012 | 5 | 1306531 | 1306538 | - | TERT\|hsa-miR-299-3p\|1 |
| NM_198255 | TERT | hsa-miR-122a | 306 | 6:00:00 | -17.6 | -13.55 | -4.04 | 0.00014 | 5 | 1306537 | 1306543 | - | TERT\|hsa-miR-122a\|1 |
| NM_198255 | TERT | hsa-miR-296 | 488 | 8:00:01 | -26.66 | -23.13 | -3.52 | 0 | 5 | 1306355 | 1306363 | - | TERT\|hsa-miR-296\|1 |
| NM_198255 | TERT | hsa-miR-650 | 373 | 7:00:01 | -16.12 | -12.66 | -3.45 | 0 | 5 | 1306470 | 1306477 | - | TERT\|hsa-miR-650\|1 |
| NM_198255 | TERT | hsa-miR-512-5p | 211 | 8:00:00 | -28.3 | -24.93 | -3.36 | 0 | 5 | 1306632 | 1306640 | - | TERT\|hsa-miR-512-5p\|3 |
| NM_198255 | TERT | hsa-miR-483 | 435 | 6:00:00 | -24.3 | -21.12 | -3.17 | 0 | 5 | 1306408 | 1306414 | - | TERT\|hsa-miR-483\|1 |
| NM_198255 | TERT | hsa-miR-320 | 554 | 7:00:01 | -9.21 | -6.15 | -3.05 | 0 | 5 | 1306289 | 1306296 | - | TERT\|hsa-miR-320\|1 |
| NM_198255 | TERT | hsa-miR-29b | 515 | 6:00:00 | -15.1 | -12.49 | -2.6 | 0 | 5 | 1306328 | 1306334 | - | TERT\|hsa-miR-29b\|1 |
| NM_198255 | TERT | hsa-miR-512-5p | 169 | 8:00:00 | -24 | -21.47 | -2.52 | 0 | 5 | 1306674 | 1306682 | - | TERT\|hsa-miR-512-5p\|1 |
| NM_198255 | TERT | hsa-miR-101 | 517 | 7:00:01 | -13.3 | -10.79 | -2.5 | 0 | 5 | 1306326 | 1306333 | - | TERT\|hsa-miR-101\|1 |
| NM_198255 | TERT | hsa-miR-29c | 515 | 6:00:00 | -14.4 | -12.49 | -1.9 | 0 | 5 | 1306328 | 1306334 | - | TERT\|hsa-miR-29c\|1 |
| NM_198255 | TERT | hsa-miR-29a | 515 | 6:00:00 | -14.4 | -12.49 | -1.9 | 0 | 5 | 1306328 | 1306334 | - | TERT\|hsa-miR-29a\|1 |
| NM_198255 | TERT | hsa-miR-346 | 35 | 6:00:00 | -20.5 | -18.63 | -1.86 | 0 | 5 | 1306808 | 1306814 | - | TERT\|hsa-miR-346\|1 |
| NM_198255 | TERT | hsa-miR-363* | 305 | 7:00:01 | -15.2 | -13.47 | -1.72 | 0.00012 | 5 | 1306538 | 1306545 | - | TERT\|hsa-miR-363*\|5 |
| NM_198255 | TERT | hsa-miR-147 | 313 | 7:00:01 | -15.57 | -13.87 | -1.69 | 0 | 5 | 1306530 | 1306537 | - | TERT\|hsa-miR-147\|1 |
| NM_198255 | TERT | hsa-miR-548a | 546 | 6:00:00 | -7.99 | -6.43 | -1.55 | 0 | 5 | 1306297 | 1306303 | - | TERT\|hsa-miR-548a\|1 |
| NM_198255 | TERT | hsa-miR-640 | 498 | 7:00:01 | -19.9 | -19.34 | -0.55 | 0 | 5 | 1306345 | 1306352 | - | TERT\|hsa-miR-640\|1 |
| NM_198255 | TERT | hsa-miR-637 | 268 | 6:00:00 | -25 | -24.45 | -0.54 | 0 | 5 | 1306575 | 1306581 | - | TERT\|hsa-miR-637\|2 |
| NM_198255 | TERT | hsa-miR-202* | 317 | 8:00:00 | -10.3 | -9.86 | -0.43 | 0 | 5 | 1306526 | 1306534 | - | TERT\|hsa-miR-202*\|1 |
| NM_198255 | TERT | hsa-miR-668 | 437 | 7:00:00 | -21.49 | -21.13 | -0.35 | 0 | 5 | 1306406 | 1306413 | - | TERT\|hsa-miR-668\|1 |
| NM_198255 | TERT | hsa-miR-565 | 275 | 8:00:01 | -25.33 | -25.07 | -0.25 | 0 | 5 | 1306568 | 1306576 | - | TERT\|hsa-miR-565\|1 |
| NM_198255 | TERT | hsa-miR-320 | 278 | 8:00:00 | -21.91 | -22.29 | 0.38 | 0 | 5 | 1306565 | 1306573 | - | TERT\|hsa-miR-320\|2 |
| NM_198255 | TERT | hsa-miR-661 | 98 | 8:00:00 | -30.92 | -31.41 | 0.49 | 0 | 5 | 1306745 | 1306753 | - | TERT\|hsa-miR-661\|2 |
| NM_198255 | TERT | hsa-miR-181b | 171 | 7:00:01 | -19.9 | -20.58 | 0.68 | 0 | 5 | 1306672 | 1306679 | - | TERT\|hsa-miR-181b\|3 |
| NM_198255 | TERT | hsa-miR-412 | 395 | 8:00:01 | -18.2 | -18.9 | 0.7 | 0 | 5 | 1306448 | 1306456 | - | TERT\|hsa-miR-412\|1 |
| NM_198255 | TERT | hsa-miR-181b | 133 | 7:00:01 | -21.7 | -22.43 | 0.73 | 0 | 5 | 1306710 | 1306717 | - | TERT\|hsa-miR-181b\|1 |
| NM_198255 | TERT | hsa-miR-506 | 372 | 6:00:00 | -10.5 | -11.37 | 0.87 | 0 | 5 | 1306471 | 1306477 | - | TERT\|hsa-miR-506\|1 |
| NM_198255 | TERT | hsa-miR-612 | 217 | 7:00:01 | -21.5 | -22.45 | 0.95 | 0 | 5 | 1306626 | 1306633 | - | TERT\|hsa-miR-612\|1 |
| NM_198255 | TERT | hsa-miR-363* | 378 | 7:00:00 | -15.91 | -17.04 | 1.13 | 0.00025 | 5 | 1306465 | 1306472 | - | TERT\|hsa-miR-363*\|3 |
| NM_198255 | TERT | hsa-miR-661 | 24 | 6:00:00 | -18.9 | -20.48 | 1.58 | 0 | 5 | 1306819 | 1306825 | - | TERT\|hsa-miR-661\|1 |
| NM_198255 | TERT | hsa-miR-181d | 171 | 7:00:01 | -18.7 | -20.58 | 1.88 | 0 | 5 | 1306672 | 1306679 | - | TERT\|hsa-miR-181d\|2 |
| NM_198255 | TERT | hsa-miR-767-3p | 33 | 6:00:00 | -16.3 | -18.29 | 1.99 | 0 | 5 | 1306810 | 1306816 | - | TERT\|hsa-miR-767-3p\|1 |
| NM_198255 | TERT | hsa-miR-491 | 285 | 8:00:01 | -17.21 | -19.44 | 2.23 | 0.00022 | 5 | 1306558 | 1306566 | - | TERT\|hsa-miR-491\|1 |
| NM_198255 | TERT | hsa-miR-150 | 113 | 6:00:00 | -17.93 | -20.3 | 2.37 | 0.00085 | 5 | 1306730 | 1306736 | - | TERT\|hsa-miR-150\|2 |
| NM_198255 | TERT | hsa-miR-502 | 466 | 7:00:01 | -20.2 | -22.6 | 2.4 | 0 | 5 | 1306377 | 1306384 | - | TERT\|hsa-miR-502\|1 |

| | | | | | | | | | | | | | |
|---|---|---|---|---|---|---|---|---|---|---|---|---|---|
| NM_198255 | TERT | hsa-miR-384 | 317 | 6:00:00 | -7.41 | -9.86 | 2.45 | 0 | 5 | 1306526 | 1306532 | - | TERT\|hsa-miR-384\|2 |
| NM_198255 | TERT | hsa-miR-328 | 273 | 7:00:00 | -20.5 | -23.03 | 2.53 | 0 | 5 | 1306570 | 1306577 | - | TERT\|hsa-miR-328\|1 |
| NM_198255 | TERT | hsa-miR-138 | 41 | 8:00:00 | -18.1 | -20.79 | 2.69 | 0 | 5 | 1306802 | 1306810 | - | TERT\|hsa-miR-138\|1 |
| NM_198255 | TERT | hsa-miR-513 | 494 | 8:00:01 | -19.9 | -22.63 | 2.73 | 0 | 5 | 1306349 | 1306357 | - | TERT\|hsa-miR-513\|1 |
| NM_198255 | TERT | hsa-miR-181c | 171 | 7:00:01 | -17.6 | -20.58 | 2.98 | 0 | 5 | 1306672 | 1306679 | - | TERT\|hsa-miR-181c\|3 |
| NM_198255 | TERT | hsa-miR-654 | 383 | 6:00:00 | -15.79 | -18.86 | 3.07 | 0.00071 | 5 | 1306460 | 1306466 | - | TERT\|hsa-miR-654\|1 |
| NM_198255 | TERT | hsa-miR-181d | 133 | 7:00:01 | -19.33 | -22.43 | 3.1 | 0 | 5 | 1306710 | 1306717 | - | TERT\|hsa-miR-181d\|3 |
| NM_198255 | TERT | hsa-miR-493-5p | 456 | 6:00:00 | -19.1 | -22.3 | 3.2 | 0 | 5 | 1306387 | 1306393 | - | TERT\|hsa-miR-493-5p\|1 |
| NM_198255 | TERT | hsa-miR-491 | 382 | 6:00:00 | -16.69 | -19.93 | 3.24 | 0.00071 | 5 | 1306461 | 1306467 | - | TERT\|hsa-miR-491\|4 |
| NM_198255 | TERT | hsa-miR-520a* | 424 | 7:00:01 | -14.7 | -18.45 | 3.75 | 0 | 5 | 1306419 | 1306426 | - | TERT\|hsa-miR-520a*\|1 |
| NM_198255 | TERT | hsa-miR-519e* | 396 | 6:00:00 | -14.85 | -18.9 | 4.05 | 0 | 5 | 1306447 | 1306453 | - | TERT\|hsa-miR-519e*\|1 |
| NM_198255 | TERT | hsa-miR-9 | 442 | 8:00:01 | -15.6 | -20.07 | 4.47 | 0 | 5 | 1306401 | 1306409 | - | TERT\|hsa-miR-9\|1 |
| NM_198255 | TERT | hsa-miR-181a | 171 | 7:00:01 | -16.1 | -20.58 | 4.48 | 0 | 5 | 1306672 | 1306679 | - | TERT\|hsa-miR-181a\|1 |
| NM_198255 | TERT | hsa-miR-192 | 498 | 7:00:01 | -14.7 | -19.34 | 4.64 | 0 | 5 | 1306345 | 1306352 | - | TERT\|hsa-miR-192\|1 |
| NM_198255 | TERT | hsa-miR-525 | 424 | 7:00:01 | -13.8 | -18.45 | 4.65 | 0 | 5 | 1306419 | 1306426 | - | TERT\|hsa-miR-525\|1 |
| NM_198255 | TERT | hsa-miR-384 | 426 | 8:00:01 | -13.6 | -18.51 | 4.91 | 0 | 5 | 1306417 | 1306425 | - | TERT\|hsa-miR-384\|1 |
| NM_198255 | TERT | hsa-miR-574 | 171 | 7:00:01 | -15.6 | -20.58 | 4.98 | 0 | 5 | 1306672 | 1306679 | - | TERT\|hsa-miR-574\|2 |
| NM_198255 | TERT | hsa-miR-516-5p | 391 | 7:00:01 | -14.7 | -19.87 | 5.17 | 0 | 5 | 1306452 | 1306459 | - | TERT\|hsa-miR-516-5p\|1 |
| NM_198255 | TERT | hsa-miR-454-5p | 484 | 7:00:01 | -17.19 | -22.4 | 5.21 | 0 | 5 | 1306359 | 1306366 | - | TERT\|hsa-miR-454-5p\|1 |
| NM_198255 | TERT | hsa-miR-574 | 133 | 7:00:01 | -17 | -22.43 | 5.43 | 0 | 5 | 1306710 | 1306717 | - | TERT\|hsa-miR-574\|1 |
| NM_198255 | TERT | hsa-miR-542-3p | 52 | 7:00:00 | -13.4 | -18.85 | 5.45 | 0 | 5 | 1306791 | 1306798 | - | TERT\|hsa-miR-542-3p\|1 |
| NM_198255 | TERT | hsa-miR-489 | 52 | 6:00:00 | -12.92 | -18.85 | 5.93 | 0 | 5 | 1306791 | 1306797 | - | TERT\|hsa-miR-489\|1 |
| NM_198255 | TERT | hsa-miR-215 | 498 | 7:00:01 | -13.3 | -19.34 | 6.04 | 0 | 5 | 1306345 | 1306352 | - | TERT\|hsa-miR-215\|1 |
| NM_198255 | TERT | hsa-miR-181c | 133 | 7:00:01 | -16.29 | -22.43 | 6.14 | 0 | 5 | 1306710 | 1306717 | - | TERT\|hsa-miR-181c\|2 |
| NM_198255 | TERT | hsa-miR-612 | 198 | 7:00:01 | -23.51 | -29.79 | 6.28 | 0 | 5 | 1306645 | 1306652 | - | TERT\|hsa-miR-612\|2 |
| NM_198255 | TERT | hsa-miR-363* | 265 | 7:00:00 | -20.9 | -27.23 | 6.33 | 0 | 5 | 1306578 | 1306585 | - | TERT\|hsa-miR-363*\|4 |
| NM_198255 | TERT | hsa-miR-512-5p | 127 | 6:00:00 | -19.93 | -26.44 | 6.51 | 0 | 5 | 1306716 | 1306722 | - | TERT\|hsa-miR-512-5p\|2 |
| NM_198255 | TERT | hsa-miR-619 | 391 | 7:00:00 | -13.3 | -19.87 | 6.57 | 0 | 5 | 1306452 | 1306459 | - | TERT\|hsa-miR-619\|1 |
| NM_198255 | TERT | hsa-miR-181a | 133 | 7:00:01 | -15.84 | -22.43 | 6.59 | 0 | 5 | 1306710 | 1306717 | - | TERT\|hsa-miR-181a\|2 |
| NM_198255 | TERT | hsa-miR-491 | 243 | 8:00:00 | -19.51 | -26.51 | 7 | 0 | 5 | 1306600 | 1306608 | - | TERT\|hsa-miR-491\|2 |
| NM_198255 | TERT | hsa-miR-510 | 169 | 6:00:00 | -14.39 | -21.47 | 7.08 | 0 | 5 | 1306674 | 1306680 | - | TERT\|hsa-miR-510\|2 |
| NM_198255 | TERT | hsa-miR-604 | 45 | 6:00:00 | -14.7 | -21.91 | 7.21 | 0 | 5 | 1306798 | 1306804 | - | TERT\|hsa-miR-604\|1 |
| NM_198255 | TERT | hsa-miR-510 | 211 | 6:00:00 | -17.7 | -24.93 | 7.23 | 0 | 5 | 1306632 | 1306638 | - | TERT\|hsa-miR-510\|3 |
| NM_198255 | TERT | hsa-miR-647 | 201 | 6:00:00 | -22 | -29.45 | 7.45 | 0 | 5 | 1306642 | 1306648 | - | TERT\|hsa-miR-647\|1 |
| NM_198255 | TERT | hsa-miR-622 | 249 | 7:00:01 | -18.4 | -25.95 | 7.55 | 0 | 5 | 1306594 | 1306601 | - | TERT\|hsa-miR-622\|1 |
| NM_198255 | TERT | hsa-miR-220 | 447 | 6:00:00 | -13.64 | -21.54 | 7.9 | 0 | 5 | 1306396 | 1306402 | - | TERT\|hsa-miR-220\|1 |
| NM_198255 | TERT | hsa-miR-617 | 115 | 7:00:01 | -15.2 | -23.15 | 7.95 | 0.00062 | 5 | 1306728 | 1306735 | - | TERT\|hsa-miR-617\|1 |
| NM_198255 | TERT | hsa-miR-609 | 94 | 6:00:00 | -21.61 | -29.92 | 8.31 | 0.00028 | 5 | 1306749 | 1306755 | - | TERT\|hsa-miR-609\|1 |
| NM_198255 | TERT | hsa-miR-515-5p | 396 | 6:00:00 | -10.45 | -18.9 | 8.45 | 0 | 5 | 1306447 | 1306453 | - | TERT\|hsa-miR-515-5p\|1 |
| NM_198255 | TERT | hsa-miR-432* | 388 | 7:00:00 | -11.5 | -19.99 | 8.49 | 0.00012 | 5 | 1306455 | 1306462 | - | TERT\|hsa-miR-432*\|1 |
| NM_198255 | TERT | hsa-miR-181b | 213 | 7:00:01 | -16.6 | -25.13 | 8.53 | 0 | 5 | 1306630 | 1306637 | - | TERT\|hsa-miR-181b\|2 |
| NM_198255 | TERT | hsa-miR-596 | 248 | 6:00:00 | -17.11 | -25.73 | 8.62 | 0 | 5 | 1306595 | 1306601 | - | TERT\|hsa-miR-596\|1 |
| NM_198255 | TERT | hsa-miR-141 | 134 | 6:00:00 | -13.8 | -22.59 | 8.79 | 0 | 5 | 1306709 | 1306715 | - | TERT\|hsa-miR-141\|1 |
| NM_198255 | TERT | hsa-miR-205 | 163 | 6:00:00 | -15.51 | -24.53 | 9.02 | 0 | 5 | 1306680 | 1306686 | - | TERT\|hsa-miR-205\|1 |
| NM_198255 | TERT | hsa-miR-149 | 274 | 7:00:01 | -14.26 | -23.5 | 9.24 | 0 | 5 | 1306569 | 1306576 | - | TERT\|hsa-miR-149\|1 |
| NM_198255 | TERT | hsa-miR-326 | 270 | 7:00:01 | -15.3 | -24.61 | 9.31 | 0 | 5 | 1306573 | 1306580 | - | TERT\|hsa-miR-326\|2 |
| NM_198255 | TERT | hsa-miR-510 | 127 | 7:00:00 | -17 | -26.44 | 9.44 | 0 | 5 | 1306716 | 1306723 | - | TERT\|hsa-miR-510\|1 |
| NM_198255 | TERT | hsa-miR-607 | 432 | 7:00:01 | -12.4 | -22.01 | 9.61 | 0 | 5 | 1306411 | 1306418 | - | TERT\|hsa-miR-607\|1 |
| NM_198255 | TERT | hsa-miR-181d | 213 | 7:00:01 | -15.35 | -25.13 | 9.78 | 0 | 5 | 1306630 | 1306637 | - | TERT\|hsa-miR-181d\|1 |
| NM_198255 | TERT | hsa-miR-181c | 213 | 7:00:01 | -15.3 | -25.13 | 9.83 | 0 | 5 | 1306630 | 1306637 | - | TERT\|hsa-miR-181c\|1 |
| NM_198255 | TERT | hsa-miR-218 | 221 | 6:00:00 | -14.2 | -24.83 | 10.63 | 0 | 5 | 1306622 | 1306628 | - | TERT\|hsa-miR-218\|1 |
| NM_198255 | TERT | hsa-miR-181a | 213 | 7:00:01 | -14.4 | -25.13 | 10.73 | 0 | 5 | 1306630 | 1306637 | - | TERT\|hsa-miR-181a\|3 |
| NM_198255 | TERT | hsa-miR-615 | 257 | 6:00:00 | -17.4 | -28.17 | 10.77 | 0 | 5 | 1306586 | 1306592 | - | TERT\|hsa-miR-615\|1 |
| NM_198255 | TERT | hsa-miR-642 | 78 | 8:00:01 | -17.4 | -28.33 | 10.93 | 0.00033 | 5 | 1306765 | 1306773 | - | TERT\|hsa-miR-642\|1 |
| NM_198255 | TERT | hsa-miR-581 | 460 | 7:00:01 | -13.9 | -25.3 | 11.4 | 0 | 5 | 1306383 | 1306390 | - | TERT\|hsa-miR-581\|1 |
| NM_198255 | TERT | hsa-miR-200a | 134 | 6:00:00 | -11.01 | -22.59 | 11.58 | 0 | 5 | 1306709 | 1306715 | - | TERT\|hsa-miR-200a\|1 |
| NM_198255 | TERT | hsa-miR-574 | 213 | 7:00:01 | -13.2 | -25.13 | 11.93 | 0 | 5 | 1306630 | 1306637 | - | TERT\|hsa-miR-574\|3 |
| NM_198255 | TERT | hsa-miR-644 | 92 | 6:00:00 | -17.7 | -29.9 | 12.2 | 0.00057 | 5 | 1306751 | 1306757 | - | TERT\|hsa-miR-644\|1 |
| NM_198255 | TERT | hsa-miR-9* | 278 | 6:00:00 | -8.63 | -22.29 | 13.66 | 0 | 5 | 1306565 | 1306571 | - | TERT\|hsa-miR-9*\|1 |
| NM_198255 | TERT | hsa-miR-585 | 68 | 7:00:01 | -13.62 | -28.17 | 14.55 | 0.00075 | 5 | 1306775 | 1306782 | - | TERT\|hsa-miR-585\|1 |
| NM_198255 | TERT | hsa-miR-326 | 73 | 7:00:01 | -15.1 | -29.83 | 14.73 | 0.00012 | 5 | 1306770 | 1306777 | - | TERT\|hsa-miR-326\|1 |
| NM_198255 | TERT | hsa-miR-150 | 417 | 6:00:00 | -14.4 | -32.14 | 17.74 | 0 | 5 | 1306426 | 1306432 | - | TERT\|hsa-miR-150\|4 |

**hTERT microRNA predictions using Miranda Database**

*** The predicted microRNA should be prioritized based on column F and G(Score and p value). A higher score or lower p value indicates a higher binding affinity.**

| microRNA | CHR | START | END | STRAND | SCORE* | PVALUE_OG* | TRANSCRIPT_ID | EXTERNAL_NAME |
|---|---|---|---|---|---|---|---|---|
| hsa-miR-512-5p | 5 | 1306632 | 1306657 | - | 17.8786 | 3.45E-05 | ENST00000310581 | TERT |
| hsa-miR-512-5p | 5 | 1306674 | 1306697 | - | 17.7728 | 3.45E-05 | ENST00000310581 | TERT |
| mmu-miR-705 | 5 | 1306467 | 1306487 | - | 17.61 | 3.31E-02 | ENST00000310581 | TERT |
| hsa-miR-548a | 5 | 1306289 | 1306310 | - | 17.1127 | 2.47E-03 | ENST00000310581 | TERT |
| hsa-miR-632 | 5 | 1306807 | 1306825 | - | 17.0597 | 5.42E-03 | ENST00000310581 | TERT |
| mmu-miR-298 | 5 | 1306474 | 1306495 | - | 17.0064 | 3.39E-02 | ENST00000310581 | TERT |
| rno-miR-343 | 5 | 1306764 | 1306783 | - | 16.9657 | 3.41E-03 | ENST00000310581 | TERT |
| hsa-miR-608 | 5 | 1306577 | 1306603 | - | 16.7785 | 6.90E-03 | ENST00000310581 | TERT |
| mmu-miR-744 | 5 | 1306484 | 1306505 | - | 16.7705 | 5.88E-04 | ENST00000310581 | TERT |
| hsa-miR-9 | 5 | 1306401 | 1306424 | - | 16.7149 | 1.63E-02 | ENST00000310581 | TERT |
| hsa-miR-661 | 5 | 1306745 | 1306766 | - | 16.64 | 4.33E-02 | ENST00000310581 | TERT |
| mmu-miR-693-3p | 5 | 1306677 | 1306699 | - | 16.6091 | 5.37E-03 | ENST00000310581 | TERT |
| hsa-miR-299-3p | 5 | 1306531 | 1306553 | - | 16.5813 | 1.49E-02 | ENST00000310581 | TERT |
| mmu-miR-685 | 5 | 1306501 | 1306521 | - | 16.5568 | 1.79E-02 | ENST00000310581 | TERT |
| hsa-miR-320 | 5 | 1306565 | 1306588 | - | 16.3975 | 4.12E-02 | ENST00000310581 | TERT |
| hsa-miR-30e-3p | 5 | 1306681 | 1306702 | - | 16.3687 | 1.03E-03 | ENST00000310581 | TERT |
| hsa-miR-30a-3p | 5 | 1306681 | 1306700 | - | 16.2624 | 1.03E-03 | ENST00000310581 | TERT |
| mmu-miR-720 | 5 | 1306651 | 1306668 | - | 16.1824 | 4.47E-03 | ENST00000310581 | TERT |
| hsa-miR-648 | 5 | 1306620 | 1306638 | - | 16.0879 | 1.32E-03 | ENST00000310581 | TERT |
| hsa-miR-138 | 5 | 1306802 | 1306818 | - | 16.0649 | 2.86E-05 | ENST00000310581 | TERT |
| mmu-miR-673 | 5 | 1306324 | 1306345 | - | 16.0498 | 5.19E-04 | ENST00000310581 | TERT |
| hsa-miR-363* | 5 | 1306578 | 1306599 | - | 15.9435 | 4.68E-05 | ENST00000310581 | TERT |
| hsa-miR-663 | 5 | 1306483 | 1306504 | - | 15.9435 | 2.68E-03 | ENST00000310581 | TERT |
| rno-miR-333 | 5 | 1306619 | 1306638 | - | 15.8919 | 2.98E-02 | ENST00000310581 | TERT |
| hsa-miR-181c | 5 | 1306630 | 1306651 | - | 15.8372 | 1.92E-03 | ENST00000310581 | TERT |
| rno-miR-343 | 5 | 1306333 | 1306354 | - | 15.7846 | 3.41E-03 | ENST00000310581 | TERT |
| hsa-miR-363* | 5 | 1306494 | 1306514 | - | 15.7309 | 4.68E-05 | ENST00000310581 | TERT |
| rno-miR-664 | 5 | 1306712 | 1306733 | - | 15.7309 | 5.08E-03 | ENST00000310581 | TERT |
| hsa-miR-658 | 5 | 1306474 | 1306498 | - | 15.6249 | 3.17E-04 | ENST00000310581 | TERT |
| hsa-miR-363* | 5 | 1306465 | 1306486 | - | 15.6247 | 4.68E-05 | ENST00000310581 | TERT |
| hsa-miR-181c | 5 | 1306672 | 1306692 | - | 15.6247 | 1.92E-03 | ENST00000310581 | TERT |
| hsa-miR-640 | 5 | 1306345 | 1306367 | - | 15.5955 | 2.63E-03 | ENST00000310581 | TERT |
| mmu-miR-712 | 5 | 1306679 | 1306699 | - | 15.5955 | 2.69E-03 | ENST00000310581 | TERT |
| hsa-miR-181b | 5 | 1306672 | 1306691 | - | 15.5184 | 1.92E-03 | ENST00000310581 | TERT |
| hsa-miR-432* | 5 | 1306455 | 1306475 | - | 15.4887 | 4.46E-02 | ENST00000310581 | TERT |
| hsa-miR-105 | 5 | 1306413 | 1306433 | - | 15.4624 | 2.35E-03 | ENST00000310581 | TERT |
| hsa-miR-648 | 5 | 1306385 | 1306403 | - | 15.4401 | 1.32E-03 | ENST00000310581 | TERT |
| hsa-miR-491 | 5 | 1306600 | 1306622 | - | 15.3396 | 4.80E-03 | ENST00000310581 | TERT |
| mmu-miR-675-5p | 5 | 1306738 | 1306759 | - | 15.0932 | 1.43E-05 | ENST00000310581 | TERT |
| hsa-miR-605 | 5 | 1306319 | 1306341 | - | 15.0222 | 9.21E-03 | ENST00000310581 | TERT |
| mmu-miR-720 | 5 | 1306712 | 1306729 | - | 14.8791 | 4.47E-03 | ENST00000310581 | TERT |
| hsa-miR-668 | 5 | 1306713 | 1306737 | - | 14.8106 | 2.43E-03 | ENST00000310581 | TERT |
| hsa-miR-668 | 5 | 1306406 | 1306428 | - | 14.8106 | 2.43E-03 | ENST00000310581 | TERT |
| hsa-miR-542-5p | 5 | 1306352 | 1306372 | - | 14.7743 | 4.83E-02 | ENST00000310581 | TERT |
| hsa-miR-550 | 5 | 1306315 | 1306335 | - | 14.668 | 6.84E-03 | ENST00000310581 | TERT |
| hsa-miR-574 | 5 | 1306710 | 1306730 | - | 14.6341 | 1.41E-03 | ENST00000310581 | TERT |
| hsa-miR-518c | 5 | 1306326 | 1306347 | - | 14.5618 | 5.08E-03 | ENST00000310581 | TERT |
| hsa-miR-518e | 5 | 1306327 | 1306348 | - | 14.4555 | 5.08E-03 | ENST00000310581 | TERT |
| hsa-miR-192 | 5 | 1306345 | 1306367 | - | 14.4205 | 8.48E-03 | ENST00000310581 | TERT |
| hsa-miR-574 | 5 | 1306653 | 1306672 | - | 14.3137 | 1.41E-03 | ENST00000310581 | TERT |
| hsa-miR-560 | 5 | 1306587 | 1306606 | - | 14.1739 | 5.34E-03 | ENST00000310581 | TERT |

**hTERT microRNA predictions using miRBase Database**

| Rfam ID | Score | Energy | Base P | Poisson P | Org P | Start | End |
|---|---|---|---|---|---|---|---|
| **hsa-miR-512-5p** | 17.8786 | -32.4 | 7.50E-03 | 3.45E-05 | 3.45E-05 | 186 | 211 |
| **hsa-miR-512-5p** | 17.7728 | -27.73 | 8.33E-03 | 3.45E-05 | 3.45E-05 | 146 | 169 |
| **hsa-miR-548a** | 17.1127 | -13.45 | 2.10E-02 | 2.07E-02 | 2.47E-03 | 533 | 554 |
| **hsa-miR-632** | 17.0597 | -21.25 | 1.53E-02 | 1.52E-02 | 5.42E-03 | 18 | 36 |
| **hsa-miR-608** | 16.7785 | -32.56 | 5.19E-02 | 5.06E-02 | 6.90E-03 | 240 | 266 |
| **hsa-miR-9** | 16.7149 | -16.86 | 2.32E-02 | 2.29E-02 | 1.63E-02 | 419 | 442 |
| **hsa-miR-661** | 16.64 | -27.51 | 5.79E-02 | 5.62E-02 | 4.33E-02 | 77 | 98 |
| **hsa-miR-299-3p** | 16.5813 | -21.67 | 1.50E-02 | 1.49E-02 | 1.49E-02 | 290 | 312 |
| **hsa-miR-320** | 16.3975 | -20.15 | 4.21E-02 | 4.12E-02 | 4.12E-02 | 255 | 278 |
| **hsa-miR-30e-3p** | 16.3687 | -25.24 | 3.73E-02 | 3.73E-02 | 1.03E-03 | 141 | 162 |
| **hsa-miR-30a-3p** | 16.2624 | -29.88 | 4.32E-02 | 4.23E-02 | 1.03E-03 | 143 | 162 |
| **hsa-miR-648** | 16.0879 | -21.6 | 2.57E-02 | 1.32E-03 | 1.32E-03 | 205 | 223 |
| **hsa-miR-138** | 16.0649 | -15.99 | 4.00E-02 | 3.92E-02 | 2.86E-05 | 25 | 41 |
| **hsa-miR-363*** | 15.9435 | -21.36 | 4.77E-02 | 4.68E-05 | 4.68E-05 | 244 | 265 |
| **hsa-miR-663** | 15.9435 | -26.2 | 6.07E-02 | 5.89E-02 | 2.68E-03 | 339 | 360 |
| **hsa-miR-181c** | 15.8372 | -15.06 | 4.41E-02 | 2.95E-03 | 1.92E-03 | 192 | 213 |
| **hsa-miR-363*** | 15.7309 | -15.64 | 5.96E-02 | 4.68E-05 | 4.68E-05 | 329 | 349 |
| **hsa-miR-658** | 15.6249 | -28.94 | 7.66E-02 | 7.38E-02 | 3.17E-04 | 345 | 369 |
| **hsa-miR-181c** | 15.6247 | -20.18 | 5.43E-02 | 2.95E-03 | 1.92E-03 | 151 | 171 |
| **hsa-miR-363*** | 15.6247 | -13.75 | 6.66E-02 | 4.68E-05 | 4.68E-05 | 357 | 378 |
| **hsa-miR-640** | 15.5955 | -20.11 | 5.26E-02 | 5.12E-02 | 2.63E-03 | 476 | 498 |
| **hsa-miR-181b** | 15.5184 | -18.54 | 7.89E-02 | 2.95E-03 | 1.92E-03 | 152 | 171 |
| **hsa-miR-432*** | 15.4887 | -16.32 | 4.57E-02 | 4.46E-02 | 4.46E-02 | 368 | 388 |
| **hsa-miR-105** | 15.4624 | -22.12 | 5.69E-02 | 5.53E-02 | 2.35E-03 | 410 | 430 |
| **hsa-miR-648** | 15.4401 | -24.85 | 5.23E-02 | 1.32E-03 | 1.32E-03 | 440 | 458 |
| **hsa-miR-491** | 15.3396 | -17.52 | 8.09E-02 | 7.77E-02 | 4.80E-03 | 221 | 243 |
| **hsa-miR-605** | 15.0222 | -28.78 | 7.95E-02 | 7.65E-02 | 9.21E-03 | 502 | 524 |
| **hsa-miR-668** | 14.8106 | -24.06 | 9.22E-02 | 4.00E-03 | 2.43E-03 | 106 | 130 |
| **hsa-miR-668** | 14.8106 | -17.12 | 9.22E-02 | 4.00E-03 | 2.43E-03 | 415 | 437 |
| **hsa-miR-542-5p** | 14.7743 | -21.45 | 6.40E-02 | 6.20E-02 | 4.83E-02 | 471 | 491 |
| **hsa-miR-550** | 14.668 | -23.49 | 9.00E-02 | 8.61E-02 | 6.84E-03 | 508 | 528 |
| **hsa-miR-574** | 14.6341 | -13.01 | 5.11E-02 | 2.43E-03 | 1.41E-03 | 113 | 133 |
| **hsa-miR-518c** | 14.5618 | -23.42 | 8.33E-02 | 7.99E-02 | 5.08E-03 | 496 | 517 |
| **hsa-miR-518e** | 14.4555 | -26.94 | 8.04E-02 | 7.99E-02 | 5.08E-03 | 495 | 516 |
| **hsa-miR-192** | 14.4205 | -15.16 | 9.66E-02 | 9.21E-02 | 8.48E-03 | 476 | 498 |
| **hsa-miR-574** | 14.3137 | -15.92 | 7.14E-02 | 2.43E-03 | 1.41E-03 | 171 | 190 |
| **hsa-miR-560** | 14.1739 | -24.16 | 7.59E-02 | 7.31E-02 | 5.34E-03 | 237 | 256 |
| | | | | | | | |
| | | | | | | | |
| **other species:** | | | | | | | |
| **mmu-miR-720** | 14.8791 | -24.85 | 9.77E-02 | 4.47E-03 | 4.47E-03 | 114 | 131 |
| **mmu-miR-675-5p** | 15.0932 | -23.02 | 5.45E-02 | 5.31E-02 | 1.43E-05 | 84 | 105 |
| **mmu-miR-712** | 15.5955 | -23.92 | 6.08E-02 | 5.90E-02 | 2.69E-03 | 144 | 164 |
| **rno-miR-343** | 15.7846 | -28.92 | 8.50E-02 | 3.41E-03 | 3.41E-03 | 489 | 510 |
| **rno-miR-664** | 15.7309 | -18.12 | 5.58E-02 | 5.43E-02 | 5.08E-03 | 110 | 131 |
| **rno-miR-333** | 15.8919 | -18.49 | 4.06E-02 | 3.98E-02 | 2.98E-02 | 205 | 224 |
| **mmu-miR-673** | 16.0498 | -24.17 | 5.60E-02 | 5.45E-02 | 5.19E-04 | 498 | 519 |
| **mmu-miR-720** | 16.1824 | -26.87 | 2.88E-02 | 4.47E-03 | 4.47E-03 | 175 | 192 |
| **mmu-miR-685** | 16.5568 | -18.44 | 1.80E-02 | 1.79E-02 | 1.79E-02 | 322 | 342 |
| **mmu-miR-693-3p** | 16.6091 | -24.73 | 3.52E-02 | 3.45E-02 | 5.37E-03 | 144 | 166 |
| **mmu-miR-744** | 16.7705 | -25.12 | 2.23E-02 | 2.21E-02 | 5.88E-04 | 338 | 359 |
| **mmu-miR-298** | 17.0064 | -28.65 | 3.45E-02 | 3.39E-02 | 3.39E-02 | 348 | 369 |
| **rno-miR-343** | 16.9657 | -22.02 | 3.44E-02 | 3.41E-03 | 3.41E-03 | 60 | 79 |
| **mmu-miR-705** | 17.61 | -31.64 | 3.37E-02 | 3.31E-02 | 3.31E-02 | 356 | 376 |

**hTERT microRNA predictions using Sanger and RNA22 (overlap) Database**

| Overlap between Sanger and RNA22 |
|---|
| hsa-miR-105 |
| hsa-miR-337 |
| hsa-miR-409-5p |
| hsa-miR-484 |
| hsa-miR-491 |
| hsa-miR-493-3p |
| hsa-miR-505 |
| hsa-miR-510 |
| hsa-miR-512-5p |
| hsa-miR-518c |
| hsa-miR-518d |
| hsa-miR-524 |
| hsa-miR-542-5p |
| hsa-miR-550 |
| hsa-miR-560 |
| hsa-miR-564 |
| hsa-miR-565 |
| hsa-miR-567 |
| hsa-miR-571 |
| hsa-miR-572 |
| hsa-miR-574 |
| hsa-miR-608 |
| hsa-miR-611 |
| hsa-miR-640 |
| hsa-miR-648 |
| hsa-miR-658 |
| hsa-miR-663 |
| hsa-miR-768-3p |
| hsa-miR-768-5p |
| mmu-miR-665 |
| mmu-miR-669b |
| mmu-miR-673 |
| mmu-miR-675-5p |
| mmu-miR-689 |
| mmu-miR-692 |
| mmu-miR-693-3p |
| mmu-miR-699 |
| mmu-miR-700 |
| mmu-miR-704 |
| mmu-miR-712 |
| mmu-miR-717 |
| mmu-miR-720 |
| rno-miR-327 |
| rno-miR-333 |
| rno-miR-664 |

# MicroRNA Expression Profiling in Human Ovarian Cancer: *miR-214* Induces Cell Survival and Cisplatin Resistance by Targeting *PTEN*

**Hua Yang, William Kong, Lili He, Jian-Jun Zhao, Joshua D. O'Donnell, Jiawang Wang, Robert M. Wenham, Domenico Coppola, Patricia A. Kruk, Santo V. Nicosia, and Jin Q. Cheng**

Departments of Interdisciplinary Oncology and Pathology, H. Lee Moffitt Cancer Center and Research Institute and University of South Florida College of Medicine, Tampa, Florida

## Abstract

**MicroRNAs (miRNA) represent a novel class of genes that function as negative regulators of gene expression. Recently, miRNAs have been implicated in several cancers. However, aberrant miRNA expression and its clinicopathologic significance in human ovarian cancer have not been well documented. Here, we show that several miRNAs are altered in human ovarian cancer, with the most significantly deregulated miRNAs being *miR-214, miR-199a*, miR-200a, miR-100, miR-125b*, and *let-7* cluster. Further, we show the frequent deregulation of *miR-214, miR-199a*, miR-200a*, and *miR-100* in ovarian cancers. Significantly, *miR-214* induces cell survival and cisplatin resistance through targeting the 3′-untranslated region (UTR) of the *PTEN*, which leads to down-regulation of PTEN protein and activation of Akt pathway. Inhibition of Akt using Akt inhibitor, API-2/triciribine, or introduction of *PTEN* cDNA lacking 3′-UTR largely abrogates *miR-214*–induced cell survival. These findings indicate that deregulation of miRNAs is a recurrent event in human ovarian cancer and that *miR-214* induces cell survival and cisplatin resistance primarily through targeting the PTEN/Akt pathway.** [Cancer Res 2008;68(2):425–33]

## Introduction

MicroRNAs (miRNA) are a class of 22-nucleotide noncoding RNAs, which are evolutionarily conserved and function as negative regulators of gene expression. Like conventional protein-coding mRNA, miRNAs are transcribed by RNA polymerase II, spliced, and polyadenylated (called primitive miRNA or pri-miRNA). However, unlike mRNA, the pri-miRNAs contain a stem-loop structure that can be recognized and excised by the RNA interference machinery to generate hairpin "precursor" miRNAs (pre-miRNA) that are ~70 nucleotides in animals or ~100 nucleotides in plants. Pre-miRNAs are cleaved by the cytoplasmic RNase III Dicer into a 22-nucleotide miRNA duplex: one strand (miRNA*) of the short-lived duplex is degraded, whereas the other strand serves as a mature miRNA. The mature miRNA then guides a complex called miRNA-containing ribonucleo-protein particles to the complementary site(s) in the 3′-untranslated region (UTR) of a target mRNA. Consequently, translation blockade or mRNA degradation will occur depending on whether it is partially matched or completely matched with the target genes, respectively (1). Moreover, the levels of individual miRNAs are dramatically changed in different cell types and different developmental stages, suggesting that miRNA plays a role in cell growth, differentiation, and programmed cell death (1, 2).

miRNAs are aberrantly expressed or mutated in human cancer, indicating that they may function as a novel class of oncogenes or tumor suppressor genes (3–9). The first evidence of involvement of miRNAs in human cancer came from molecular studies characterizing the 13q14 deletion in human chronic lymphocytic leukemia, which revealed two miRNAs, *miR-15a* and *miR-16-1* (3). Subsequently, miRNA deregulation was detected in other human malignancies, including breast carcinoma (4, 5), primary glioblastoma (6, 7), lung cancer (8), papillary thyroid carcinoma (9), colon carcinoma (10), and pancreatic tumors (11, 12). For instance, the *miR-17-92* cluster is up-regulated in B-cell lymphomas and lung cancer. *miR-143* and *miR-145* are down-regulated in colon carcinomas. A decrease in *let-7* is detected in human lung carcinomas and restoration of its expression induces cell growth inhibition in lung cancer cells (13). The *BIC* gene, which contains the *miR-155*, is up-regulated in some Burkitt's lymphomas and several other types of lymphomas (14, 15).

In this report, we show deregulation of several miRNAs in human ovarian cancer. The aberrant expression of *miR-214, miR-199a*, miR-200a*, and *miR-100* was detected in a near or over half of ovarian cancers, especially in late-stage and high-grade tumors. Significantly, we showed that *miR-214* negatively regulates PTEN by binding to its 3′-UTR leading to inhibition of PTEN translation and activation of Akt pathway. Consequently, *miR-214* induces cell survival and cisplatin resistance, which were overridden by either small-molecule Akt inhibitor or expression of PTEN cDNA lacking 3′-UTR.

## Materials and Methods

**Cell lines and human tissue samples.** Human ovarian cancer cell lines and human immortalized ovarian surface epithelial (HIOSE) cell lines were described previously (16). HIOSE cells were grown in 199/MDCB 105 (1:1) medium (Sigma) supplemented with 5% fetal bovine serum. Frozen human primary ovarian tumor and normal ovarian tissues were obtained from the Tissue Procurement Facility at H. Lee Moffitt Cancer Center.

**miRNA array and Northern blot analysis.** Oligonucleotide arrays were printed with trimer oligonucleotide probes (antisense to miRNAs) specific for 515 human and mouse miRNAs on GeneScreen Plus (NEN) membranes, and miRNA expression profiling was performed and analyzed as previously described (7). Briefly, total RNAs were isolated from 10 HIOSE cell lines and 10 primary serous ovarian carcinomas with Trizol reagent (Invitrogen). Low-molecular weight RNAs were enriched from total RNAs using Microcon YM-100 columns (Millipore). The low-molecular weight RNAs were labeled with [$\gamma$-$^{32}$P]ATP and then hybridized to the miRNA array. To ensure accuracy of the hybridizations, each labeled RNA sample was hybridized with three separate membranes. In addition, eight oligonucleotides with nonmatching any known miRNA were used as hybridization controls. Hybridization signals for each spot of the array and background values at 15

**Requests for reprints:** Jin Q. Cheng, H. Lee Moffitt Cancer Center and Research Institute, 12902 Magnolia Drive, SRB3, Tampa, FL 33612. Phone: 813-745-6915; Fax: 813-745-3928; E-mail: jin.cheng@moffitt.org.



doi:10.1158/0008-5472.CAN-07-2488

empty spots were measured. Raw data were further automatically processed in Microsoft Excel. Hybridization signals that failed to exceed the average background value by more than three SDs were excluded from analysis.

For Northern blot analysis, 20 μg RNA was separated on 15% denaturing polyacrylamide gel and then electroblotted onto a Zeta-Probe GT Blotting Membrane (Bio-Rad). Following transfer, the membrane was dried and UV cross-linked. The probes were prepared using the StarFire Oligonucleotide Labeling System (Integrated DNA Technologies) according to the manufacturer's protocol. The blots were hybridized overnight at 50°C in a buffer containing 5× SSC, 20 mmol/L $Na_2HPO_4$ (pH 7.2), 7% SDS, 1× Denhardt's, and 0.2 mg/mL salmon sperm DNA and then washed with 1× SSC/1% SDS buffer at 50°C (13). The probe sequences are as follows: hsa-*miR-199a**, 5′-AACCAATGTGCAGACTACTGTA-3′; hsa-*miR-214*, 5′-CTGCCTGTC-TGTGCCTGCTGT-3′; hsa-*miR-100*, 5′-CACAAGTTCGGATCTACGGGTT-3′; and hsa-*miR-200a*, 5′-ACATCGTTACCAGACAGTGTTA-3′.

**RNase protection assay and quantitative reverse transcription-PCR.** Expression of miRNAs was also analyzed by RNase protection or *mir*Vana reverse quantitative transcription-PCR (qRT-PCR) miRNA detection assay. For RNase protection assay, enriched small RNA was purified using the miRVana miRNA Isolation kit (Ambion). The *mir*Vana miRNA probe construction kit (Ambion) was used to synthesize the $^{32}$P-labeled *miR-214* probe. Probe hybridization and RNase protection were then carried out using the *mir*Vana miRNA detection kit (Ambion) according to the manufacturer's instructions. After hybridization and RNase treatment, the double-strand products were resolved in a 15% polyacrylamide 8 mol/L urea denaturing gel and visualized using phosphoimaging and autoradiography. *mir*Vana qRT-PCR was performed according to the manufacturer's protocol (Ambion). PCR products were analyzed by electrophoresis on a 7.5% polyacrylamide gel in 0.5× Tris-borate EDTA and visualized by ethidium bromide staining.

**Antisense inhibition of miRNA expression.** 2′-*O*-methyl (2′-*O*-me) oligoribonucleotides were synthesized by Integrated DNA Technologies. The sequences of 2′-*O*-me-anti-*miR-214* and 2′-*O*-me-anti-*miR-199a** are as follows: 5′-CUGCCUGUCUGUGCCUGCUGU-3′ and 5′-AACCAAUGUGCAGA-CUACUGUA-3′. 2′-*O*-me-scrambled miR (5′-AAAACCUUUUGACCGAGCGU-GUU-3′) was used as a control. Cells were grown in six-well plate ($1.7 \times 10^6$ per well) for 24 h and transfected with 150 pmol/L/well of 2′-*O*-me oligoribonucleotides using Lipofectamine 2000. RNA and protein were extracted after 72 h of transfection.

**Cloning and expression of miRNAs.** Expression plasmids of *miR-214* and *miR-199a** were created by PCR amplification using human genomic DNA as a template. The primers are the following: *miR-214*, 5′-CACCTTTCTCCCTTTCCCCTTACTCTCC-3′ (sense) and 5′-TTTCATAGG-CACCACTCACTTTAC-3′ (antisense), and *miR-199a**, 5′-CACCGCCCAGA-AGCCACGATCCCAAACC-3′ (sense) and 5′-TGCCTTTCCCCAGTGCCTC-TTCTC-3′ (antisense). The PCR products (392 bp containing pri-miRNA) were cloned into pcDNA3.1/V5-His-Topo expression vector (Invitrogen) and confirmed by DNA sequencing. The expression of miRNA was carried out by transfection of the plasmid into the cells using Lipofectamine 2000.

**Target *in vitro* reporter assay.** For luciferase reporter experiments, the 3′-UTR segments of PTEN predicted to interact with *miR-214* were amplified by PCR from human genomic DNA and inserted into the *Mlu*I and *Hin*dIII sites of pGL3 vector immediately downstream from the stop codon of luciferase (Promega). A2780CP and HIOSE-80 cells were cotransfected in 12-well plates with 0.4 μg of the firefly luciferase report vector and 0.08 μg of the control vector containing *Renilla* luciferase, pRL-TK (Promega), as well as with or without 0.5 μg of Topo-*miR-214*. Firefly and *Renilla* luciferase activities were measured consecutively using dual-luciferase assays (16).

**Cell viability and apoptosis assays.** Cell viability was examined with 3-(4,5-dimethylthiazol-2-yl)-2,5-diphenyltetrazolium bromide (MTT) assay as previously described (17). Apoptosis was detected with Annexin V and caspase-3/7 activity (17, 18). For detection of caspase-3/7 activity, cells were cultured in 96-well plates and treated with the agents indicated in the figure legends and analyzed using Caspase-Glo 3/7 Assay kit (Promega) according to the manufacturer's instructions. Statistical analysis was done using two-sample *t* test, assuming equal variance, and *P* value was calculated based on two-tailed test.

**miRNA locked nucleic acid *in situ* hybridization of formalin-fixed, paraffin-embedded tissue section.** A miRNA locked nucleic acid (LNA) probe was prepared by 3′-end labeling with digoxigenin-ddUTP terminal transferase using the Dig-3′-End Labeling kit (Roche). Following deparaffinization and proteinase K digestion, slides were prehybridized for 1 h and then hybridized with 10 nmol/L miRNA LNA probe in a hybridization buffer (Roche) for 12 h. After three consecutive washes in 4× SSC/50% formamide, 2× SSC, and 0.1× SSC, sections were treated with a blocking buffer (Roche) for 1 h and incubated with anti-DIG-AP Fab fragments (Roche) for 12 h. Following wash for three times in 1× maleic acid and 0.3% Tween 20 buffer, reactions were detected in a detection solution [100 mmol/L Tris-HCl (pH 9.5) and 100 mmol/L NaCl] in the presence of nitroblue tetrazolium and 5-bromo-4-chloro-3-indolyl phosphate (Promega) and then visualized under a microscope.

## Results

**Frequent deregulation of *miR-199a**, *miR-214*, *miR-200a*, and *miR-100* in human ovarian cancer.** miRNA profiles have been reported in different types of tumors derived from different organs (3–12), including ovarian cancer (5). However, the frequency and pathobiological significance of aberrant miRNA expression in human ovarian cancer have not been well documented. We initially analyzed miRNA expression in 10 human ovarian epithelial tumors and 10 "normal" HIOSE cell line pools by hybridization of the array containing 515 miRNAs. After normalization of control oligos, the differential expression of miRNAs between ovarian tumors and normal ovarian surface epithelial cells was quantified using a phosphorimager. Thirty-six of the 515 miRNAs showed differential expression with *P* values derived from the nonparametric Wilcoxon/Kruskal-Wallis test being <0.05. Of them, 14 miRNAs that changed >1-fold were confirmed by Northern blot and/or qRT-PCR analysis (Fig. 1*A* and *B*; data not shown). To further validate our results, *miR-199a*, miR-214, miR-200a*, and *miR-100*, four of the most differentially expressed miRNAs, were analyzed in 30 primary ovarian cancers (Table 1). As compared with normal ovarian cells, more than half of the primary tumors exhibited elevated levels of *miR-199a** (53%, 16 of 30) and *miR-214* (56%, 17 of 30) and down-regulated *miR-100* (76%, 23 of 30). Moreover, increased *miR-200a* was detected in 43% of primary ovarian carcinomas examined (Table 1). Further, although the number of specimens is relatively small, the deregulation of *miR-199a*, miR-214*, and *miR-200a* seems to be associated with high-grade and late-stage tumors (Table 2). These data suggest that alterations of these three miRNAs could be involved in ovarian cancer progression.

**The *miR-214* targets *PTEN* leading to activation of the Akt pathway.** Because *miR-214* was one of the most frequently up-regulated miRNAs in the ovarian tumors (Table 2; Fig. 1) and has recently been shown to play an important role in zebrafish muscle development (19), we next examined its potential targets by searching the PicTar and miRBase database as well as sequence alignment analysis using GCG version 11.1. Among the candidates targeted, 3′-UTR of human *PTEN* contains a putative region (nucleotides 3257–3264, NM_000314) that matches to the seed sequence of hsa-*miR-214*, which is also conserved in mouse and rat (Fig. 2*A*). To examine whether *PTEN* is indeed the target of *miR-214*, a *miR-214*–negative cell line HIOSE-80 (Figs. 2*B* and 3*A*) was transfected with pcDNA3.1/V5-His-Topo-*miR-214*. The cells transfected with pcDNA3.1/V5-His-Topo vector alone and pcDNA3.1/V5-His-Topo-*miR-199a** were used as controls. Immunoblotting and

**A**

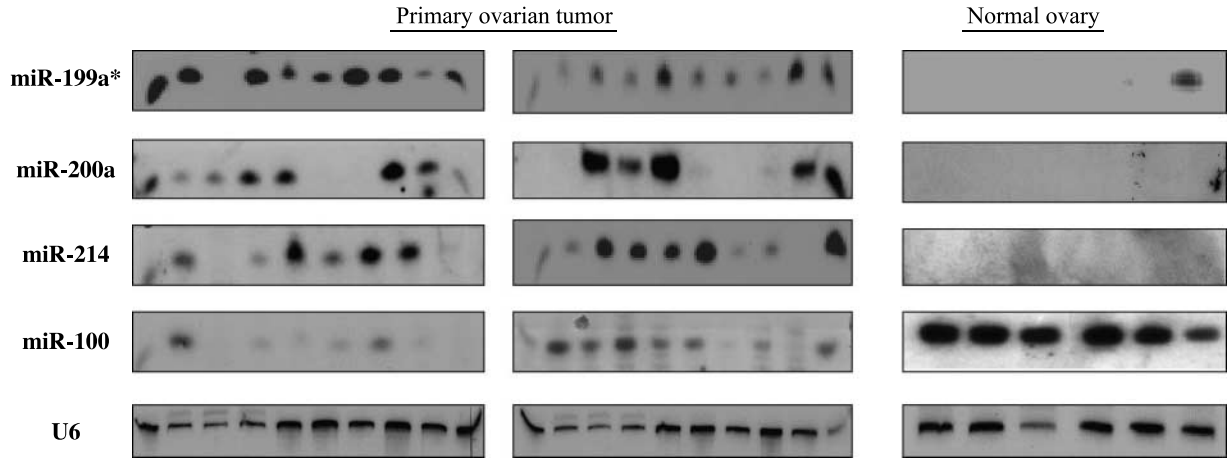


**B**

| | Relative expression level | | Fold Change |
|---|---|---|---|
| | Normal | Tumor | (Tumor : normal) |
| miR-493-5p | 261.99 | 177.17 | -1.48 |
| miR-494 | 3256.87 | 1639.41 | -1.99 |
| miR-199a* | 108.02 | 729.00 | +6.75 |
| miR-424 | 49.19 | 200.86 | +4.08 |
| miR-302d | 38.27 | 171.88 | +4.49 |
| miR-320 | 81.87 | 228.32 | +2.79 |
| miR-214 | 180.62 | 1558.75 | +8.63 |
| miR-200a | 116.94 | 959.91 | +5.75 |
| miR-125b | 9997.24 | 1104.53 | -5.05 |
| miR-100 | 1469.68 | 156.85 | -9.37 |
| miR-let-7a | 10316.96 | 3093.66 | -3.33 |
| miR-let-7c | 8247.15 | 1161.16 | -7.10 |
| miR-let-7b | 5252.75 | 692.60 | -7.58 |
| miR-29a | 340.85 | 450.03 | +1.32 |

**Figure 1.** miRNA expression profile and frequent deregulation of miR-199*, miR-200a, miR-214, and miR-100 in human primary ovarian cancer. *A,* Northern blot analysis. Total RNA (20 μg) from human primary ovarian tumors and normal ovary tissue was separated on a denaturing 15% polyacrylamide gel and transferred to a GeneScreen Plus membrane. The blot was hybridized with indicated probes. *B,* list of deregulated miRNAs at >1-fold in human ovarian cancer versus normal ovary.

RT-PCR analyses revealed that PTEN protein but not mRNA was considerably decreased in *miR-214*–transfected HIOSE-80 cells (Fig. 2*B*). In contrast, knockdown of *miR-214* by 2′-*O*-me *miR-214* in A2780CP cells, which express high levels of endogenous *miR-214* (Fig. 3*A*), increased the protein level of PTEN (Fig. 2*B*). Further, the phosphorylation levels of Akt, a major target of PTEN (20), and Akt substrates glycogen synthase kinase 3β and p70S6K were elevated by ectopic expression of *miR-214* and decreased by knockdown of *miR-214* (Fig. 2*B*), suggesting that *miR-214* targets the PTEN/Akt pathway.

To further show that PTEN is negatively regulated by *miR-214*, we constructed luciferase reporters with wild-type (pGL3-PTEN-3′-UTR) and mutated (pGL3-PTENmut-3′-UTR) 3′-UTR of PTEN (Fig. 2*A*). Both the wild-type and the mutant reporters were introduced into A2780CP (*miR-214* positive) and HIOSE-80 (*miR-214* negative) cells, respectively. Luciferase activity of the wild-type, but not mutant, PTEN-3′-UTR reporter was significantly suppressed in *miR-214*–positive A2780CP cells but not in *miR-214*–negative HOSE-80 cells. Moreover, ectopic expression of *miR-214* in HIOSE-80 cells inhibited the wild-type but not the mutated reporter activity (Fig. 2*C*).

Having observed that *miR-214* negatively regulates PTEN in cell culture system, we asked if this regulation is seen *in vivo*. Inverse correlation of expression of PTEN and *miR-214* was investigated in

**Table 1.** Alterations of miRNA and tumor histopathology

| Histology | No. | miR-199a* | | miR-214 | | miR-200a | | miR-100 | |
|---|---|---|---|---|---|---|---|---|---|
| | | Low/no | High* | Low/no | High | Low/no | High | Normal | Down |
| Serous cystadenocarcinoma | 14 | 5 | 9 | 4 | 10 | 8 | 6 | 6 | 8 |
| Mucinous cystadenocarcinoma | 6 | 2 | 4 | 2 | 4 | 3 | 3 | 1 | 5 |
| Endometrioid carcinoma | 5 | 3 | 2 | 3 | 2 | 3 | 2 | 0 | 5 |
| Granulosa cell tumor | 1 | 1 | 0 | 0 | 1 | 1 | 0 | 0 | 1 |
| Clear cell cystadenocarcinoma | 3 | 2 | 1 | 3 | 0 | 2 | 1 | 0 | 3 |
| Mixed tumor | 1 | 1 | 0 | 1 | 0 | 0 | 1 | 0 | 1 |
| Normal ovary | 10 | 10 | 0 | 10 | 0 | 10 | 0 | 10 | 0 |

*Intensity of signal is ≥2-fold compared with that of normal ovary and/or HIOSE cells.

primary ovarian tumor specimens. Of the 30 primary ovarian tumors examined, 13 exhibited down-regulation of PTEN and 17 had overexpression of *miR-214* (Table 1). Among 17 tumors with elevated *miR-214*, 11 (65%) had decreased PTEN levels ($P < 0.0001$; Fig. 2*D*). These data further support the findings that the *PTEN* is a direct target of *miR-214*.

***miR-214* is an antiapoptotic factor that is associated with cisplatin resistance.** Because Akt is a major cell survival pathway and its activation plays a key role in multiple drug resistance, including cisplatin (20, 21), we next examined the effects of *miR-214* on cell survival and cisplatin resistance. Figure 3*A* shows that expression levels of *miR-214* are low in immortalized human surface epithelial cell lines HIOSE-80 and MCC-3 as well as A2780S and OV119 cells compared with other ovarian cancer cell lines examined. Because A2780S and OV119 cells are sensitive to cisplatin (22), we ectopically expressed *miR-214* in these two cell lines and examined if expression of miR-214 renders the cells resistant to cisplatin-induced cell death. Following the transfection of pcDNA3.1/V5-His-Topo-*miR-214* and G418 selection, stable pool cells were obtained and the expression of *miR-214* was confirmed by qRT-PCR (Fig. 3*B*). The cells transfected with *miR-214* and pcDNA3.1/V5-His-Topo vector were treated with cisplatin or vehicle DMSO. As shown in Fig. 3*C* and *D*, the expression of *miR-214* confers the cells resistant to cisplatin-induced cell death, suggesting that *miR-214* is an antiapoptotic factor.

Having shown an elevated level of *miR-214* in cisplatin-resistant A2780CP cells (Fig. 3*A*), we next examined if knockdown of *miR-214* is able to override cisplatin resistance. A2780CP cells were transfected with 2′-*O*-me-anti-*miR-214*. The cells transfected with 2′-*O*-me-scrambled miR were used as control. Following 72 h of transfection, qRT-PCR analysis showed that level of *miR-214* was significantly decreased in the cells treated with 2′-*O*-me-anti-*miR-214* (Fig. 4*A*). Further, the cells were treated with cisplatin or vehicle DMSO. Cell viability analysis revealed that knockdown of *miR-214* alone reduced cell survival ~20% in A2780CP cells. Moreover, blocking *miR-214* expression considerably sensitized A2780CP cells to cisplatin-induced apoptosis (Fig. 4*B* and *C*). Taken collectively, these data indicate that *miR-214* could play an important role in cisplatin resistance.

**Akt inhibitor, API-2/triciribine/TCN, or introduction of PTEN cDNA lacking 3′-UTR reduces cell survival and CDDP resistance induced by *miR-214*.** Because ectopic expression of *miR-214* reduces PTEN expression leading to activation of Akt pathway (Fig. 2*B* and *C*) and inhibition of the cisplatin-induced cell death (Fig. 3*C* and *D*), we next reasoned that inhibition of Akt should override *miR-214*–induced cell survival and cisplatin resistance. We have previously identified a specific Akt inhibitor, API-2/triciribine, which is currently in clinical trial (17). To test this hypothesis, *miR-214*–transfected A2780S cells were treated with API-2/triciribine, in combination with or without cisplatin. The cells transfected with Topo vector were used as control. As shown in Fig. 5*A*, API-2 abrogated *miR-214*–activated Akt and significantly inhibited *miR-214*–induced cell survival and cisplatin resistance.

It has been documented that miRNAs negatively regulate the expression of their targets primarily through base-pairing interactions in the mRNA 3′-UTR, leading to mRNA degradation or translational

**Table 2.** miRNA expression level and tumor grade and clinical stage

| | | No. | miR-199a* | | | miR-214 | | | miR-200a | | | miR-100 | | |
|---|---|---|---|---|---|---|---|---|---|---|---|---|---|---|
| | | | Low/no | High | *P** | Low/no | High | *P* | Low/no | High | *P* | Normal | Down | *P* |
| Grade | 1-2 | 13 | 10 | 3 | 0.004 | 9 | 4 | 0.012 | 10 | 3 | 0.01 | 4 | 9 | 0.39 |
| | 3 | 17 | 4 | 13 | | 4 | 13 | | 5 | 12 | | 3 | 14 | |
| Stage | I-II | 12 | 9 | 3 | 0.011 | 7 | 5 | 0.087 | 9 | 3 | 0.049 | 4 | 8 | 0.15 |
| | III-IV | 18 | 5 | 13 | | 6 | 12 | | 8 | 10 | | 3 | 15 | |

*Statistical analysis was done using two-sample *t* test and *P* value was calculated based on two-tailed test.

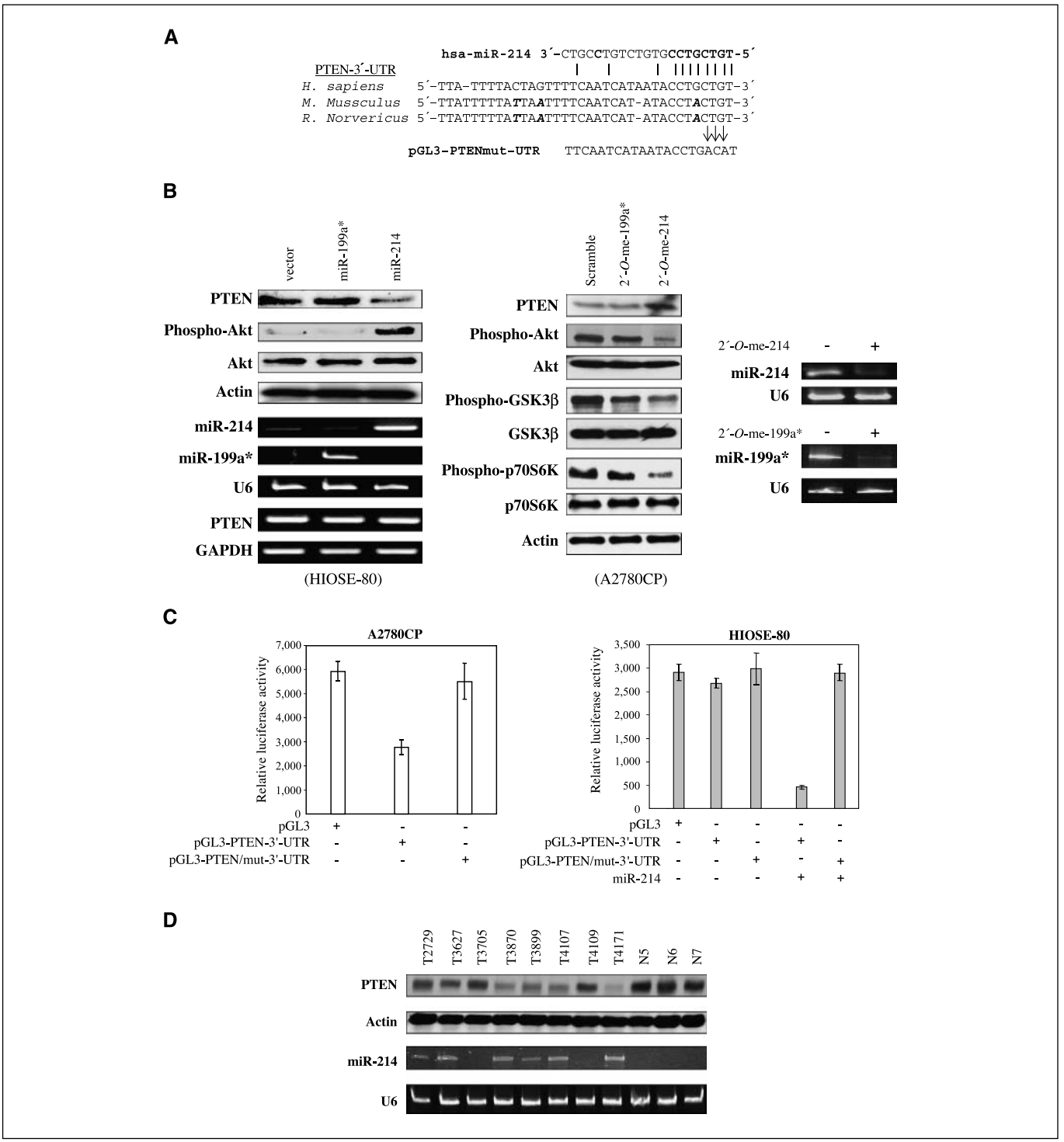


**Figure 2.** *miR-214* negatively regulates PTEN through binding to 3′-UTR of the *PTEN. A,* sequence alignment of human *miR-214* with 3′-UTR of *PTEN*. The seed sequence of *miR-214* (*top*) matches 3′-UTR of *PTEN* (*middle*). *Bottom,* mutations of the 3′-UTR of *PTEN* for creating the mutant luciferase reporter construct. *B, rows 1* to *4, miR-214* reduces PTEN protein but not mRNA levels. HIOSE-80 cells (*left*) were transfected with pcDNA3.1/V5-His-Topo-*miR-214*, pcDNA3.1/V5-His-Topo-*miR199a**, and vector alone and immunoblotted with indicated antibodies; *rows 5* and *6,* the expression of *miR-214* and *miR-199a** was determined by qRT-PCR; *row 8,* PTEN mRNA level was measured by RT-PCR. U6 (*row 7*) and glyceraldehyde-3-phosphate dehydrogenase (*GAPDH*; *row 9*) were used for controls. *Middle* and *right,* knockdown of *miR-214* inducing PTEN expression. A2780CP cells were transfected with antisense 2′-*O*-me oligonucleotide targeting *miR-214* at concentration of 150 pmol/L/well (6-well plate) with Lipofectamine 2000. Anti-*miR199a** and scramble 2′-*O*-me oligonucleotide were used as controls. *Middle,* after incubation of 72 h, cells were lysed and immunoblotted with indicated antibodies; *right,* inhibition of *miR-214* and *miR-199a** expression by 2′-*O*-me oligonucleotide in A2780CP cells was shown by qRT-PCR. *GSK3β,* glycogen synthase kinase 3β. *C, miR-214* inhibits wild-type but not mutated PTEN-3′-UTR reporter activity. *miR-214*–positive A2780CP cells (*left*) and *miR-214*–negative HIOSE-80 cells (*right*) were transiently transfected with indicated plasmids. Following 36 h of incubation, cells were subjected to luciferase assay. *Columns,* mean of three independent experiments; *bars,* SD. *D, rows 1* and *2,* representative tumor and normal tissue lysates were analyzed by Western blot with indicated antibodies; *row 3,* expression of *miR-214* was analyzed by qRT-PCR; *row 4,* U6 was used as a control.

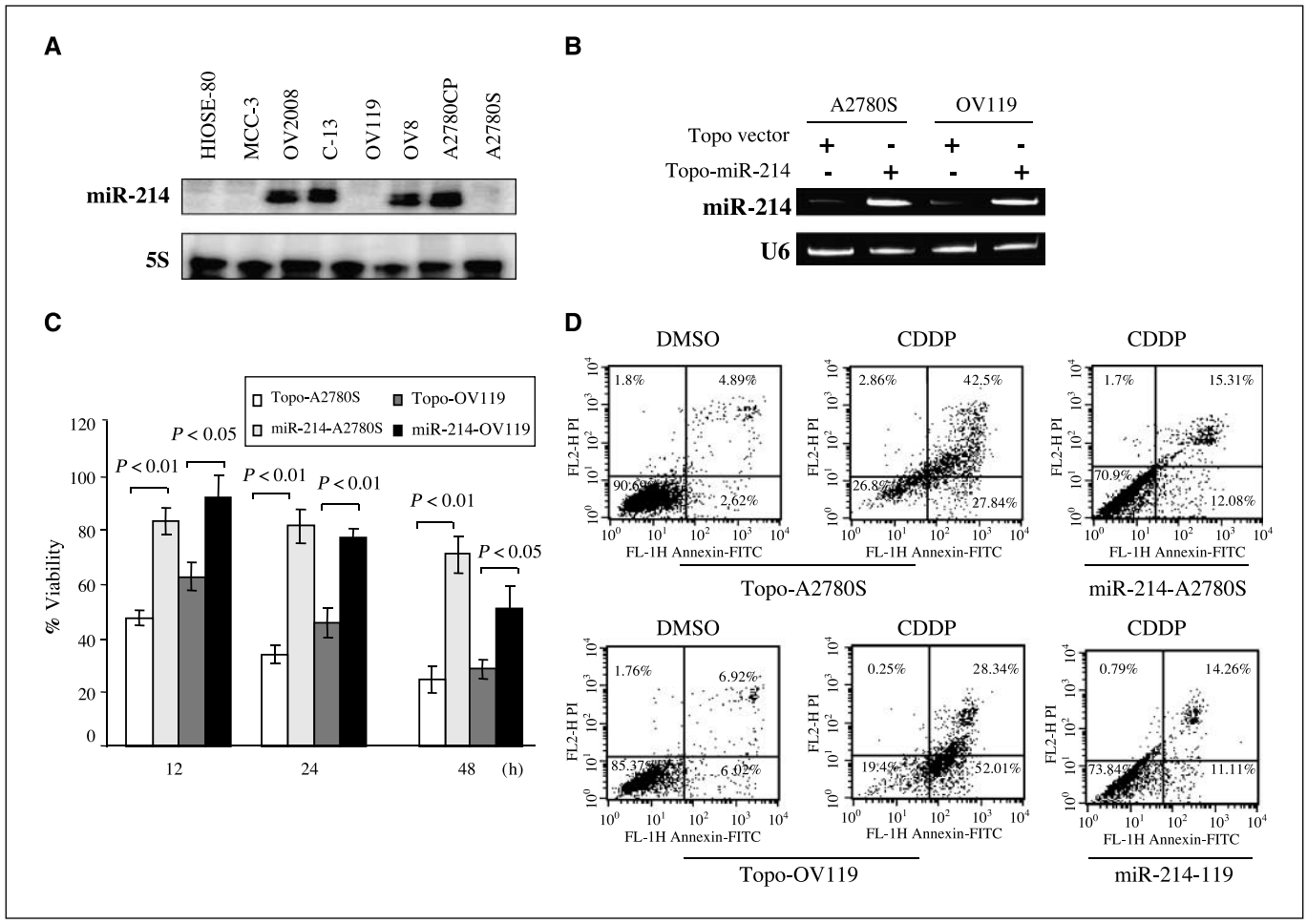


**Figure 3.** Ectopic expression of *miR-214* induces ovarian cancer cells resistant to cisplatin-induced apoptosis. *A, top,* RNase protection analysis of *miR-214* expression in ovarian cancer cell lines and immortalized human ovarian surface epithelial cells; *bottom,* 5S was used as control. *B,* ectopic expression of *miR-214*. A2780S and OV119 cells, which express low levels of endogenous *miR-214*, were transfected with pcDNA3.1/V5-His-Topo-*miR-214* or vector alone. Following G418 selection, cells were subjected to qRT-PCR analysis for expression of *miR-214* (*top*) and U6 (*bottom*). *C* and *D,* expression of *miR-214* renders A2780S and OV119 cells resistant to cisplatin. The vector (Topo)-transfected and *miR-214*–transfected cells were treated with cisplatin or DMSO for different time points. *C,* cell viability was detected by MTT assay. *D,* after 48 h of the treatment, cells were labeled with Annexin V and analyzed by flow cytometry.

inhibition, which depends on whether it is partially matched or completely matched with the target genes. Because *miR-214* down-regulates PTEN through binding to 3′-UTR of *PTEN* mRNA (Fig. 2), ectopic expression of PTEN by transfection of the cDNA that only contains the coding region of *PTEN* should escape the regulation by *miR-214* and thus attenuate or decrease *miR-214* function. To this end, pcDNA-*PTEN* lacking 3′-UTR was introduced into *miR-214*–transfected A2780S cells and then treated with or without cisplatin for 24 h. As shown in Fig. 5*B*, expression of PTEN decreased Akt activation induced by *miR-214* and sensitized the *miR-214*-A2780S cells to cisplatin-induced apoptosis. These results further indicate that the PTEN/Akt pathway is a major target of *miR-214* and largely mediates *miR-214* antiapoptotic function.

Although adjuvant chemotherapy with cisplatin achieves clinical response in ~80% of patients, the tumor recurs in most patients within 3 years following treatment due to the development of chemoresistance (23). Having shown that *miR-214* is involved in cisplatin resistance in ovarian cancer cell lines, we next examined if *miR-214* is involved in cisplatin resistance in patients with ovarian cancer (e.g., more frequent overexpression in chemoresistant/recurrent tumors than in sensitive/primary lesions). Among 30 primary ovarian tumors examined, 11 patients with recurrent (chemoresistant) ovarian cancer were readmitted at H. Lee Moffitt Cancer Center. miRNA LNA *in situ* hybridization (LNA-ISH) analysis revealed that *miR-214* levels were low or undetectable in eight primary tumors but elevated in their recurrent lesions (Fig. 5*C*; data not shown). The remaining tumors expressed high level of *miR-214* in both primary and recurrent tumors. These data further suggest that *miR-214* plays an important role in chemoresistance.

## Discussion

Profiles of miRNA have been reported in different types of human malignancy (3–12). Thus far, there is a miRNA DNA copy number study of human ovarian cancer in combination with breast cancer and melanoma using high-resolution array-based comparative genomic hybridization. In this study, a high proportion of genomic loci containing miRNA genes exhibited DNA copy number alterations in ovarian and breast cancers and melanoma (5). In the present report, we performed miRNA expression profiling in normal HIOSE and epithelial ovarian carcinomas and showed that up-regulation of *miR-214, miR-199a**, and *miR-200a* and

down-regulation of *miR-100* are recurrent events and that alterations of the first three miRNAs seem to be associated with late-stage and high-grade ovarian tumors (Table 2). This finding suggests that deregulation of *miR-214, miR-199a**, and *miR-200a* could contribute to ovarian tumor progression rather than initiation.

Although members of the *let-7* family, *miR-21, miR-145, miR-221*, and *miR-155*, are often deregulated in several cancers, including carcinomas of breast, lung, and colon (24), there are miRNAs deregulated in specific neoplasms. For example, *miR-122a*, a liver-specific miRNA, is down-regulated in hepatocellular carcinoma (25); *miR-204* and *miR-211* are up-regulated in insulinomas (26). Accumulated evidence shows that miRNA expression signatures correlate well with specific clinical cancer characteristics and can be used to classify normal and cancerous tissues as well as subtype

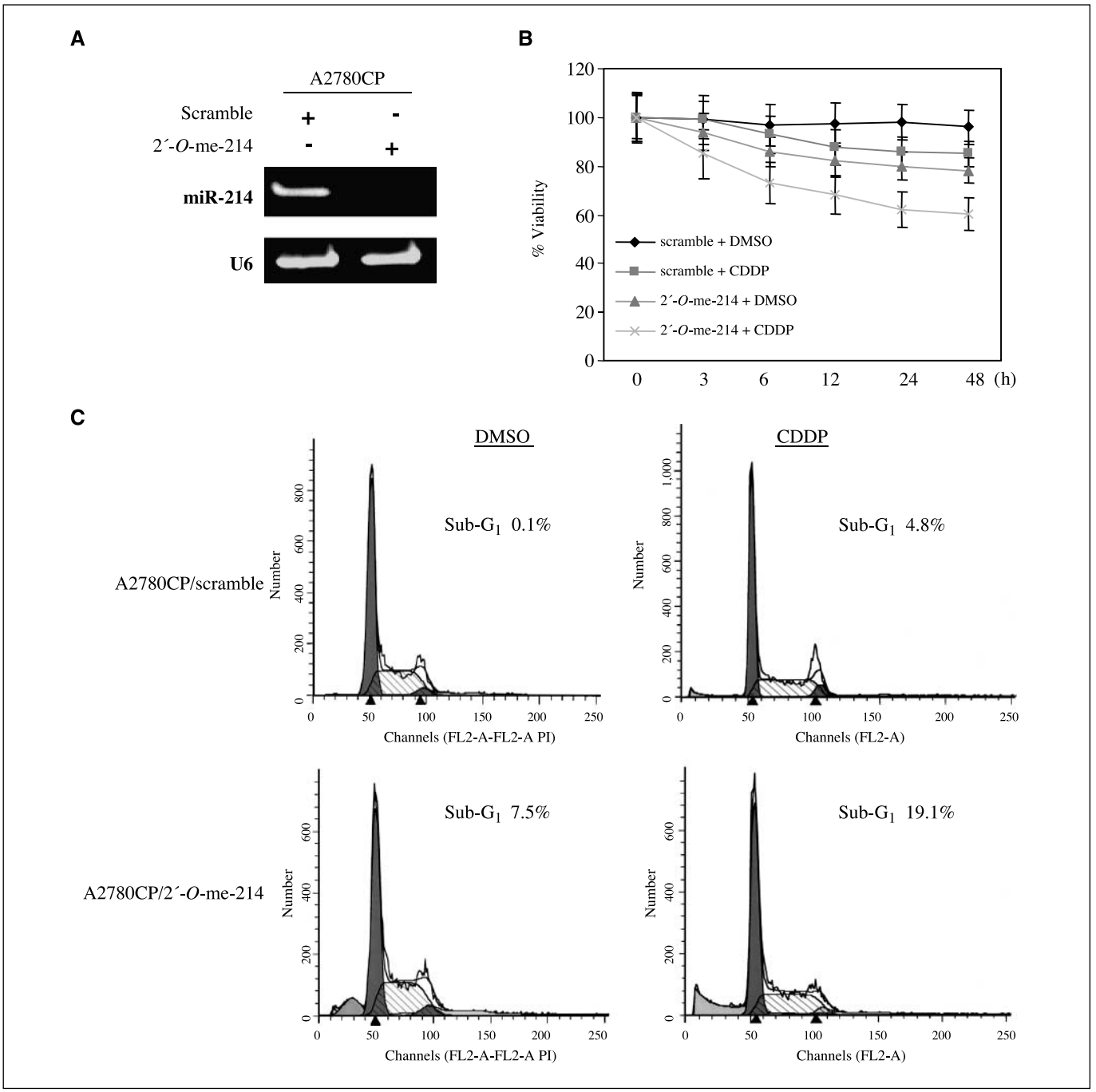


**Figure 4.** Knockdown of *miR-214* sensitizes A2780CP cells to cisplatin. *A,* A2780CP, a cisplatin-resistant cell line and expressing elevated levels of endogenous *miR-214*, was transfected with 2′-*O*-me-anti-miR-214 or scramble 2′-*O*-me oligonucleotides and assayed with qRT-PCR with primers of *miR-214* (*top*) and U6 (*bottom*). *B,* MTT assay. The 2′-*O*-me-anti-miR-214–transfected or scramble 2′-*O*-me–transfected A2780CP cells were treated with 20 μmol/L of cisplatin or DMSO vehicle for the indicated times and examined for cell viability. *C,* flow cytometry. Indicated cells were treated with cisplatin or DMSO for 12 h and the sub-$G_1$ population was identified by flow cytometry.

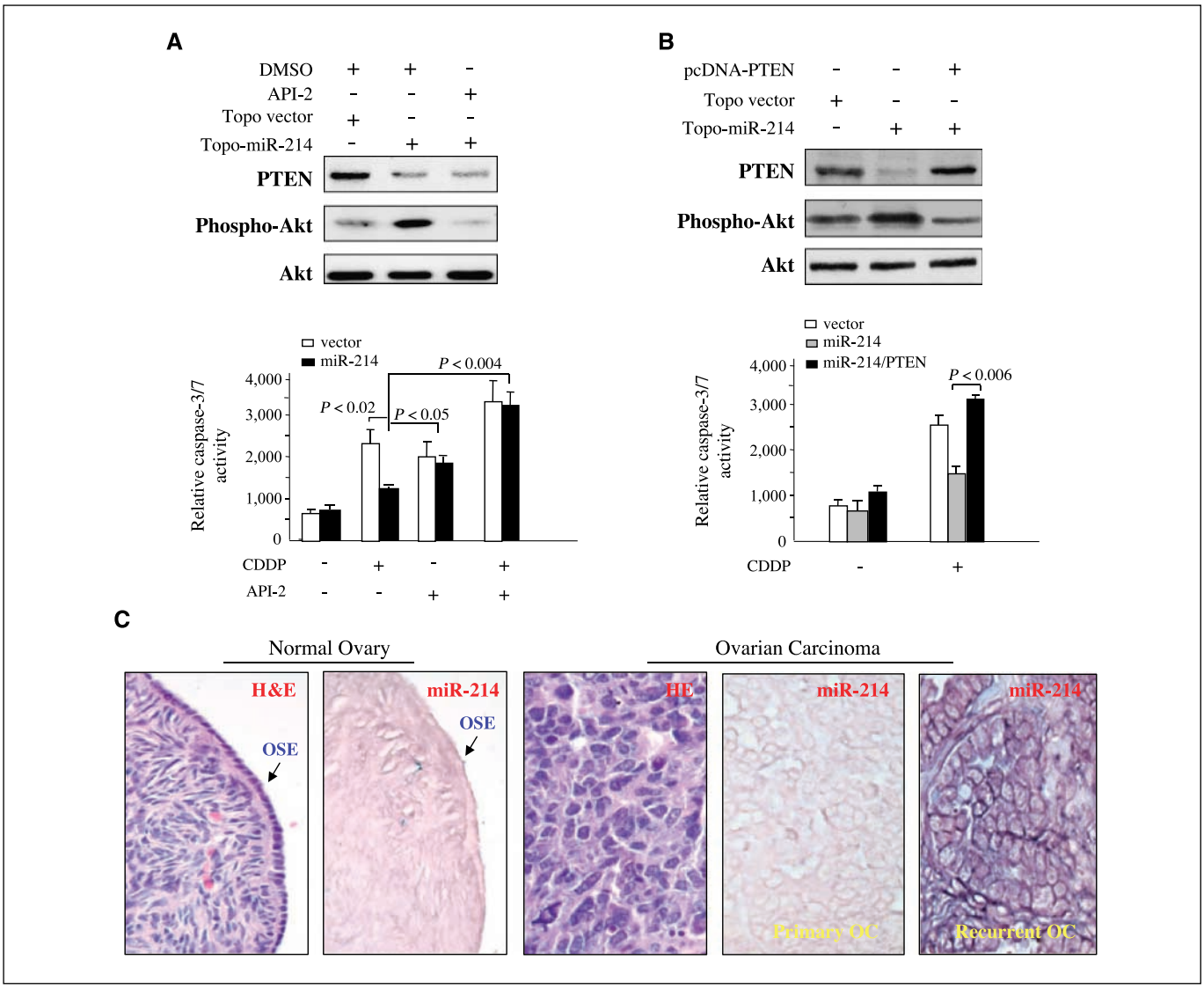


**Figure 5.** Inhibition of Akt or transfection of PTEN cDNA lacking 3′-UTR overrides *miR-214*–induced cell survival. *A,* Topo-*miR-214* and vector stably transfected A2780S cells were treated with Akt inhibitor API-2/triciribine (10 μmol/L) and/or cisplatin (20 μmol/L). The cells treated with DMSO were used as control. After 24 h of treatment, cells were subjected to immunoblotting analysis with indicated antibodies (*top*) and assayed for caspase-3/7 activity (*bottom*). *B, top,* A2780S cells were stably transfected with indicated plasmids and assayed for expression of PTEN, phospho-Akt-S473, and total Akt; *bottom,* after treatment with or without cisplatin for 24 h, cells were examined for caspase-3/7 activity. *C,* LNA-ISH. *miR-214* was labeled with digoxigenin-ddUTP using the Dig-3′-End Labeling kit and hybridized to paraffin sections of normal ovary (*middle left*) as well as a patient with primary and recurrent/cisplatin-resistant ovarian serous carcinoma (*middle right* and *right*). *Left* and *middle,* H&E staining. Unlike normal ovarian surface epithelial cells (*middle left*) and primary tumor (*middle right*), recurrent/cisplatin-resistant tumor (*right*) expresses high level of *miR-214. OC,* ovarian carcinoma.

of malignancy (27–29). Therefore, miRNA signatures might be more effective than mRNA signatures in categorizing, detecting, and predicting the course of human cancers as well as in characterizing developmental origins of tumors (29). Our study showed different expression patterns of miRNAs between ovarian cancer and normal HIOSE cells. Whereas deregulation of *let-7, miR-100, miR-214, miR-200a*, and *miR-125* has been detected in other tumors, alterations of other miRNAs, including *miR-424* and *miR-494*, were to the best of our knowledge only observed in ovarian cancer. Further investigation is required for evaluating these miRNAs as specific markers in ovarian tumors.

Previous studies have shown that miRNA could serve as "oncogene" or "tumor suppressor gene" and regulate different cellular processes by targeting hundreds of genes. We showed that *miR-214* is highly expressed in the cisplatin-resistant A2780CP cell line compared with its corresponding cisplatin-sensitive cell line A2780S. Knockdown of *miR-214* overrides cisplatin resistance in A2780CP cells, whereas ectopic expression of *miR-214* renders A2780S and OV119 cells resistant to cisplatin-induced apoptosis. It has been well documented that constitutive activation of Akt contributes to chemoresistance in different types of tumors, including ovarian carcinoma (20). *miR-214* blocks PTEN translation leading to activation of the Akt pathway (Fig. 2). These indicate that miR-214 plays an important role in cisplatin resistance by targeting PTEN/Akt pathway. Although alterations of several oncogenes (e.g., Ras, Src, and Bcl2) and tumor suppressor genes (e.g., p53, RB, and p16) are closely associated with chemoresistance, the involvement of miRNA in this process has not been

documented. Thus, our study provided direct evidence that miRNA is of critical importance in chemoresistance of human ovarian cancer.

Mutation of *PTEN* has been detected only in endometrioid ovarian cancer (30). However, down-regulation of PTEN protein is frequently detected in serous and mucinous epithelial ovarian tumors (31). The mechanism of down-regulation of PTEN was thought to be promoter hypermethylation. However, the demethylation agent 5-aza-2′-deoxycytidine failed to restore PTEN protein expression, suggesting that PTEN is highly regulated at the translational level and that methylation of the *PTEN* gene plays a subordinate role in ovarian cancer (32). In the present study, we showed that PTEN is negatively regulated by *miR-214* at the protein level and that down-regulation of PTEN largely correlates with elevated levels of *miR-214* in ovarian cancer (Fig. 2*D*). Therefore, these data indicate that *miR-214* could be a causal factor of the down-regulation of PTEN in human ovarian cancer.

In summary, our study suggests that deregulation of *miR-214, miR-199a*, miR-200a*, and *miR-100* is a frequent event in ovarian cancer. Alteration of *miR-214, miR-199a**, and *miR-200a* seems to be associated with tumor progression. Further, *miR-214* induces cell survival and cisplatin resistance by targeting the PTEN/Akt pathway. Therefore, these miRNAs could play an important role in the pathogenesis of this malignancy and are potential targets for ovarian cancer intervention. Further investigations are required for characterization of miRNAs as prognostic and/or diagnostic markers in ovarian cancers by examining a large series of specimens as well as their *in vivo* role in ovarian tumor development by creating transgenic and/or knockout mice.

## Acknowledgments

Received 7/9/2007; revised 9/13/2007; accepted 11/8/2007.

**Grant support:** NIH and Department of Defense.

The costs of publication of this article were defrayed in part by the payment of page charges. This article must therefore be hereby marked *advertisement* in accordance with 18 U.S.C. Section 1734 solely to indicate this fact.

We thank the Tissue Procurement, DNA Sequence and Flow Cytometry Core Facilities at H. Lee Moffitt Cancer Center for providing cancer specimens, sequencing, and cell cycle analysis.

## References

**1.** Lagos-Quintana M, Rauhut R, Lendeckel W, Tuschl T. Identification of novel genes coding for small expressed RNAs. Science 2001;294:853–8.

**2.** Bartel DP. MicroRNAs: genomics, biogenesis, mechanism, and function. Cell 2004;116:281–97.

**3.** Calin GA, Dumitru CD, Shimizu M, et al. Frequent deletions and down-regulation of micro-RNA genes miR15 and miR16 at 13q14 in chronic lymphocytic leukemia. Proc Natl Acad Sci U S A 2002;99:15524–9.

**4.** Iorio MV, Ferracin M, Liu CG, et al. MicroRNA gene expression deregulation in human breast cancer. Cancer Res 2005;65:7065–70.

**5.** Zhang L, Huang J, Yang N, et al. microRNAs exhibit high frequency genomic alterations in human cancer. Proc Natl Acad Sci U S A 2006;103:9136–41.

**6.** Lu J, Getz G, Miska EA, et al. MicroRNA expression profiles classify human cancers. Nature 2005;435:834–8.

**7.** Chan JA, Krichevsky AM, Kosik KS. MicroRNA-21 is an antiapoptotic factor in human glioblastoma cells. Cancer Res 2005;65:6029–33.

**8.** Takamizawa J, Konishi H, Yanagisawa K, et al. Reduced expression of the let-7 microRNAs in human lung cancers in association with shortened postoperative survival. Cancer Res 2004;64:3753–6.

**9.** He H, Jazdzewski K, Li W, et al. The role of microRNA genes in papillary thyroid carcinoma. Proc Natl Acad Sci U S A 2005;102:19075–80.

**10.** Volinia S, Calin GA, Liu CG. A microRNA expression signature of human solid tumors defines cancer gene targets. Proc Natl Acad Sci U S A 2006; 103:2257–61.

**11.** Lee EJ, Gusev Y, Jiang J, et al. Expression profiling identifies microRNA signature in pancreatic cancer. Int J Cancer 2007;120:1046–54.

**12.** Gaur A, Jewell DA, Liang Y, et al. Characterization of microRNA expression levels and their biological correlates in human cancer cell lines. Cancer Res 2007;67: 2456–68.

**13.** Johnson SM, Grosshans H, Shingara J, et al. RAS is regulated by the let-7 microRNA family. Cell 2005;120: 635–47.

**14.** Metzler M, Wilda M, Busch K, Viehmann S, Borkhardt A. High expression of precursor microRNA-155/BIC RNA in children with Burkitt lymphoma. Genes Chromosomes Cancer 2004;39:167–9.

**15.** Eis PS, Tam W, Sun L, et al. Accumulation of miR-155 and BIC RNA in human B cell lymphomas. Proc Natl Acad Sci U S A 2005;102:3627–32.

**16.** Yang H, Ou CC, Feldman RI, Nicosia SV, Kruk PA, Cheng JQ. Aurora-A kinase regulates telomerase activity through c-Myc in human ovarian and breast epithelial cells. Cancer Res 2004;64:463–7.

**17.** Yang L, Dan HC, Sun M, et al. Akt/protein kinase B signaling inhibitor-2, a selective small molecule inhibitor of Akt signaling with antitumor activity in cancer cells overexpressing Akt. Cancer Res 2004;64:4394–9.

**18.** Yuan ZQ, Feldman RI, Sussman GE, Coppola D, Nicosia SV, Cheng JQ. AKT2 inhibition of cisplatin-induced JNK/p38 and Bax activation by phosphorylation of ASK1: implication of AKT2 in chemoresistance. J Biol Chem 2003;278:23432–40.

**19.** Flynt AS, Li N, Thatcher EJ, Solnica-Krezel L, Patton JG. Zebrafish miR-214 modulates Hedgehog signaling to specify muscle cell fate. Nat Genet 2007;39:259–63.

**20.** Testa JR, Bellacosa A. AKT plays a central role in tumorigenesis. Proc Natl Acad Sci U S A 2001;98: 10983–5.

**21.** Altomare DA, Wang HQ, Skele KL, et al. AKT and mTOR phosphorylation is frequently detected in ovarian cancer and can be targeted to disrupt ovarian tumor cell growth. Oncogene 2004;23:5853–7.

**22.** Yan X, Fraser M, Qiu Q, Tsang BK. Over-expression of PTEN sensitizes human ovarian cancer cells to cisplatin-induced apoptosis in a p53-dependent manner. Gynecol Oncol 2006;102:348–55.

**23.** Aghajanian C. Clinical update: novel targets in gynecologic malignancies. Semin Oncol 2004;31:22–6.

**24.** Negrini M, Ferracin M, Sabbioni S, Croce CM. MicroRNAs in human cancer: from research to therapy. J Cell Sci 2007;120:1833–40.

**25.** Kutay H, Bai S, Datta J, et al. Downregulation of miR-122 in the rodent and human hepatocellular carcinomas. J Cell Biochem 2006;99:671–8.

**26.** Roldo C, Missiaglia E, Hagan JP, et al. MicroRNA expression abnormalities in pancreatic endocrine and acinar tumors are associated with distinctive pathologic features and clinical behavior. J Clin Oncol 2006;24: 4677–84.

**27.** Cummins JM, Velculescu VE. Implications of micro-RNA profiling for cancer diagnosis. Oncogene 2006;25: 6220–7.

**28.** Dalmay T, Edwards DR. MicroRNAs and the hallmarks of cancer. Oncogene 2006;25:6170–5.

**29.** Tricoli JV, Jacobson JW. MicroRNA: potential for cancer detection, diagnosis, and prognosis. Cancer Res 2007;67:4553–5.

**30.** Obata K, Morland SJ, Watson RH, et al. Frequent PTEN/MMAC mutations in endometrioid but not serous or mucinous epithelial ovarian tumors. Cancer Res 1998;58:2095–7.

**31.** Kurose K, Zhou XP, Araki T, Cannistra SA, Maher ER, Eng C. Frequent loss of PTEN expression is linked to elevated phosphorylated Akt levels, but not associated with p27 and cyclin D1 expression, in primary epithelial ovarian carcinomas. Am J Pathol 2001;158:2097–106.

**32.** Schondorf T, Ebert MP, Hoffmann J, et al. Hypermethylation of the PTEN gene in ovarian cancer cell lines. Cancer Lett 2004;207:215–20.

## Correction: miRNA Profiling in Ovarian Cancer and *miR-214* Targets PTEN

In the article on miRNA profiling in ovarian cancer and *miR-214* targets PTEN in the January 15, 2008 issue of *Cancer Research* (1), the first sentence of the section "Target *in vitro* reporter assay" on page 426 should read as follows: For luciferase reporter experiments, the 3′-UTR segments of PTEN predicted to interact with *miR-214* were amplified by PCR from human genomic DNA and inserted into the *Mlu*I and *Hin*dIII sites of pMIR-Reporter (Ambion) immediately downstream from the stop codon of luciferase.

**1.** Yang H, Kong W, He L, Zhao J-J, O'Donnell JD, Wang J, Wenham RM, Coppola D, Kruk PA, Nicosia SV, Cheng JQ. MicroRNA expression profiling in human ovarian cancer: *miR-214* induces cell survival and cisplatin resistance by targeting *PTEN*. Cancer Res 2008;68:425–33.


doi:10.1158/0008-5472.CAN-68-5-COR4

# Genomic and epigenetic alterations deregulate microRNA expression in human epithelial ovarian cancer

Lin Zhang[a,b,c], Stefano Volinia[d], Tomas Bonome[e], George Adrian Calin[d], Joel Greshock[f,g], Nuo Yang[a], Chang-Gong Liu[d], Antonis Giannakakis[a,h], Pangiotis Alexiou[i], Kosei Hasegawa[a], Cameron N. Johnstone[j], Molly S. Megraw[k], Sarah Adams[a,b], Heini Lassus[l], Jia Huang[f], Sippy Kaur[l], Shun Liang[a], Praveen Sethupathy[k], Arto Leminen[l], Victor A. Simossis[i], Raphael Sandaltzopoulos[h], Yoshio Naomoto[m], Dionyssios Katsaros[n], Phyllis A. Gimotty[o], Angela DeMichele[j], Qihong Huang[p], Ralf Bützow[l], Anil K. Rustgi[j], Barbara L. Weber[f,g], Michael J. Birrer[e], Artemis G. Hatzigeorgiou[c,f,i,k], Carlo M. Croce[c,d], and George Coukos[a,b,c,f]

[a]Center for Research on Early Detection and Cure of Ovarian Cancer and Gynecology, [f]Abramson Family Cancer Research Institute, and Departments of [b]Obstetrics, [j]Medicine, [k]Genetics, and [o]Biostatistics and Epidemiology, University of Pennsylvania, Philadelphia, PA 19104; [d]Departments of Molecular Virology, Immunology, and Medical Genetics, Ohio State University, Columbus, OH 43210; [e]Cell and Cancer Biology Branch, National Cancer Institute, National Institutes of Health, Bethesda, MD 20814; [h]Laboratory of Gene Expression, Modern Diagnostic and Therapeutic Methods, Democritus University of Thrace, 68100 Alexandroupolis, Greece; [i]Institute of Molecular Oncology, Biomedical Sciences Research Center ''Alexander Fleming'', 166 72 Varkiza, Greece; [l]Department of Obstetrics and Gynecology, University of Helsinki, 00290, Helsinki, Finland; [m]Department of Surgical Oncology, Okayama University, Okayama 700-8530, Japan; [n]Department of Obstetrics and Gynecology, University of Turin, 10124 Turin, Italy; and [p]The Wistar Institute, 3601 Spruce Street, Philadelphia, PA 19104

Contributed by Carlo M. Croce, February 20, 2008 (sent for review December 15, 2007)

**MicroRNAs (miRNAs) are an abundant class of small noncoding RNAs that function as negative gene regulators. miRNA deregulation is involved in the initiation and progression of human cancer; however, the underlying mechanism and its contributions to genome-wide transcriptional changes in cancer are still largely unknown. We studied miRNA deregulation in human epithelial ovarian cancer by integrative genomic approach, including miRNA microarray ($n = 106$), array-based comparative genomic hybridization ($n = 109$), cDNA microarray ($n = 76$), and tissue array ($n = 504$). miRNA expression is markedly down-regulated in malignant transformation and tumor progression. Genomic copy number loss and epigenetic silencing, respectively, may account for the down-regulation of ≈15% and at least ≈36% of miRNAs in advanced ovarian tumors and miRNA down-regulation contributes to a genome-wide transcriptional deregulation. Last, eight miRNAs located in the chromosome 14 miRNA cluster (*Dlk1-Gtl2* domain) were identified as potential tumor suppressor genes. Therefore, our results suggest that miRNAs may offer new biomarkers and therapeutic targets in epithelial ovarian cancer.**

Dlk1-Gtl2 domain | noncoding RNA

Cancer is a disease involving multistep changes in the genome. Studies on cancer genome have so far focused mainly on protein-coding genes, whereas little is presently known on alterations of functional noncoding sequences in cancer (1, 2). MicroRNAs (miRNAs) are endogenous noncoding small RNAs, which negatively regulate gene expression (3–6). In human cancer, miRNAs might function as either oncogenes (7–11) or tumor suppressor genes (12–15). Increasing evidence shows that expression of miRNAs is deregulated in human cancer (1, 2). High-throughput miRNA quantification technologies have provided powerful tools to study global miRNA profiles. It has become progressively obvious that, although the number of miRNAs (≈600) is much smaller than that of the protein-coding genes (≈22,000), miRNA expression signatures reflect more accurately the developmental lineage or tissue origin of human cancers (16). Large-scale studies in human cancer further demonstrated that miRNA expression signatures are associated with specific tumor subtypes and clinical outcomes (16–22). More than half of the miRNAs have been aligned to genomic fragile sites or regions associated with cancers (23), and our group and others have provided evidence that miRNA genes are involved by copying abnormalities in cancer (7, 12, 24). In addition, recent studies suggest that epigenetic alterations might play a critical role in regulating miRNA expression in human cancers (25). Finally, several key proteins in the miRNA biogenesis pathway may be dysfunctional (26) or deregulated in cancer (27–30), which may enhance tumorigenesis (31). Therefore, DNA copy number abnormalities, epigenetic alterations, and/or defects in the miRNA biogenetic machinery might each contribute to miRNA deregulation in human cancer.

Epithelial ovarian cancer (EOC), the most common ovarian malignancy, continues to be the leading cause of death among gynecological malignancies (24). Here, we used integrative genomic approaches to perform a comprehensive analysis of miRNome alterations associated with malignant transformation of the ovarian surface epithelium and/or ovarian tumor stage progression. Our findings indicate that numerous miRNAs are down-regulated in EOC and that this down-regulation can be attributed to genomic copy number loss or more often to epigenetic silencing. Several important miRNA alterations with putative oncogenic or tumor suppressor function were found, including a miRNA cluster in *Dlk1-Gtl2* domain that may represent an important therapeutic target in cancer.

## Results

**microRNA Expression Profiles Classify Malignant from Nonmalignant Ovarian Surface Epithelium.** Most EOC are believed to originate from the ovarian surface epithelium (OSE). Because the OSE represents only a minimal part of the whole normal ovary, whole ovary may not be a suitable normal tissue control for EOC (32).

Author contributions: S.V., T.B., G.A.C., J.G., N.Y., C.-G.L., A.G., and P.A. contributed equally to this work; L.Z., S.V., G.A.C., B.L.W., M.J.B., A.G.H., C.M.C., and G.C. designed research; T.B., J.G., N.Y., C.-G.L., A.G., P.A., K.H., C.N.J., M.S.M., S.A., H.L., J.H., S.K., S.L., P.S., A.L., V.A.S., and R.S. performed research; J.G., Y.N., D.K., P.A.G., A.D., Q.H., R.B., A.K.R., B.L.W., and A.G.H. contributed new reagents/analytic tools; L.Z., S.V., J.G., A.G.H., and G.C. analyzed data; and L.Z., A.G.H., C.M.C., and G.C. wrote the paper;.

The authors declare no conflict of interest.

[c]To whom correspondence may be addressed. E-mail: linzhang@mail.med.upenn.edu, hatzigeorgiou@fleming.gr, carlo.croce@osumc.edu, or gcks@mail.med.upenn.edu.

[g]Present address: Translational Medicine and Genetics, GlaxoSmithKline, King of Prussia, PA 19406.

This article contains supporting information online at www.pnas.org/cgi/content/full/0801615105/DCSupplemental.

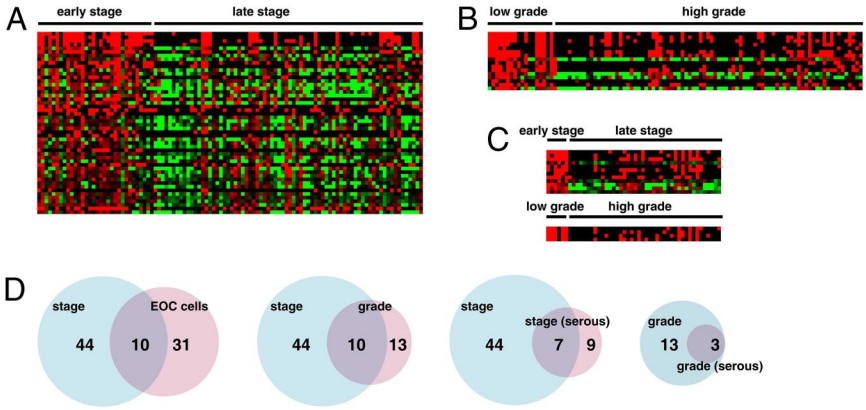


**Fig. 1.** Numerous miRNAs are down-regulated in late-stage or high-grade ovarian cancer. (*A*) Heat map showing the 44 miRNAs significantly down-regulated in late-stage relative to early-stage EOC. (*B*) Heat map showing the 13 miRNAs significantly down-regulated in high-grade relative to low-grade EOC. (*C*) Heat map showing the miRNAs significantly down-regulated in late-stage or high-grade serous EOC. (*D*) Venn diagrams of down-regulated miRNAs in different analyses.

To investigate miRNA alterations associated with OSE malignant transformation, we compared mature miRNA expression profiles in 18 EOC cell lines and four immortalized primary cultured human ovarian surface epithelium (IOSE), using TaqMan miRNA assay. Among 173 miRNAs examined, 160 miRNAs (92.5%) were detected in either IOSEs or EOC cell lines [supporting information (SI) Fig. S1*A*]. Expression of select miRNAs (mir-15a, mir-30d, mir-182, mir-386, and let-7i) was further confirmed by Northern blot. Unsupervised hierarchical clustering or 3D scaling analysis clearly segregated the two groups of cells (Fig. S1 *A* and *B*). There were 35 miRNAs expressed differentially between the EOC and IOSE ($P < 0.05$). Only four (11.4%, 4/35) were up-regulated, whereas most (88.6%, 31/35) were down-regulated in EOC compared with IOSE lines (Fig. S1*C* and Dataset S1), including the tumor suppressor miRNAs *let-7d* (13, 14, 21) and *mir-127* (25). Thus, miRNAs are deregulated in EOC and can distinguish malignant from nonmalignant ovarian epithelium. Importantly, most miRNA alterations associated with ovarian epithelial transformation are consistent with down-regulation.

**miRNA Down-Regulation in Late-Stage and High-Grade Ovarian Cancer.** Next, we sought to identify miRNA alterations associated with ovarian cancer progression *in vivo*. We analyzed 106 primary human ovarian cancer specimens of various stages or grades, using miRNA microarrays. miRNA expression profiles of early-stage (I, $n = 25$; II, $n = 8$) and late-stage (III, $n = 62$; IV, $n = 11$) EOC were compared by significance analysis of microarrays. Expression of forty-four miRNAs were significantly different between early- and late-stage EOC. Interestingly, all miRNA alterations consisted in down-regulation in late-stage tumors. These alterations included three known tumor suppressors, miRNAs, *mir-15a* (12), *mir-34a*, and *mir-34b* (15, 33–37) (Fig. 1*A* and Dataset S2). Ten miRNAs were found to be commonly down-regulated in both late-stage (relative to early tumors) and in EOC cells (relative to IOSE cells) (Fig. 1*D* and Dataset S1 and Dataset S2). In addition, we analyzed miRNA expression differences between the low-grade (0, $n = 4$; 1, $n = 18$) and high-grade (2, $n = 17$; 3, $n = 68$) EOC. Thirteen miRNAs exhibited significant difference and all were down-regulated in high-grade compared with the low-grade EOC (Fig. 1*B* and Dataset S3). Ten of 13 miRNAs were commonly down-regulated with stage or grade advancement (Fig. 1*D*). These results were further validated by stem-loop real-time RT-PCR. From 21 randomly selected miRNAs among the 44 that were down-regulated in late stage, 17 were confirmed to be significantly down-regulated ($P < 0.05$, early stage $n = 30$; late stage $n = 66$) (Fig. S2). Four additional miRNAs were down-regulated in late stage but did not reach statistical significance (Fig. S2). Because the prevalence of histotypes is different among EOC stages (nonserous histotypes prevail among early-stage tumors, whereas serous histotype prevails among late-stage tumors), we tested whether similar miRNA expression differences were detectable in a within-histotype analysis. We analyzed separately serous EOC samples, the most common EOC histotype. Again, we found that miRNA alterations consisted of down-regulation in late-stage or high-grade tumors (Fig. 1*C* and Dataset S4 and Dataset S5). Taking the primary tumor microarray data and cell line TaqMan data together, we conclude that, during ovarian cancer tumorigenesis and progression, numerous miRNAs are down-regulated by as-yet-unknown mechanisms.

**Drosha and Dicer Are Not Deregulated in Ovarian Cancer.** The RNases Drosha and Dicer serve as key regulatory proteins in miRNA biogenesis pathway and their alterations may contribute to widespread miRNA deregulation in cancer (20, 31). Thus, we examined the mRNA expression level of Drosha and Dicer in the same set of EOC samples used for miRNA microarray. There was no significant expression difference in Drosha or Dicer expression between early and late stage EOC (Fig. S3 *A* and *B*). Similar levels of Drosha or Dicer were found also in EOC cell lines and IOSE (Fig. S3 *C* and *D*). Finally, similar levels of Drosha or Dicer were found in different stage EOC tumors in two independent public cDNA microarrays (Oncomine; Fig. S3 *E* and *F*). Next, we analyzed the expression levels of Drosha and Dicer proteins in tissue arrays containing 504 EOC specimens. Immunostaining intensity of these proteins was scored as 1–4, and expression differences between early and late stages were examined by $\chi^2$ test. Consistent with the mRNA expression levels, we did not find any significant difference in the expression of Drosha or Dicer between early- and late-stage tumors (Fig. S3 *G* and *H*). This result agrees with a recent report showing no substantial down-regulation of the miRNA processing machinery in human tumors (16). To further assess the impact of Drosha or Dicer expression on EOC biology, we performed survival analysis using this tissue array. There was no correlation between the expression levels of either protein and the patient survival (Fig. S4). These results indicate that the observed down-regulation of numerous miRNAs in advanced EOC cannot be attributed to alterations in the key RNases of the miRNA biogenesis pathway.

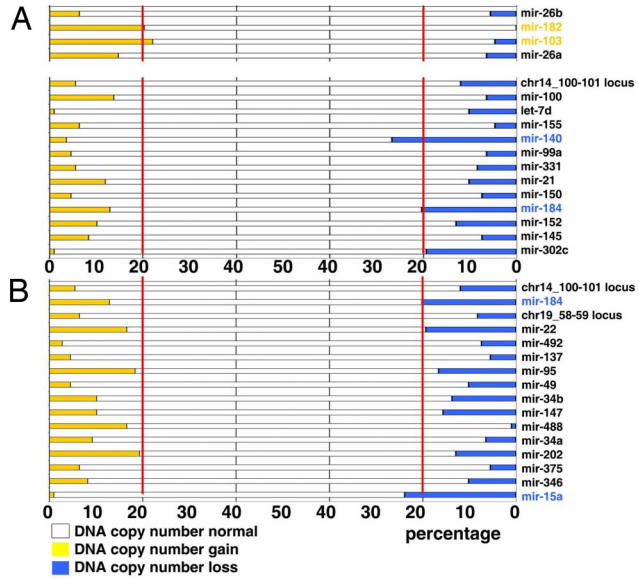


**Fig. 2.** DNA copy number deletions contribute to down-regulation of miRNAs. (*A*) DNA copy number status of 17 genomic loci containing miRNAs differentially expressed between IOSE cells and EOC cell lines. (*Upper*) Four up-regulated miRNAs. (*Lower*) Thirteen down-regulated miRNAs. Red lines indicate the designated cut-off for significant alterations (20%). (*B*) DNA copy number status of 16 genomic loci containing miRNAs significantly down-regulated in late-stage EOC. Red lines indicate the designated cut-off for significant alterations (20%).

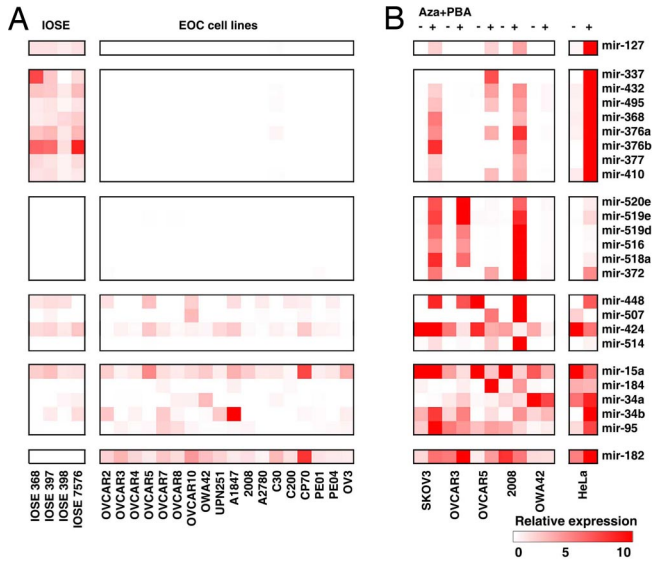


**Fig. 3.** Epigenetic alterations silence miRNA expression in ovarian cancer. (*A*) Heat map depicts expression of 24 miRNAs in IOSE cells and EOC cell lines analyzed by real-time RT-PCR. (*B*) Expression of the same 24 miRNAs in five EOC cell lines and HeLa cells after treatment with demethylating agent 5-aza-2′-deoxycytidine (5-Aza-CdR) and the histone deacetylase inhibitor 4-phenylbutyric acid (PBA) for 6 days.

**DNA Copy Number Loss Contributes to the Down-Regulation of miRNAs.** miRNAs are frequently located in cancer-associated regions of the human genome (23), and we have reported that genomic loci containing miRNA genes are frequently altered in human cancers (24). Thus, we examined the chromosomal distribution of miRNAs that were found down-regulated in advanced EOC. Twenty-five of the miRNAs that were down-regulated in late-stage EOC aggregate in <1-Mb clusters in three chromosomes (Fig. S5). These clustered miRNA loci were considered chromosome regions of interest in further aCGH analysis. We first analyzed miRNAs that are deregulated in EOC cell lines. We excluded *mir-222*, *mir-224*, and *mir-424*, which are located in chromosome X (not included in our aCGH platform), and *mir-124*, which exhibits multiple copies in different genomic loci. The remaining 31 miRNA are located in 17 euchromosomic loci. Two of four (50.0%) loci containing miRNA up-regulated in EOC lines relative to IOSE (*mir-182* and *mir-103*) exhibited amplification (Fig. 2*A*). Two of 13 (15.3%) loci containing miRNA down-regulated in EOC lines relative to IOSE (*mir-140* and *mir-184*) exhibited deletion (Fig. 2*A*). Next, we analyzed miRNAs down-regulated in late-stage EOC, again excluding miRNAs located in chromosome X and miRNAs with multiple copies in different genomic loci. This analysis comprised 30 miRNAs located in 16 euchromosomic loci. Two of 16 loci (12.5%, *mir-15a* and *mir-184*) were significantly deleted. None of these loci exhibited amplification in late-stage EOC (Fig. 2*B*).

To further confirm that DNA copy number alterations correlate with concordant miRNA deregulation in EOC, we analyzed two representative miRNAs with opposite alterations. We found that locus chr7*_129-130*, containing *mir-182*, was amplified in 28.9% of EOC (Fig. S6*A*). In both primary tumors and cell lines, DNA copy number amplification correlated with miRNA expression (Fig. S6 *B* and *C*). Importantly, forced expression of *mir-182* in EOC cell line significantly promoted tumor growth *in vivo*, confirming the role of *mir-182* as a putative oncogene (unpublished data). We also analyzed *mir-15a*, a known tumor suppressor gene (12, 38, 39). *mir-15a* was deleted in 23.9% of EOC (Fig. S6*D*). A positive correlation between the deletion of locus chr*13_49-50* and reduced expression of *mir-15a* was found in both primary tumors and cell lines (Fig. S6 *E–G*). Thus, DNA copy number alteration is one important mechanism of miRNA deregulation in EOC.

**Epigenetic Alterations Silence miRNA Expression.** Epigenetic mechanisms play an important role in chromatin remodeling and the regulation of protein-coding genes and miRNA in human cancer (25). Importantly, three genomic loci at chromosomes 14, 19, and X harbor 25 miRNAs down-regulated in EOC (Fig. S5), and these loci may be regulated through imprinting or epigenetic mechanisms (40). Therefore, we analyzed IOSE and EOC cell lines by real-time RT-PCR for expression of 18 from these 25 clustered miRNAs and 5 miRNAs not located in these clusters. *mir-127* was chosen as experimental control, because it is epigenetically regulated in human cancer (25). All eight miRNAs located in chromosome 14 cluster (*mir-337*, *mir-432*, *mir-495*, *mir-368*, *mir-376a*, *mir-376b*, *mir-377*, and *mir-419*) were expressed in all four IOSE, but in no EOC cell line. None of the six miRNAs located in chromosome 19 cluster (*mir-520e*, *mir-519e*, *mir-519d*, *mir-516*, *mir-518a*, and *mir-372*) were detected in IOSE or EOC cell lines. Finally, three of four miRNAs located in chromosome X cluster (*mir-448*, *mir-507*, and *mir-424*) were expressed in both IOSE and EOC cell lines (Fig. 3*A*).

To investigate whether epigenetic mechanisms are responsible for miRNA down-regulation in EOC, five EOC cell lines were treated with the DNA demethylating agent 5-aza-2′-deoxycytidine (5-Aza-CdR) and the histone deacetylase (HDAC) inhibitor 4-phenylbutyric acid (PBA) (25). Seven of eight miRNAs at the chromosome 14 cluster, six of six miRNAs at the chromosome 19 cluster, two of four miRNAs at the chromosome X cluster, and one of five miRNAs located at other chromosomes were up-regulated by this treatment in at least two cell lines (Fig. 3*B*). Interestingly, treatment restored the expression of *miR-34b*, a tumor suppressor miRNA regulated by p53, in all six cell lines. This result was also confirmed by Northern blot (Fig. S7 *A* and *B*). Taken together, expression of at least 16 of 44 (36.4%)

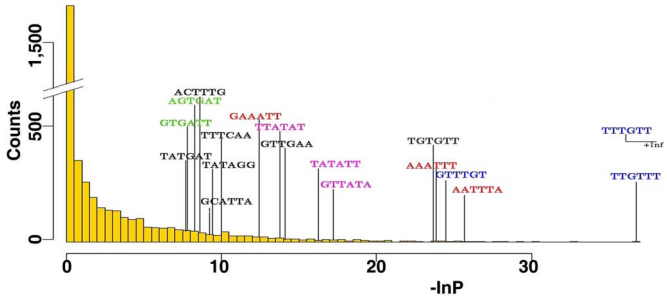


**Fig. 4.** miRNA deregulation affects mRNA transcripts. Histograms of negative natural logarithms of 4,096 *P* values derived from one-tailed Wilcoxon rank sum test applied to the distributions of each hexamer occurrence in the 3′ UTRs of all up-regulated versus unchanged mRNA transcripts.

miRNAs that are down-regulated in late-stage EOC was restored by DNA demethylation or histone deacetylase inhibiting drugs. These *in vitro* results suggest that epigenetic silencing is an important mechanism contributing to the widespread miRNA down-regulation in late-stage EOC.

**MicroRNA Deregulation Affects mRNA Transcripts.** miRNAs can down-regulate mRNA expression by controlling mRNA stability or cleaving target mRNAs. We then asked whether the marked down-regulation of miRNAs observed between early- and late-stage EOC has implications on the transcriptome, i.e., whether it is associated with up-regulation of specific mRNAs. To address this question, we used Affymetrix cDNA microarrays to analyze the genome-wide transcriptional changes between early- and late-stage EOC in samples previously analyzed by miRNA microarray. In total, 76 EOC specimens (8 early-stage and 68 late-stage) were analyzed, and 2,279 transcripts were identified as significantly different between early- and late-stage EOC ($P < 0.05$). Of these, 1,266 were up-regulated in late-stage EOC. Thus, we collected 948 genes representing the 1,266 up-regulated Affymetrix transcripts and 15,212 annotated genes whose expression was unchanged between early- and late-EOC. Following the method described by Krutzfeld *et al.* (41), we calculated the number of nonoverlapping occurrences of each possible hexamer in every 3′ UTR sequence of those genes, divided it by the length of the UTR, and applied one-tailed Wilcoxon rank sum to each normalized hexamer count distribution in up-regulated versus unchanged UTRs (Fig. 4 and Fig. S8). Several hexamers were significantly overrepresented in the up-regulated genes ($P < 0.001$) and in parallel corresponded to the first seed positions (miRNA nucleotides 1–6, 2–7, and 3–8) in miRNAs that were down-regulated in the late-stage EOC. Twelve miRNAs had seed region complementary to the top scoring hexamers (Fig. 4 and Fig. S8*B*) and were considered significant candidates possibly contributing to the corresponding mRNA up-regulation in late-stage EOC. We also observed an enrichment in up-regulated genes for having at least two hexamers corresponding to the microRNA seed positions (Fig. S8*C*). Of note, 5 of the top 12 miRNAs identified were located in the chromosome 14 cluster (*Dlk1-Gtl2* domain) (42) (Fig. 4, Fig. S5*B*, and Fig. S8*B*). This finding indicates that miRNA alterations are not simply "bystander events" during EOC advancement but that they may serve as tumor suppressor genes whose loss mediates oncogenesis.

**miRNA Cluster at *Dlk1-Gtl2* Domain Is Commonly Altered in Epithelial Cancers.** Because *mir-377*, *mir-368*, and *mir-495*, three of the eight miRNAs located in the *Dlk1-Gtl2* domain of chromosome 14, are also silenced by epigenetic mechanisms in bladder cancer (25), we asked whether down-regulation of miRNAs in this cluster is a common molecular event in human epithelial malignancy. Four miRNAs in this cluster were randomly selected for the analysis in 23 benign breast lesions, 73 invasive ductal carcinomas (IDC), and paired colon cancer and normal colon tissue specimens from 18 patients. All miRNAs were down-regulated in tumors, with all but one (*mir-376a*) in breast cancer and one (*mir-368*) in colon cancer reaching statistical significance (Fig. S9). Thus, down-regulation of chromosome 14 miRNA cluster is an event common to many human epithelial tumors. The above results collectively suggest that those eight miRNAs located in chromosome 14 cluster (*Dlk1-Gtl2* domain) are commonly regulated and may play a role as tumor suppressor genes in solid tumors, because (*i*) they are down-regulated in advanced relative to early-stage EOC and in invasive breast and colon cancer, (*ii*) they are silenced by epigenetic alterations in EOC and bladder cancer (25), and (*iii*) their down-regulation is associated with up-regulation of numerous potential mRNA targets in late-stage EOC. Importantly, this chromosome region has been identified as a cancer susceptibility locus in mouse (43). Therefore, we further analyzed the putative mRNA targets of these eight miRNAs. mRNA targets identified with the above method for each of these miRNAs are listed in Dataset S6. Gene ontology (GO) analysis (18) revealed that these miRNAs are highly associated with two important biological processes implicated in human carcinogenesis, namely cell cycle regulation and immune response (Dataset S7).

**Down-Regulation of miRNA Cluster at *Dlk1-Gtl2* Domain Is Associated with Poor Survival.** We asked whether deregulation of the miRNAs at the *Dlk1-Gtl2* domain affects tumor behavior at an advanced stage. Nonsupervised clustering of eight *Dlk1-Gtl2* domain miRNA expression signature classified 73 late-stage EOC in two distinct clusters, cluster 1, with global low expression of these miRNAs ($n = 38$), and cluster 2, with relatively global high expression ($n = 35$) (Fig. 5*A*). Sixty-four tumors with histological sections and clinical follow-up were available for analysis. Patients in cluster 1 were at significantly greater risk with shorter 5-year survival than those in cluster 2 ($P = 0.024$, log-rank test, Fig. 5*B*). Because miRNAs located at *Dlk1-Gtl2* domain appear to regulate mRNAs involved in the control of cell cycle, we examined the tumor proliferation index (percentage of Ki67-positive cells in tumor islets). Tumors in cluster 1 exhibited significantly higher proliferation index (49.0) than cluster 2 (32.7, $P = 0.017$, Fig. 5 *C–E*). Thus, down-regulation of miRNAs located at *Dlk1-Gtl2* domain is associated with higher tumor proliferation and shorter patient survival.

## Discussion

According to recent high-throughput studies, global expression of miRNAs is seemingly deregulated in most cancer types (1, 16–20). Interestingly, miRNA expression may be widely down-regulated in human tumors relative to normal tissues, as revealed by bead-based flow cytometry (16) or miRNA microarray (44). However, other microarray studies reported a tumor-specific mixed pattern of down-regulation and up-regulation of select miRNA genes (17–19). The choice of control samples may therefore be critical in the interpretation of those results. For example, normal ovaries are mainly comprised of stroma and the surface epithelium represents only a minimal part; thus, the whole ovary may not serve as an optimal control for EOC studies. We accordingly compared EOC cell lines with ovarian surface epithelial cells to investigate the miRNA alterations associated with OSE malignant transformation. Our findings indicate that the miRNome is largely down-regulated in association with OSE malignant transformation and EOC progression, which is in agreement with recent reports (45, 46). This result further suggests that certain miRNAs may function as tumor suppressor genes and justifies why abrogation of miRNAs at large may in fact be a hallmark of human cancers (16).

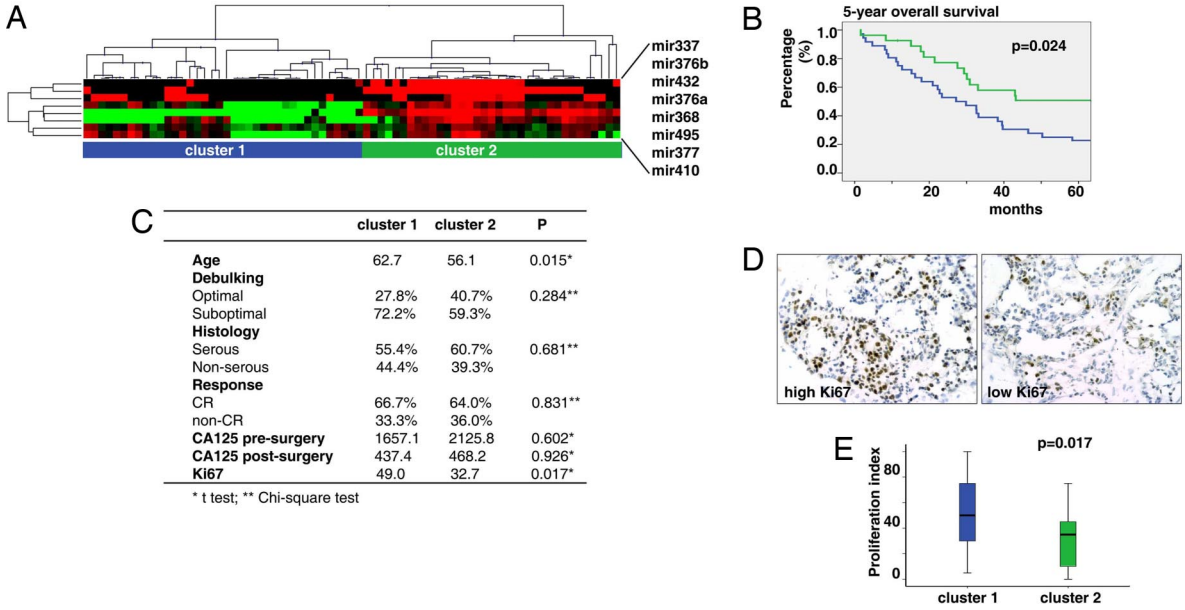


**Fig. 5.** Down-regulation of miRNA cluster at the *Dlk1-Gtl2* domain is associated with poor survival. (*A*) Nonsupervised clustering of the eight *Dlk1-Gtl2* domain miRNA expression signatures classifies 73 late-stage EOC in two distinct clusters (cluster 1, $n = 38$; cluster 2, $n = 35$). (*B*) Five-year survival of patients with advanced stage EOC whose tumors belong to cluster 1 (blue) or cluster 2 (green). (*C*) Summary of clinicopathologic characteristics of patients in the two clusters. (*D*) Examples of high and low proliferation index based on Ki67 immunohistochemistry staining in late-stage EOC. (*E*) Summary of proliferation index in tumors from the two clusters.

DNA copy number abnormalities (23, 24), epigenetic alterations (25), mutations (17), transcriptional deregulation (15), and defective miRNA biogenesis pathway (31) may contribute to the miRNA deregulation in human cancer. In EOC, we showed that: (*i*) Drosha and Dicer, key proteins in miRNA biogenesis pathway, are not altered and, thus, are unlikely to contribute to the miRNA deregulation between early- and late-stage EOC; (*ii*) deletions occur in up to 15% of genomic loci harboring miRNAs that are down-regulated, suggesting that genomic loss contributes to miRNA down-regulation in EOC; and (*iii*) at least one-third of down-regulated miRNAs may be silenced by epigenetic alterations. For example, *miR-15a* was down-regulated and its DNA copy number was deleted in EOC. *miR-34b*, a tumor suppressor miRNA regulated by p53 (15, 33–37), was also down-regulated in EOC but because of epigenetic silencing. Complementary mechanisms, including transcriptional regulation, may cooperate in miRNA deregulation. For example, *mir-34b* is regulated by p53, and p53 loss could cooperate with epigenetic mechanisms to down-regulate *mir-34b*. However, different mechanisms may regulate miRNA in opposite directions. For example, genomic gain may increase *mir-182* expression in EOC, but *mir-182* is silenced epigenetically in some EOC cell lines (Fig. 5*B*) and bladder cancer (25). Thus, final expression will depend on the net effect of these mechanisms. In addition, this study carried out the very first analysis to link miRNA microarray to cDNA microarray data to provide, through seed sequences, molecular evidence that miRNA down-regulation can indeed result in specific genome-wide transcriptional up-regulation.

Finally, a putative tumor suppressor miRNA cluster located at chromosome 14 (*Dlk1-Gtl2* domain) was identified. This chromosome region is a cancer susceptibility locus in the mouse (43) and AAV integration in this location induced hepatocellular carcinoma (47). Eight miRNAs located in this cluster are of particular interest, because they were suppressed in EOC cell lines in advanced EOC and invasive breast and colon cancer, they were silenced by epigenetic mechanisms, and they were predicted to up-regulate a large number of mRNA transcripts in late stage EOC that, by GO analysis, are implicated in cancer. Some of these miRNAs are also down-regulated in bladder cancer (25). miRNAs in this chromosome region are only expressed from a maternally inherited chromosome and their imprinted expression is regulated by an intergenic germ line-derived differentially methylated region located ≈200 kb upstream of the miRNA cluster (42). Importantly, tumors with lower expression of these eight miRNAs were associated with higher proliferation index and significantly shorter survival. At this point, the function of this miRNA cluster is largely unknown, but it may play a critical role in embryonic development (42, 48, 49). Our data suggest that miRNAs in this cluster function as tumor suppressor genes. Further work is required to understand their function and potential for cancer therapy.

## Materials and Methods

**Patients and Specimens.** The ovarian cancer (miRNA microarray, $n = 106$; aCGH, $n = 109$; Affymetrix cDNA microarray, $n = 76$; tissue array, $n = 504$; and qPCR validation, $n = 96$) and breast cancer ($n = 96$) specimens were collected at the University of Pennsylvania; the University of Turin, and the University of Helsinki. Detailed information is provided in *SI Methods*. The colon cancer and paired normal control specimens ($n = 18$ pairs) were provided by the cooperative human tissue network (Cooperative Human Tissue Network) and the Department of Surgical Oncology, Okayama University.

**TaqMan miRNA Assay.** Expression of mature miRNAs was analyzed by TaqMan miRNA Assay (Applied Biosystems). Detailed information is provided in *SI Methods*.

**miRNA Microarray.** miRNA microarray was performed on the microarray chip (OSU_CCC version 3.0; OSU). Detailed information is provided in *SI Methods*.

**cDNA Microarray.** cDNA microarray was performed on the human U133 + 2.0 GeneChip (Affymetrix). Detailed information is provided in *SI Methods*.

**Array-Based Comparative Genomic Hybridization (aCGH).** BAC clones included in the 1-Mb array platform were described in ref. 24. Detailed information is provided in *SI Methods*.

**Tissue Microarray.** The tissue microarray was constructed as described. A total of 504 specimens were printed in the array slides. Detailed information is provided in *SI Methods*.

**5-Aza-CdR and PBA Treatment.** Treatment was preformed as descried by Saito (25). Briefly, cells were seeded at $5 \times 10^5$ cells per T75 flask 24 h before

treatment with 5-Aza-CdR (3 $\mu$M; Sigma–Aldrich) and/or PBA (3 mM; Sigma–Aldrich). 5-Aza-CdR was removed after 24 h, whereas PBA was continuously administered by replacing the medium containing PBA every 24 h for 6 days.

**Bioinformatic Analysis.** Detailed information for miRNA target prediction and gene ontology analysis is provided in *SI Methods*.

**Statistics.** Statistical analysis was performed by using the SPSS statistics software package (SPSS). All results were expressed as mean $\pm$ SD, and $P < 0.05$ was used for significance. Kaplan–Meier curves were used to estimate 5-year rates and were compared with the use of log-rank statistics.

**ACKNOWLEDGMENTS.** We thank Vassilis Altmazoglou and Trias Thiraiou for the mapping of the Affymetric Gene ID to the Ensembl Gene ID and the initial calculation on the hexamer distribution. We thank the following investigators who developed public microarray analysis software: TM4 developed was by Dr. John Quackenbush (Harvard School of Public Health, Boston); BRB ArrayTools were developed by Drs. Richard Simon and Amy Peng Lam (National Cancer Insitute, Rockville, MD); GenePattern was developed by Dr. Jill P. Mesirov (Broad Institute, Cambridge, MA); and Cluster software was developed by Drs. Michael Eisen (Lawrence Berkeley National Laboratory, Berkeley, CA) and David Botstein (Princeton University, Princeton). We thank Dr. Nelly Auersperg (University of British Columbia, Vancouver, BC, Canada) for IOSE and access to the Canadian Ovarian Tissue Bank. This work was supported by a grants from the Ovarian Cancer Research Fund (G.C. and L.Z.), National Cancer Institute ovarian Specialized Programs of Research Excellence Grant P01-CA83638 Career Development Award (to L.Z.), American Cancer Society Grant IRG-78-002-30 (to L.Z.), the Mary Kay Ash Charitable Foundation (L.Z.), National Science Foundation Grant DBI-0238295 (to A.G.H.), and National Institutes of Health/National Institute of Diabetes and Digestive and Kidney Diseases Grant R01-DK056645 (to A.K.R. and C.N.J.).

1. Calin GA, Croce CM (2006) MicroRNA signatures in human cancers. *Nat Rev Cancer* 6:857–866.
2. Esquela-Kerscher A, Slack FJ (2006) Oncomirs—microRNAs with a role in cancer. *Nat Rev Cancer* 6:259–269.
3. Bartel DP (2004) MicroRNAs: Genomics, biogenesis, mechanism, and function. *Cell* 116:281–297.
4. Ambros V (2004) The functions of animal microRNAs. *Nature* 431:350–355.
5. He L, Hannon GJ (2004) MicroRNAs: Small RNAs with a big role in gene regulation. *Nat Rev Genet* 5:522–531.
6. Zamore PD, Haley B (2005) Ribo-gnome: The big world of small RNAs. *Science* 309:1519–1524.
7. He L, *et al.* (2005) A microRNA polycistron as a potential human oncogene. *Nature* 435:828–833.
8. O'Donnell KA, *et al.* (2005) c-Myc-regulated microRNAs modulate E2F1 expression. *Nature* 435:839–843.
9. Costinean S, *et al.* (2006) Pre-B cell proliferation and lymphoblastic leukemia/high-grade lymphoma in E(mu)-miR155 transgenic mice. *Proc Natl Acad Sci USA* 103:7024–7029.
10. Voorhoeve PM, *et al.* (2006) A genetic screen implicates miRNA-372 and miRNA-373 as oncogenes in testicular germ cell tumors. *Cell* 124:1169–1181.
11. Chan JA, Krichevsky AM, Kosik KS (2005) MicroRNA-21 is an antiapoptotic factor in human glioblastoma cells. *Cancer Res* 65:6029–6033.
12. Calin GA, *et al.* (2002) Frequent deletions and down-regulation of micro-RNA genes miR15 and miR16 at 13q14 in chronic lymphocytic leukemia. *Proc Natl Acad Sci USA* 99:15524–15529.
13. Johnson SM, *et al.* (2005) RAS is regulated by the let-7 microRNA family. *Cell* 120:635–647.
14. Mayr C, Hemann MT, Bartel DP (2007) Disrupting the pairing between let-7 and Hmga2 enhances oncogenic transformation. *Science* 315:1576–1579.
15. He L, *et al.* (2007) A microRNA component of the p53 tumour suppressor network. *Nature* 447:1130–1134.
16. Lu J, *et al.* (2005) MicroRNA expression profiles classify human cancers. *Nature* 435:834–838.
17. Calin GA, *et al.* (2005) A MicroRNA signature associated with prognosis and progression in chronic lymphocytic leukemia. *N Engl J Med* 353:1793–1801.
18. Yanaihara N, *et al.* (2006) Unique microRNA molecular profiles in lung cancer diagnosis and prognosis. *Cancer Cell* 9:189–198.
19. Volinia S, *et al.* (2006) A microRNA expression signature of human solid tumors defines cancer gene targets. *Proc Natl Acad Sci USA* 103:2257–2261.
20. Cummins JM, *et al.* (2006) The colorectal microRNAome. *Proc Natl Acad Sci USA* 103:3687–3692.
21. Shell S, *et al.* (2007) Let-7 expression defines two differentiation stages of cancer. *Proc Natl Acad Sci USA* 104:11400–11405.
22. Lu L, *et al.* (2007) Hypermethylation of let-7a-3 in epithelial ovarian cancer is associated with low insulin-like growth factor-II expression and favorable prognosis. *Cancer Res* 67:10117–10122.
23. Calin GA, *et al.* (2004) Human microRNA genes are frequently located at fragile sites and genomic regions involved in cancers. *Proc Natl Acad Sci USA* 101:2999–3004.
24. Zhang L, *et al.* (2006) microRNAs exhibit high frequency genomic alterations in human cancer. *Proc Natl Acad Sci USA* 103:9136–9141.
25. Saito Y, *et al.* (2006) Specific activation of microRNA-127 with down-regulation of the proto-oncogene BCL6 by chromatin-modifying drugs in human cancer cells. *Cancer Cell* 9:435–443.
26. Thomson JM, *et al.* (2006) Extensive post-transcriptional regulation of microRNAs and its implications for cancer. *Genes Dev* 20:2202–2207.
27. Muralidhar B, *et al.* (2007) Global microRNA profiles in cervical squamous cell carcinoma depend on Drosha expression levels. *J Pathol* 212:368–377.
28. Chiosea S, *et al.* (2007) Overexpression of Dicer in precursor lesions of lung adenocarcinoma. *Cancer Res* 67:2345–2350.
29. Chiosea S, *et al.* (2006) Up-regulation of dicer, a component of the MicroRNA machinery, in prostate adenocarcinoma. *Am J Pathol* 169:1812–1820.
30. Karube Y, *et al.* (2005) Reduced expression of Dicer associated with poor prognosis in lung cancer patients. *Cancer Sci* 96:111–115.
31. Kumar MS, *et al.* (2007) Impaired microRNA processing enhances cellular transformation and tumorigenesis. *Nat Genet* 39:673–677.
32. Zorn KK, *et al.* (2003) Choice of normal ovarian control influences determination of differentially expressed genes in ovarian cancer expression profiling studies. *Clin Cancer Res* 9:4811–4818.
33. Bommer GT, *et al.* (2007) p53-Mediated Activation of miRNA34 Candidate Tumor-Suppressor Genes *Curr Biol* 17:1298–1307.
34. Chang TC, *et al.* (2007) Transactivation of miR-34a by p53 broadly influences gene expression and promotes apoptosis. *Mol Cell* 26:745–752.
35. Raver-Shapira N, *et al.* (2007) Transcriptional activation of miR-34a contributes to p53-mediated apoptosis. *Mol Cell* 26:731–743.
36. Tarasov V, *et al.* (2007) Differential regulation of microRNAs by p53 revealed by massively parallel sequencing: miR-34a is a p53 target that induces apoptosis and G1-arrest. *Cell Cycle* 6:1586–1593.
37. Corney DC, *et al.* (2007) MicroRNA-34b and MicroRNA-34c are targets of p53 and cooperate in control of cell proliferation and adhesion-independent growth. *Cancer Res* 67:8433–8438.
38. Cimmino A, *et al.* (2005) miR-15 and miR-16 induce apoptosis by targeting BCL2. *Proc Natl Acad Sci USA* 102:13944–13949.
39. Raveche ES, *et al.* (2007) Abnormal microRNA-16 locus with synteny to human 13q14 linked to CLL in NZB mice, *Blood* 109:5079–5086.
40. Royo H, Bortolin ML, Seitz H, Cavaille J (2006) Small non-coding RNAs and genomic imprinting. *Cytogenet Genome Res* 113:99–108.
41. Krutzfeldt J, *et al.* (2005) Silencing of microRNAs *in vivo* with ''antagomirs''. *Nature* 438:685–689.
42. Seitz H, *et al.* (2004) A large imprinted microRNA gene cluster at the mouse Dlk1-Gtl2 domain. *Genome Res* 14:1741–1748.
43. Sevignani C, *et al.* (2007) MicroRNA genes are frequently located near mouse cancer susceptibility loci. *Proc Natl Acad Sci USA* 104:8017–8022.
44. Visone R, *et al.* (2007) Specific microRNAs are down-regulated in human thyroid anaplastic carcinomas. *Oncogene* 26:7590–7595.
45. Iorio MV, *et al.* (2007) MicroRNA signatures in human ovarian cancer. *Cancer Res* 67:8699–8707.
46. Yang H, *et al.* (2008) MicroRNA expression profiling in human ovarian cancer: miR-214 induces cell survival and cisplatin resistance by targeting PTEN. *Cancer Res* 68:425–433.
47. Donsante A, *et al.* (2007) AAV vector integration sites in mouse hepatocellular carcinoma. *Science* 317:477.
48. Lin SP, *et al.* (2003) Asymmetric regulation of imprinting on the maternal and paternal chromosomes at the Dlk1-Gtl2 imprinted cluster on mouse chromosome 12. *Nat Genet* 35:97–102.
49. Lin SP, *et al.* (2007) Differential regulation of imprinting in the murine embryo and placenta by the Dlk1-Dio3 imprinting control region. *Development (Cambridge, UK)* 134:417–426.

# MicroRNA Signatures in Human Ovarian Cancer

Marilena V. Iorio,[1] Rosa Visone,[2] Gianpiero Di Leva,[2] Valentina Donati,[2] Fabio Petrocca,[2] Patrizia Casalini,[1] Cristian Taccioli,[2] Stefano Volinia,[2] Chang-Gong Liu,[2] Hansjuerg Alder,[2] George A. Calin,[2] Sylvie Ménard,[1] and Carlo M. Croce[2]

[1]Molecular Biology Unit, Department of Experimental Oncology, Fondazione Istituti di Ricovero e Cura a Carattere Scientifico, Istituto Nazionale Tumori, Milano, Italy and [2]Department of Molecular Virology, Immunology and Medical Genetics and Comprehensive Cancer Center, Ohio State University, Columbus, Ohio

## Abstract

**Epithelial ovarian cancer (EOC) is the sixth most common cancer in women worldwide and, despite advances in detection and therapies, it still represents the most lethal gynecologic malignancy in the industrialized countries. Unfortunately, still relatively little is known about the molecular events that lead to the development of this highly aggressive disease. The relatively recent discovery of microRNAs (miRNA), a class of small noncoding RNAs targeting multiple mRNAs and triggering translation repression and/or RNA degradation, has revealed the existence of a new level of gene expression regulation. Multiple studies involving various types of human cancers proved that miRNAs have a causal role in tumorigenesis. Here we show that, in comparison to normal ovary, miRNAs are aberrantly expressed in human ovarian cancer. The overall miRNA expression could clearly separate normal versus cancer tissues. The most significantly overexpressed miRNAs were *miR-200a, miR-141, miR-200c*, and *miR-200b*, whereas *miR-199a, miR-140, miR-145*, and *miR-125b1* were among the most down-modulated miRNAs. We could also identify miRNAs whose expression was correlated with specific ovarian cancer biopathologic features, such as histotype, lymphovascular and organ invasion, and involvement of ovarian surface. Moreover, the levels of *miR-21, miR-203*, and *miR-205*, up-modulated in ovarian carcinomas compared with normal tissues, were significantly increased after 5-aza-2′-deoxycytidine demethylating treatment of OVCAR3 cells, suggesting that the DNA hypomethylation could be the mechanism responsible for their overexpression. Our results indicate that miRNAs might play a role in the pathogenesis of human EOC and identify altered miRNA gene methylation as a possible epigenetic mechanism involved in their aberrant expression.** [Cancer Res 2007;67(18):8699–707]

## Introduction

Epithelial ovarian cancer (EOC) is the most common gynecologic malignancy and the sixth most common cancer in women worldwide, with highly aggressive natural history causing almost 125,000 deaths yearly (1). Despite advances in detection and cytotoxic therapies, only 30% of patients with advanced-stage ovarian cancer survive 5 years after initial diagnosis (2). The high mortality of this disease is mainly due to late-stage diagnosis for >70% of ovarian cancers. In fact, when ovarian cancer is diagnosed in its early stage, that is still organ confined, the 5-year survival rate exceeds 90%. Unfortunately, only 19% of all ovarian cancers are diagnosed at this early stage. Indeed, this rather poor prognosis is due to (*a*) the insidious asymptomatic nature of this disease in its early onset, (*b*) the lack of robust and minimally invasive methods for early detection, and (*c*) tumor resistance to chemotherapy. The vast majority of human ovarian carcinomas are represented by ovarian epithelial cancers (OEC), deriving from the ovarian surface epithelium (3).

Ovarian adenocarcinomas occur as four major histologic subtypes, serous, mucinous, endometrioid, and clear cell, with serous being the most common. Current data indicate that each of these histologic types is associated with distinct morphologic and molecular genetic alterations (4), but further investigations of the molecular mechanisms promoting ovarian cancer are necessary to determine how each of the subtypes emerges.

Over the last 5 years, expression profiling technologies greatly improved, thus expanding the knowledge on cancer etiology and biomarkers with clinical applications (5, 6). However, although these technologies have provided most of the new biomarkers with potential use for diagnosis, drug development, and tailored therapy, they have thus far shed little insight into the detailed mechanisms at the origin of this neoplasia, thus suggesting that ovarian tumorigenesis may occur through novel or poorly characterized pathways.

A new class of small noncoding RNAs, named microRNAs (miRNA), was discovered recently and shown to regulate gene expression at post-transcriptional level, for the most part by binding through partial sequence homology to the 3′ untranslated region of target mRNAs and causing block of translation and/or mRNA degradation (7). miRNAs are 19 to 25 nt long molecules cleaved from 70 to 100 nt hairpin pre-miRNA precursors. The precursor is cleaved by cytoplasmic RNase III Dicer into ~22 nt miRNA duplex: one strand (miRNA*) of the short-lived duplex is degraded, whereas the other strand, which serves as mature miRNA, is incorporated into the RNA-induced silencing complex and drives the selection of target mRNAs containing antisense sequences.

Several studies have shown that miRNAs play important roles in essential processes, such as differentiation, cell growth, and cell death (8, 9).

Moreover, it has been shown that miRNAs are aberrantly expressed or mutated in cancers, suggesting that they may play a role as a novel class of oncogenes or tumor suppressor genes, depending on the targets they regulate: *let-7*, down-regulated in lung cancer, suppresses RAS (10) and HMGA2 (11, 12); *mir-15* and

**Note:** Supplementary data for this article are available at Cancer Research Online (http://cancerres.aacrjournals.org/).

**Requests for reprints:** Carlo M. Croce, Department of Molecular Virology, Immunology and Medical Genetics and Comprehensive Cancer Center, Ohio State University, Room 445C, Wiseman Hall, 400 12th Avenue, Columbus, OH 43210. Phone: 614-292-3063; Fax: 614-292-3312; E-mail: Carlo.Croce@osumc.edu.



doi:10.1158/0008-5472.CAN-07-1936

*mir-16*, deleted or down-regulated in leukemia, suppress BCL2 (13); and *mir-17-5p* and *mir-20a*, control the balance of cell death and proliferation driven by the proto-oncogene c-Myc (14). Clear evidences indicate that miRNA polycistron *mir-17-92* acts as an oncogene in lymphoma and lung cancer (15); *mir-372* and *mir-373* are novel oncogenes in testicular germ cell tumors by numbing p53 pathway (16); *miR-155*, overexpressed in B-cell lymphomas and solid tumors, leads to the development of B-cell malignancies in an *in vivo* model of transgenic mice (17).

The use of miRNA microarray technologies has been used as a powerful tool to recognize miRNAs differentially expressed between normal and tumor samples (18–20) and also to identify miRNA expression signatures associated with well-defined clinicopathologic features and disease outcome (21, 22). Several studies have also investigated the molecular mechanisms leading to an aberrant miRNA expression, identifying the presence of genomic abnormalities in miRNA genes (21, 23, 24). More recently, few evidences have shown that miRNA genes may be regulated also by epigenetic mechanisms, as changes in genomic DNA methylation pattern: *miR-127* (25) and *miR-124a* (26) are transcriptionally inactivated by CpG island hypermethylation, whereas in lung cancer, the overexpression of *let-7a-3* seems to be due to DNA hypomethylation (27).

Here, we present the results of a genome-wide miRNA expression profiling in a large set of normal and tumor ovarian tissues, showing the existence of an ovarian cancer-specific miRNA signature and identifying the altered methylation of miRNA genes as a possible epigenetic mechanism responsible for their aberrant expression.

## Materials and Methods

**Ovarian cancer samples and cell lines.** A total of 84 snap-frozen normal and malignant ovarian tissues were collected at the GOG Tissues Bank, Columbus Children's Hospital (Columbus, OH). The tissue collection used for microarray analysis included 15 normal ovarian tissue sections and 69 malignant tissues, all ovarian epithelial carcinomas, including 31 serous (29 of them showed a papillary pattern), 8 endometrioid, 4 clear cell, 9 poorly differentiated, and 1 mucinous carcinomas. The ovarian cancer cell line IGROV1 was originally derived by Dr. Bernard (Institute Gustave Roussy, Villejuf, France), from a moderately differentiated ovarian carcinoma of an untreated patient; OAW-42 was from Dr. Ulrich U. (Department of Obstetrics and Gynaecology, University of Ulm, Ulm, Germany), whereas OVCAR3, OVCAR8, and SKOV3 were purchased from the American Type Culture Collection. All the cell lines were maintained in RPMI 1640 (Life Technologies), supplemented with 10% (v/v) fetal bovine serum, 3 mmol/L L-glutamine, and 100 units/mL penicillin/streptomycin.

**miRNA microarray hybridization and quantification.** Total RNA isolation was done with Trizol (Invitrogen) according to the manufacturer's instructions. RNA labeling and hybridization on miRNA microarray chips were done as described previously (28) using 5 μg of total RNA from each sample. Hybridization was carried out on our miRNA microarray (Ohio State Comprehensive Cancer Center, version 2.0), which contains probes for 460 mature miRNAs spotted in quadruplicate (235 *Homo sapiens*, 222 *Mus musculus*, and three *Arabidopsis thaliana*) with annotated active sites. Often, more than one probe set exists for a given mature miRNA. Additionally, there are quadruplicate probes corresponding to most precursor miRNAs. Hybridization signals were detected with streptavidin-Alexa Fluor 647 conjugate and scanned images (Axon 4000B) were quantified using the GenePix 6.0 software (Axon Instruments).

**Computational analysis of miRNA microarray data.** Microarray images were analyzed by using GenePix Pro. Average values of the replicate spots of each miRNA were background subtracted, normalized, and subjected to further analysis. We did a global median normalization of ovary microarray data by using BRB ArrayTools developed by Richard Simon and Amy Peng Lam (29). Absent calls were thresholded to 4.5 before subsequent statistical analysis. This level is the average minimum intensity level detected in the experiments. miRNA nomenclature was according to the Genome Browser[3] and the miRNA database at Sanger Center[4]; in case of discrepancies, the miRNA database was followed. Differentially expressed miRNAs were identified by using the *t* test procedure within significance analysis of microarrays (SAM), a method developed at Stanford University Labs based on recent article of Tusher, Tibshirani, and Chu (30). To identify miRNA signatures, we also applied PAM, which does sample classification from gene expression data, via the "nearest shrunken centroid method" of Tibshirani, Hastie, Narasimhan, and Chu (31).

**Northern blotting.** Northern blot analysis was done as described previously. RNA samples (10 μg each) were run on 15% polyacrylamide and 7 mol/L urea Criterion precasted gels (Bio-Rad) and transferred onto Hybond-N+ membranes (Amersham). The hybridization was done at 37°C in ULTRAhyb-Oligo hybrization buffer (Ambion) for 16 h. Membranes were washed at 37°C, twice with 2× saline-sodium phosphate-EDTA and 0.5% SDS. The oligonucleotides used as probes were antisense to the sequence of the mature miRNAs (miRNA Registry[5]): miR-200a, 5′-ACATCGTTACCAGACAGTGTTA-3′; miR-141, 5′-CCATCTTTACCAGACAGTGTTA-3′; miR-199a, 5′-GAACAGGTAGTCTGAACACTGGG-3′; miR-125b1, 5′-TCACAAGTTAGGGTCTCAGGGA-3′; miR-145, 5′-AAGGGATTCCTGGGAAAACTGGAC-3′; miR-222, 5′-GAGACCCAGTAGCCAGATGTAGCT-3′; and miR-21, 5′-TCAACATCAGTCTGATAAGCTA-3′.

5S RNA or EtBr gel staining were used to normalize. Two hundred nanograms of each probe were end labeled with 100 μCi [γ-$^{32}$P]ATP using the polynucleotide kinase (Roche). Blots were stripped in boiling 0.1% SDS for 10 min before rehybridization.

**Quantitative real-time PCR.** The single tube Taqman miRNA assays were used to detect and quantify mature miRNAs on Applied Biosystems real-time PCR instruments in accordance with manufacturer's instructions (Applied Biosystems). Normalization was done with 18S rRNA. All reverse transcription reactions, including no-template controls and reverse transcriptase minus controls, were run in a GeneAmp PCR 9700 Thermocycler (Applied Biosystems). Gene expression levels were quantified using the ABI Prism 7900HT Sequence Detection System (Applied Biosystems). Comparative real-time PCR was done in triplicate, including no-template controls. Relative expression was calculated using the comparative $C_t$ method.

**Demethylating experiment.** OVCAR3 cells were seeded at low density 48 h before treatment with 10 μmol/L 5-aza-2′-deoxycytidine (5-AZA; Sigma). After 24 h of treatment, cells were collected and total RNA was isolated using Trizol reagent. Three replicates for both untreated cells and 5-AZA–treated cells were used to evaluate the miRNA expression by microarray profiling. Differentially expressed miRNAs were identified by using univariate two-class *t* test with random variance model.

## Results

**A miRNA expression signature discriminates ovarian cancer tissues from normal ovary.** We used a custom microarray platform already validated by numerous studies (19) to evaluate miRNA expression profiles on a heterogeneous set of ovarian tissues from different patients. This set included 15 normal ovarian samples, 69 ovarian malignant tumors, and 5 ovarian cancer cell lines, for a total of 89 biologically independent samples. Each tumor sample was derived from a single specimen. Description of sample characteristics is reported in Supplementary Table S1.

The unsupervised hierarchical clustering, based on all the human miRNAs spotted on the chip, generated a tree with a clear

[3] http://genome.ucsc.edu
[4] http://microrna.sanger.ac.uk/
[5] http://www.sanger.ac.uk/Software/Rfam/mirna/

distinction of samples in two main groups, represented by normal tissues and malignant tissues (Fig. 1).

To identify miRNAs differentiating normal versus cancer tissue, we used SAM and PAM tools, and the results obtained from the two types of class prediction analysis were largely overlapping. The SAM comparison between normal and cancer tissues identified 39 miRNAs (with $q$ values <1% and fold changes >3) differentially expressed, 10 up-modulated in tumors and the

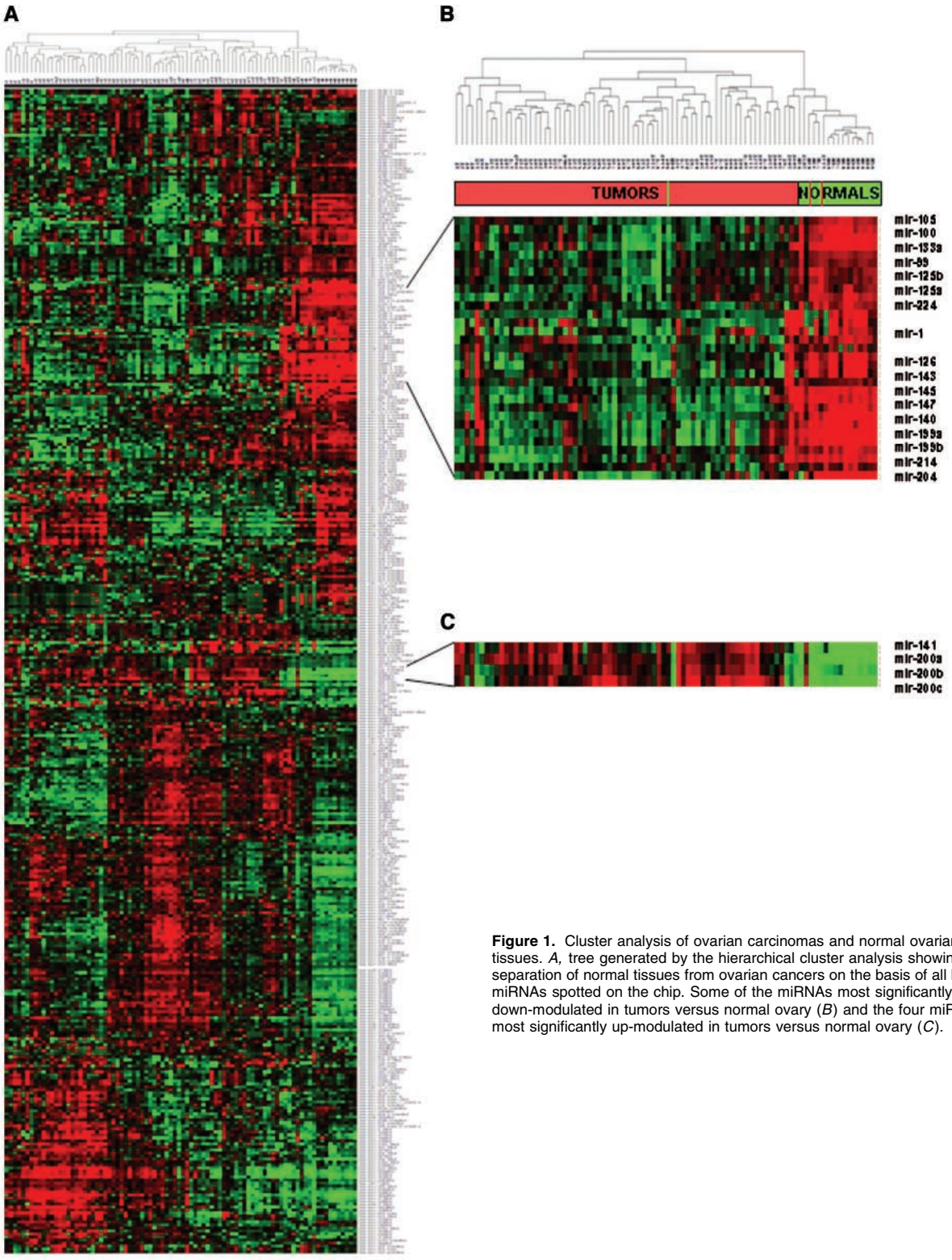


**Figure 1.** Cluster analysis of ovarian carcinomas and normal ovarian tissues. *A,* tree generated by the hierarchical cluster analysis showing the separation of normal tissues from ovarian cancers on the basis of all human miRNAs spotted on the chip. Some of the miRNAs most significantly down-modulated in tumors versus normal ovary (*B*) and the four miRNAs most significantly up-modulated in tumors versus normal ovary (*C*).

remaining down-modulated (the list is reported in Supplementary Table S2). The PAM analysis in Supplementary Fig. S1 displays the graphical representation of the probabilities (0.0–1.0) of each sample for being a cancer or a normal tissue according to the miRNA signature reported in Table 1, which describes a smaller set of 29 miRNAs, 4 up-modulated (*miR-200a, miR-200b, miR-200c*, and *miR-141*) and 25 down-modulated (being *miR-199a, miR-140, miR-145*, and *miR-125b1* among the most significant) differentiating normal versus tumor with a classification rate of 89%.

**Table 1.** PAM analysis of miRNAs differentially expressed between tumors and normals

CV confusion matrix (threshold = 3.23866)

| True/predicted | Cancer | Normal | Class error rate |
|---|---|---|---|
| Cancer | 63 | 8 | 0.112676056 |
| Normal | 1 | 14 | 0.066666667 |

Misclassification error = 0.11

| miRNAs | Cancer score | Normal score |
|---|---|---|
| hsa-mir-200c* | 0.1152 | −0.5454 |
| hsa-mir-200a* | 0.1059 | −0.5012 |
| hsa-mir-199a † | −0.098 | 0.4637 |
| hsa-mir-143 ‡ | −0.0946 | 0.4479 |
| hsa-mir-199b ‡ | −0.0887 | 0.4197 |
| hsa-mir-141* | 0.0874 | −0.4138 |
| hsa-mir-145 ‡ | −0.0734 | 0.3473 |
| hsa-mir-147* | −0.0679 | 0.3212 |
| hsa-mir-133a ‡ | −0.0671 | 0.3176 |
| hsa-mir-101* | −0.0616 | 0.2917 |
| hsa-mir-214 † | −0.0607 | 0.2873 |
| hsa-mir-100 † | −0.0535 | 0.2533 |
| hsa-mir-140* | −0.0523 | 0.2474 |
| hsa-mir-126 ‡ | −0.0501 | 0.2371 |
| hsa-mir-224 ‡ | −0.0485 | 0.2294 |
| hsa-mir-9* | −0.0481 | 0.2277 |
| hsa-mir-105 | −0.0461 | 0.2184 |
| hsa-mir-99a ‡ | −0.037 | 0.1753 |
| hsa-mir-125a ‡ | −0.0315 | 0.1489 |
| hsa-mir-211* | −0.0248 | 0.1174 |
| hsa-mir-127* | −0.0232 | 0.11 |
| hsa-mir-200b* | 0.0179 | −0.0847 |
| hsa-mir-125b-1 † | −0.0177 | 0.0837 |
| hsa-let-7c ‡ | −0.0152 | 0.0719 |
| hsa-let-7d* | −0.0138 | 0.0654 |
| hsa-mir-124a* | −0.0121 | 0.0574 |
| hsa-mir-374 | −0.0119 | 0.0563 |
| hsa-let-7a* | −0.0113 | 0.0533 |
| hsa-mir-134* | −0.0014 | 0.0068 |

NOTE: Of the 39 miRNAs found by SAM analysis, 29 miRNAs, 4 up-modulated and 25 down-modulated, were able to classify normal and tumor samples with a classification rate of 89%. The four miRNAs up-modulated were found amplified in the genomic study done by Zhang et al., 2005; among the miRNAs down-modulated, 10 of 25 were found deleted, 4 are discordant and 11 do not show any copy loss or gain in Zhang study.

*Concordant.

† Discordant.

‡ Unchanged in Zhang study.

To confirm the results obtained by microarray analysis, we carried out Northern blots (Fig. 2*A*) or real-time PCR (Fig. 2*B*) on some of the differentially expressed miRNAs. We analyzed the expression of *miR-200a* and *miR-141*, the most significantly up-modulated in ovarian carcinoma, and the miRNAs most significantly down-modulated, *miR-199a, miR-140, miR-145*, and *miR-125b1*. All the experiments confirmed the results obtained by microarray analysis.

**Biopathologic features and miRNA expression.** Considering that ovarian epithelial carcinomas occur as different histologic subtypes characterized by distinct morphologic and molecular genetic alterations, we decided to compare the miRNA profile of each of them with the normal tissue to evaluate if miRNA expression profiles are different in distinct histotypes of ovarian carcinomas. Complete lists resulting from SAM analyses are reported in Supplementary Table S3, whereas a summary is shown in the Venn diagram in Fig. 3: two of four miRNAs most significantly up-modulated (Fig. 3*A*) in tumors versus normal tissue, *miR-200a* and *miR-200c*, are up-modulated in all the three histotypes considered (serous, endometrioid, and clear cell), whereas *miR-200b* and *miR-141* up-modulation is shared by endometrioid and serous histotypes. Moreover, the endometrioid histotype shows the up-modulation of three additional miRNAs, *miR-21, miR-203*, and *miR-205*. Nineteen miRNAs, including *miR-125b1, miR199a*, and *miR-140*, are down-modulated (Fig. 3*B*) in all the three histotypes examined in comparison with normal tissue, whereas four are shared in each paired analysis of the different signatures: *miR-145*, for example, is down-modulated in both serous and clear cell carcinomas; *miR-222* is down-modulated in both endometrioid and clear cell carcinomas.

Considering the tumors classified as "mixed" and "poorly differentiated," we found that the first group revealed a signature with characteristics of different histotypes, sharing for example the overexpression of *miR-200c* and *miR-181* with the endometrioid carcinomas and the down-modulation of *miR-214* with the serous, whereas the "poorly differentiated" tumors have a quite different pattern of miRNA expression (Supplementary Table S3).

We then compared miRNA expression of different groups of tumors paired as reported in Supplementary Table S4, and in particular, we compared the two most numerous histotypes, serous and endometrioid. When considering the miRNAs differentially expressed in endometrioid carcinomas compared with serous, we found *miR-212* up-modulated and *miR-302b** and *miR-222* ($P < 0.05$, $t$ test analysis of microarray data in Fig. 4*A*) among the miRNAs most significantly down-modulated. In Fig. 4*B*, a Northern blot on a small set of samples verifies *miR-222* overexpression in serous tumors compared with endometrioid.

We then focused our attention on other clinicopathologic features associated with tumor specimens: whereas no miRNAs were found significantly differentially expressed in relation to the age of patients, other tumor characteristics seemed to affect miRNA expression, such as lymphovascular invasion and ovarian surface, tubal, uterus, and pelvic peritoneum involvement (Supplementary Table S5).

To investigate if there were miRNAs associated with different grade or stage of the disease, we did comparative analyses considering all the tumors or only the serous histotype, which was the most numerous, but we did not obtain any significant miRNA differentially expressed.

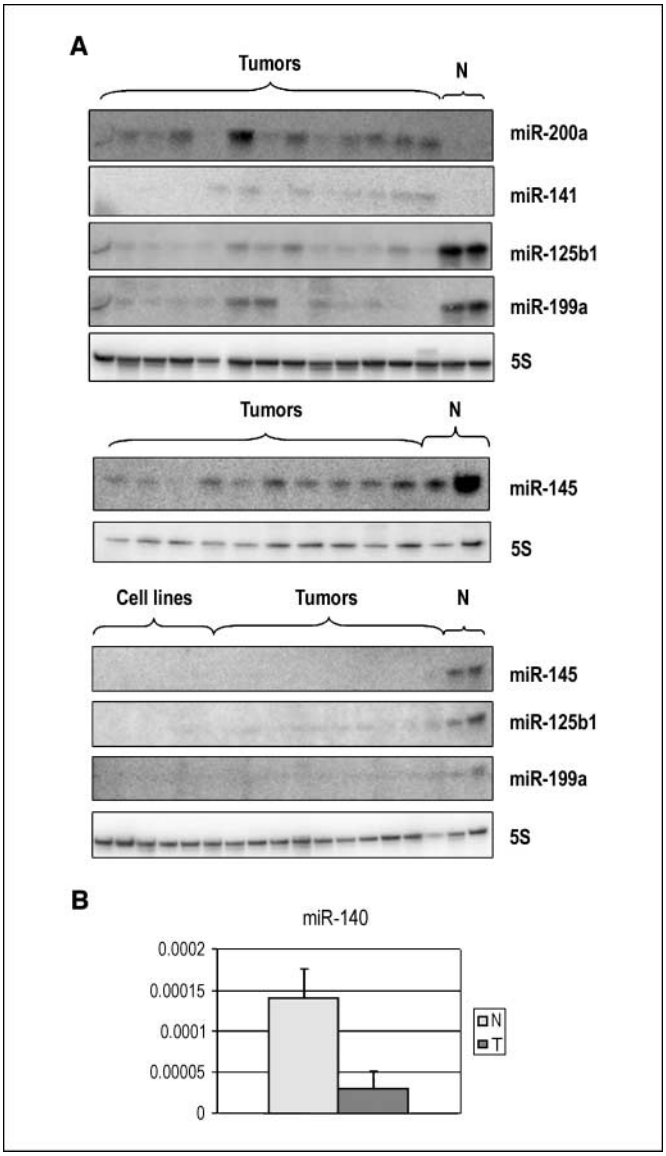


**Figure 2.** *A,* Northern blot analysis of human ovarian carcinomas with probes of miR-200a, miR-141, mir-199a, mir-125b1, and miR-145. Evaluation of miR-199a, miR-125b1, and miR-145 on human ovarian cell lines. The 5S probe was used for normalization of expression levels in the different lanes. *B,* real-time PCR was used to verify the miR-140 down-modulation in tumors compared with normal samples.

**Confirmed and potential targets for miRNA members of various signatures.** Using the DianaTarbase,[6] we looked for confirmed targets of some of the most significant miRNAs resulting from our analyses, finding some interesting data: *ERBB2* and *ERBB3* receptors, for example, are targeted by *miR-125* (32); *miR-101*, down-modulated in ovarian carcinoma, has been shown targeting the oncogene *MYCN* (33). We then analyzed their potential targets using the miRGen database[7] and evaluated for some of these molecules the expression levels in ovarian carcinoma: all the four most significantly up-modulated miRNAs, *miR-200a, miR-200b, miR-200c*, and *miR-141*, for example, have as common putative target the oncosuppressor BAP1, BRCA1-associated protein, down-modulated in ovarian cancer. The information obtained is summarized in Supplementary Table S6.

**Epigenetic regulation of miRNA expression.** To evaluate if an aberrant DNA methylation pattern could also contribute to the altered miRNA expression characterizing the human ovarian carcinoma, we analyzed the miRNA profiling of the ovarian cell line OVCAR3, before and after treatment with the demethylating agent 5-AZA. The analysis of microarray data showed 11 human miRNAs differentially expressed, 9 up-modulated and 2 down-modulated ($P < 0.001$, significance threshold of each univariate test), being *miR-21, miR-203, miR-146b, miR-205, miR-30-5p*, and *miR-30c* the most significantly induced on treatment (the miRNAs differentially expressed are listed in Fig. 5*A*, whereas the resulting hierarchical cluster tree is reported in Fig. 5*B*). Real-time PCRs to verify the up-modulation of the five most significantly induced miRNAs are described in Fig. 5 as graphical representation of miRNA expression levels (Fig. 5*C*), and *miR-21* was also validated by Northern blot (Fig. 5*D*).

Interestingly, *miR-21, miR-203*, and *miR-205* are overexpressed in ovarian carcinomas compared with normal tissues (see SAM analysis in Supplementary Table S2 and Venn Diagram in Fig. 3): the reactivation of these miRNA genes after demethylating treatment suggests that the hypomethylation could be the mechanism responsible for their overexpression *in vivo*. We confirmed the overexpression of *miR-21*, the most significant miRNA induced on treatment, doing a Northern blotting (Supplementary Fig. S2*A*) on a panel of human ovarian carcinomas and two normal tissues. Moreover, using the CpG Island Searcher Program (34), we verified that *miR-21* and *miR-203* are associated with CpG islands, being the *miR-203* embedded in a CpG island 875 bp long and the *miR-21* characterized by a CpG island ≈2 kb upstream the mature sequence (Supplementary Fig. S2*B*), whereas *miR-205* does not show any CpG island in a region spanning 2 kb upstream its mature form.

## Discussion

In this study, we show that miRNAs are aberrantly expressed in human ovarian cancer. The overall miRNA expression could clearly separate normal versus cancer tissues, identifying a number of miRNAs altered in human ovarian cancer and probably involved in the development of this neoplasia.

The expression of all the four miRNAs we found most significantly up-modulated, *miR-200a* and *miR-141*, belonging to the same family; *miR-200b* (localized in the same region of *miR-200a,* at chromosome 1p36.33); and *miR-200c* (localized in the same region of *miR-141,* at chromosome 12p13.31), is concordant with the results obtained at genomic level by Zhang et al. (24), suggesting that the mechanism driving their up-modulation could be the amplification of the miRNA genes. Interestingly, all these miRNAs have a common putative target: the oncosuppressor BAP1, BRCA1-associated protein (24). The altered expression of GATA factors, found and proposed as the underlying mechanism for dedifferentiation in ovarian carcinogenesis (35), may also be driven by miRNA deregulation. In particular, GATA6, lost or excluded from the nucleus in 85% of ovarian tumors, may be regulated by *miR-200a*, and GATA4, absent in the majority of ovarian cancer cell lines, may be targeted by *miR-200b* (Supplementary Table S5).

Among the down-modulated genes, notably, we found *miR-125b1*, altered also in breast cancer, as well as *miR-145* (18); *mir-199a*,

[6] http://www.diana.pcbi.upenn.edu/tarbase.html
[7] http://www.diana.pcbi.upenn.edu/miRGen.html

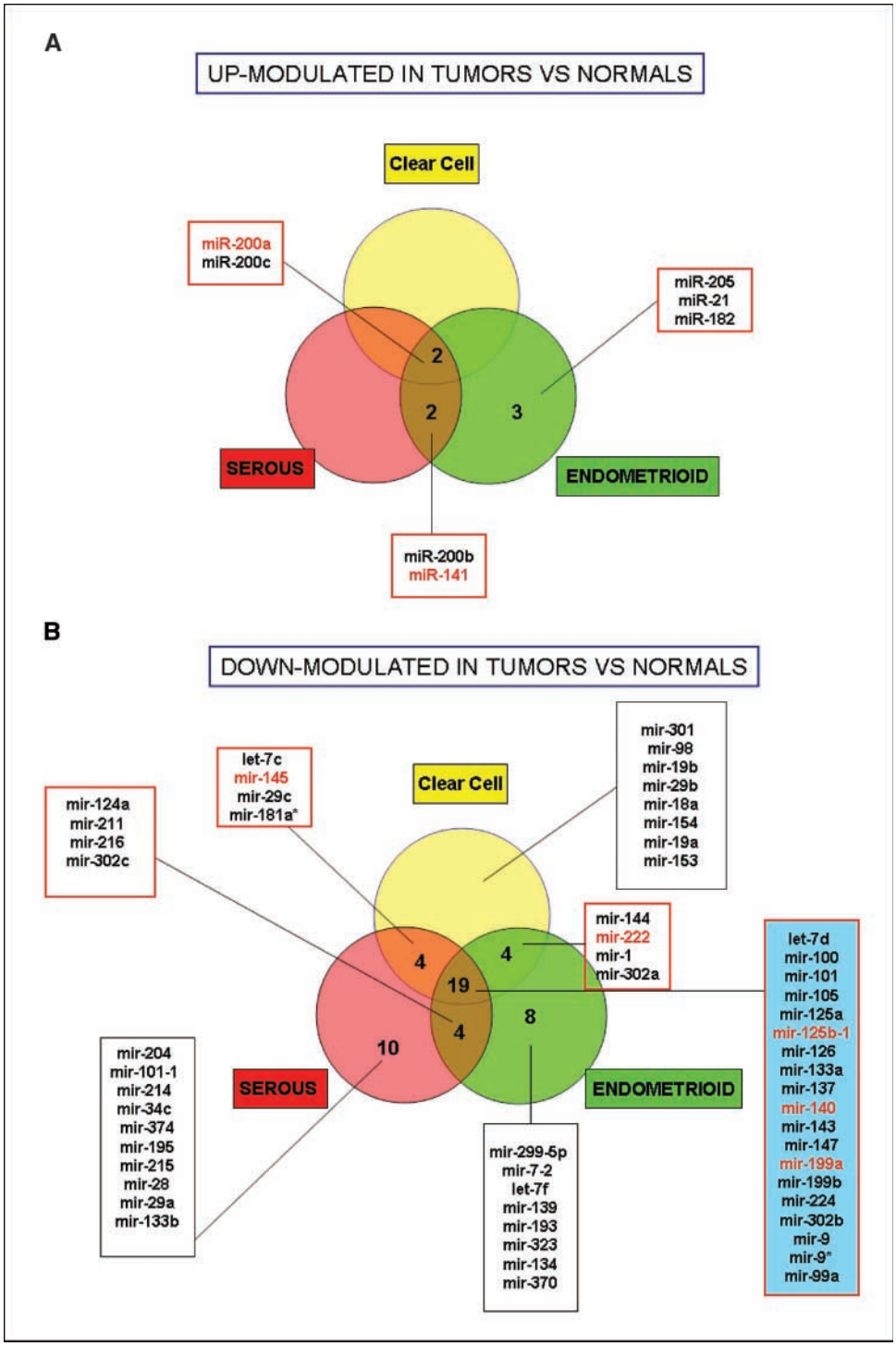


**Figure 3.** Venn diagram showing the miRNA signatures characterizing different ovarian carcinoma histotypes (serous, endometrioid, and clear cell) compared with the normal tissue (*A*, miRNAs up-modulated; *B*, miRNAs down-modulated).

recently shown down-modulated in other tumors, as hepatocellular carcinoma (36); and *miR-140*, deleted in ovarian carcinoma (24). Interestingly, *miR-140* is indeed located at chromosome 6q22, a fragile region often deleted in ovarian tumor, and it is predicted to target important molecules as c-SRK, MMP13, and FGF2.

Even if the normal control available in this study is represented by whole normal ovary, our data could identify a number of miRNAs altered in human ovarian carcinoma and probably involved in the biology of this malignancy.

In fact, the miRNA signatures obtained comparing different histotypes of ovarian carcinomas (serous, endometrioid, clear cell, and mixed) with the normal tissue are overlapping in most cases, but they also reveal a number of miRNAs that seem to be "histotype specific": the endometrioid tumors, for example, share with the others the four most significantly up-modulated miRNAs (*miR-200a, miR-200b, miR-200c,* and *miR-141*) but also present overexpression of *miR-21*, known to be misregulated in numerous solid tumors (18, 37, 38) and to exert an antiapoptotic role in different

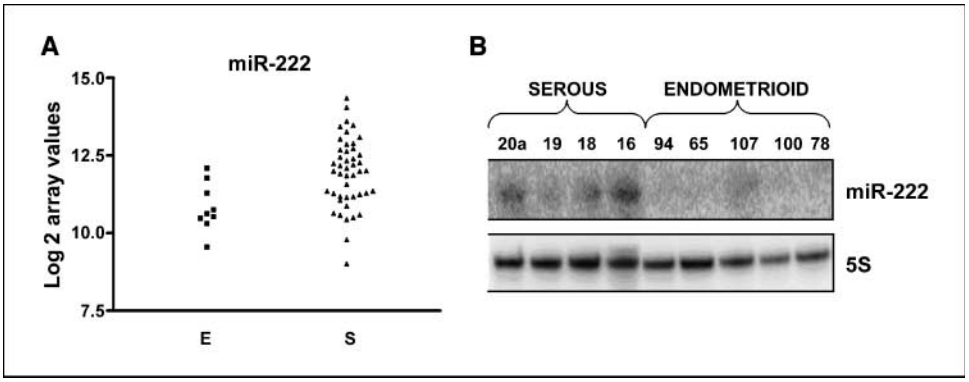


**Figure 4.** *t* test graphic representation of miR-222 microarray data expression in serous (*S*) and endometrioid (*E*) tumors (*A*) and verification by Northern blot on a smallest set of samples (*B*).

cellular systems (39, 40), *miR-205* and *miR-182*. Endometrioid tumors also present down-modulation of several miRNAs in comparison with the other classes of tumors, for example, *miR-222*, already shown targeting c-Kit (41), being involved in cancer (42–44) and down-modulated under folate-deficient conditions (45).

These differences enforce the fact that different histotypes represent biologically and pathogenetically distinct entities of EOCs, although they are currently treated with identical therapeutic strategies. Microarray analysis has confirmed recently that different histotypes (serous, mucinous, endometrioid, and clear cell) show the alteration of different pathways, probably reflecting the gene expression pattern of the organ of origin (respectively fallopian tubes, colonic mucosa, and endometrium; ref. 46).

Notably, many of the miRNAs differentially expressed are predicted to target molecules involved in pathways differentially activated depending on the histotype. *miR-212*, for example, down-modulated in serous carcinoma, has as putative target WT1, overexpressed in this subgroup of ovarian carcinomas (47). Another putative target of *miR-212* is BRCA1: mutated in

A

| miR name | FDR | Ratio of geom means AZA/NT |
|---|---|---|
| hsa-mir-21 | 0.002013 | 4.277 |
| hsa-mir-203 | 0.0067368 | 3.826 |
| hsa-mir-146b | 0.0095114 | 2.968 |
| hsa-mir-205 | 0.0121302 | 2.877 |
| hsa-miR-30a-5p | 0.0160979 | 2.047 |
| hsa-miR-96 | 0.0161969 | 0.476 |
| hsa-mir-155 | 0.018638 | 1.784 |
| hsa-mir-383 | 0.018638 | 0.474 |
| hsa-miR-30c | 0.018638 | 2.286 |
| hsa-mir-193b | 0.018638 | 2.09 |
| hsa-mir-202 | 0.018638 | 1.782 |

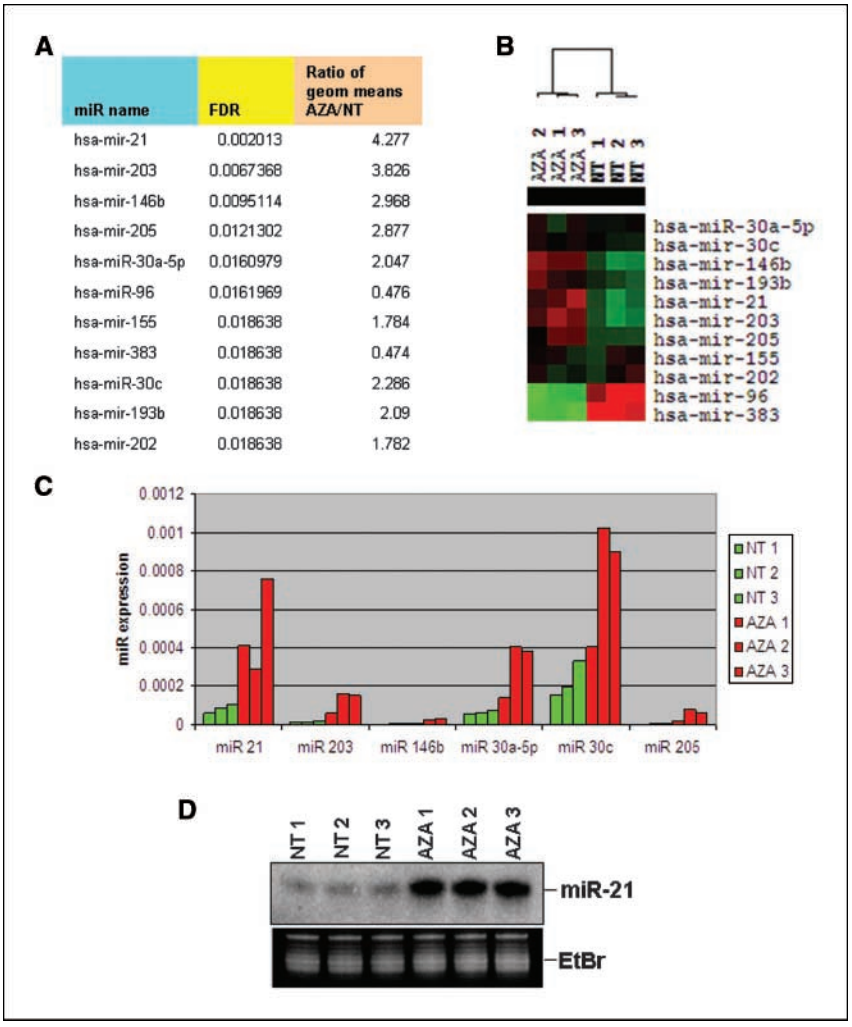


**Figure 5.** Expression pattern of miRNAs in OVCAR3 cell line before and after treatment with the demethylating agent 5-AZA. *A,* table reporting the most significant miRNAs differentially expressed resulting from the microarray profiling. *B,* hierarchical cluster tree representation. *C,* real-time PCR to verify the up-modulation of the five most significantly induced miRNAs, reported as graphical representation of miRNA expression levels. *Columns,* independent experiment resulting from the average of three technical replicates. *D,* Northern blot showing the up-modulation of miR-21 after treatment, normalized with EtBr gel staining.

hereditary ovarian cancer, this molecule has been found recently involved also in the pathoetiology of sporadic OEC, where a loss of gene function due to epigenetic alterations has been observed more commonly (48). The decreased BRCA1 expression could be determined by overexpression of one or more miRNAs.

*miR-299-5p* and *miR-135b*, up-modulated in serous histotype compared with endometrioid, are supposed to target, respectively, Delta-like 1 (DLK1) and msh homeobox 2 (MSX2), overexpressed in endometrioid carcinomas (47). Compared with the other tumors, clear cell carcinomas show expression levels of *miR-30-5p* and of *miR-20a* opposite (46) to two putative targets, retinol binding protein 4 (RBP4) and solute carrier 40-iron-regulated transporter, member 1 (SLC40A1), respectively. Compared with the normal tissue, clear cell carcinoma also shows lower expression of *miR-18a, miR-19a*, and *miR-19b*, suggesting a possible down-modulation of the *cluster 17-92* (already validated as deleted by Zhang et al.). This cluster, involved in the intricate regulation mediated by E2F1 and c-Myc, seems to have a duplex nature of putative oncogene, as suggested recently in B-cell lymphoma (15), or tumor suppressor: in hepatocellular carcinoma, for example, loss of heterozygosity at the locus coding the *miR-17-92 cluster* (13q31) has been reported (49). In ovarian carcinoma, at least in clear cell histotype, it could also exert a role of oncosuppressor. Our data suggest indeed that miRNAs may have a regulatory role in the process of differentiation leading to the development of a specific subtype of EOC. Interestingly, poorly differentiated carcinomas have a quite different pattern of miRNA expression, showing up-modulation of several miRNAs in comparison with normal ovary. More intriguingly, one of them, *miR-373*, has been described recently as putative oncogene in testicular germ cell tumors (16).

The absence of miRNAs significantly differentially expressed in relation to tumor stage or grade might be explained by the fact that our set of samples is mostly represented by advanced stage tumors, as expected considering the late diagnosis of this kind of neoplasia; however, the difference in size among the different groups of samples could have represented a limit for the statistical analysis. Alternatively, miRNAs might be important for the development of human ovarian carcinoma but not for the progression of the disease.

Resulting from our analyses, a number of miRNAs overexpressed but not reported as amplified in Zhang study, as well as down-modulated but not deleted, the involvement of an epigenetic regulatory mechanism could actually exert a role on miRNA expression in human EOC. Indeed, among the most significant miRNAs induced after demethylating treatment of an ovarian cell line, we found *miR-21, miR-203*, and *miR-205* up-modulated in ovarian cancer. Moreover, *miR-203* and *miR-21* are associated with a CpG island (miR-203 is embedded in a CpG island, whereas *miR-21* has a CpG island $\approx$2 kb upstream its mature sequence), supporting the idea that the demethylation leads to the reactivation of these miRNA genes. Notably, *miR-21* has already been described up-modulated in several human tumors and having an antiapoptotic role in different cellular models. These data suggest that the DNA hypomethylation could be an epigenetic mechanism responsible for the *in vivo* overexpression of potentially oncogenic miRNAs.

To the best of our knowledge, this is the first report describing a complete miRNA expression profiling in human EOCs, focused on the identification of miRNAs differentially expressed in carcinomas versus normal ovary and in different subgroups of tumors. Our data suggest the important role that miRNAs can exert on the pathogenesis and on the development of different histotypes of ovarian carcinoma and identify altered DNA methylation as a possible epigenetic mechanism responsible for the aberrant expression of miRNAs not affected by genomic changes.

## Acknowledgments

Received 5/24/2007; accepted 7/10/2007.

**Grant support:** Associazione Italiana per la Ricerca sul Cancro. Fondazione Italiana per la Ricerca sul Cancro fellowship (M.V. Iorio). National Cancer Institute Program Project grants (C.M. Croce). Kimmel Foundation Scholar award and CLL Global Research Foundation (G.A. Calin).

The costs of publication of this article were defrayed in part by the payment of page charges. This article must therefore be hereby marked *advertisement* in accordance with 18 U.S.C. Section 1734 solely to indicate this fact.

We thank Dr. Elda Tagliabue for the scientific discussion and her useful advice.

## References

1. Cannistra SA. Cancer of the ovary. N Engl J Med 2004; 351:2519–29.
2. Greenlee RT, Hill-Harmon MB, Murray T, Thun M. Cancer statistics, 2001. CA Cancer J Clin 2001; 51:15–36.
3. Feeley KM, Wells M. Precursor lesions of ovarian epithelial malignancy. Histopathology 2001;38:87–95.
4. Bell DA. Origins and molecular pathology of ovarian cancer. Mod Pathol 2005;18 Suppl 2:S19–32.
5. Schwartz DR, Kardia SL, Shedden KA, et al. Gene expression in ovarian cancer reflects both morphology and biological behavior, distinguishing clear cell from other poor-prognosis ovarian carcinomas. Cancer Res 2002;62:4722–9.
6. De Cecco L, Marchionni L, Gariboldi M, et al. Gene expression profiling of advanced ovarian cancer: characterization of a molecular signature involving fibroblast growth factor 2. Oncogene 2004;23:8171–83.
7. He L, Hannon GJ. MicroRNAs: small RNAs with a big role in gene regulation. Nat Rev Genet 2004;5:522–31.
8. Miska EA. How microRNAs control cell division, differentiation, and death. Curr Opin Genet Dev 2005; 5:563–8.
9. Zamore PD, Haley B. Ribo-gnome: the big world of small RNAs. Science 2005;309:1519–24.
10. Johnson SM, Grosshans H, Shingara J, et al. RAS is regulated by the let-7 microRNA family. Cell 2005;120: 635–47.
11. Mayr C, Hemann MT, Bartel D. Disrupting the pairing between let-7 and HMGA2 enhances oncogenic transformation. Science 2007;315:1576–9.
12. Lee YS, Dutta A. The tumor suppressor microRNA let-7 represses the HMGA2 oncogene. Genes Dev 2007; 21:1025–30.
13. Cimmino A, Calin GA, Fabbri M, et al. miR-15 and miR-16 induce apoptosis by targeting BCL2. Proc Natl Acad Sci U S A 2005;102:13944–9.
14. O'Donnell KA, Wentzel EA, Zeller KI, Dang CV, Mendell JT. c-Myc-regulated microRNAs modulate E2F1 expression. Nature 2005;435:839–43.
15. He L, Thomson JM, Hemann MT, et al. A microRNA polycistron as a potential human oncogene. Nature 2005;435:828–33.
16. Voorhoeve PM, le Sage C, Schrier M, et al. A genetic screen implicates miRNA-372 and miRNA-373 as oncogenes in testicular germ cell tumors. Cell 2006; 124:1169–81.
17. Costinean S, Zanesi N, Pekarsky Y, et al. Pre-B cell proliferation and lymphoblastic leukemia/high-grade lymphoma in E(mu)-miR155 transgenic mice. Proc Natl Acad Sci U S A 2006;103:7024–9.
18. Iorio MV, Ferracin M, Liu CG, et al. MicroRNA gene expression deregulation in human breast cancer. Cancer Res 2005;65:7065–70.
19. Calin GA, Croce CM. MicroRNA signatures in human cancers. Nat Rev Cancer 2006;6:857–66.
20. Esquela-Kerscher A, Slack FJ. Oncomirs—microRNAs with a role in cancer. Nat Rev Cancer 2006;6:259–69.
21. Calin GA, Ferracin M, Cimmino A, et al. MicroRNA signature associated with prognosis and progression in chronic lymphocytic leukemia. N Engl J Med 2005;353: 1793–801.
22. Yanaihara N, Caplen N, Bowman E, et al. Unique microRNA molecular profiles in lung cancer diagnosis and prognosis. Cancer Cell 2006;9:189–98.
23. Calin GA, Croce CM. MicroRNAs and chromosomal abnormalities in cancer cells. Oncogene 2006; 25:6202–10.
24. Zhang L, Huang J, Yang N, et al. MicroRNAs exhibit high frequency genomic alterations in human cancer. Proc Natl Acad Sci U S A 2006;103:9136–41.
25. Saito Y, Liang G, Egger G, et al. Specific activation of microRNA-127 with downregulation of the proto-oncogene BCL6 by chromatin-modifying drugs in human cancer cells. Cancer Cell 2006;9:435–43.
26. Lujambio A, Ropero S, Ballestar E, et al. Genetic unmasking of an epigenetically silenced microRNA in human cancer cells. Cancer Res 2007;67:1424–9.
27. Brueckner B, Stresemann C, Kuner R, et al. The

human let-7a-3 locus contains an epigenetically regulated microRNA gene with oncogenic function. Cancer Res 2007;67:1419–23.
**28.** Liu CG, Calin GA, Meloon B, et al. An oligonucleotide microchip for genomewide microRNA profiling in human and mouse tissues. Proc Natl Acad Sci U S A 2004;101:9740–4.
**29.** Wright GW, Simon RM. A random variance model for detection of differential gene expression in small microarray experiments. Bioinformatics 2003;19:2448–55.
**30.** Tusher VG, Tibshirani R, Chu G. Significance analysis of microarrays applied to the ionizing radiation response. Proc Natl Acad Sci U S A 2001;98:5116–21.
**31.** Tibshirani R, Hastie T, Narasimhan B, Chu G. Diagnosis of multiple cancer types by shrunken centroids of gene expression. Proc Natl Acad Sci U S A 2002;99:6567–72.
**32.** Scott GK, Goga A, Bhaumik D, et al. Coordinate suppression of ERBB2 and ERBB3 by enforced expression of micro-RNA miR-125a or miR-125b. J Biol Chem 2007;282:1479–86.
**33.** Lewis BP, Shih IH, Jones-Rhoades MW, Bartel DP, Burge CB. Prediction of mammalian microRNA targets. Cell 2003;115:787–98.
**34.** Takai D, Jones PA. The CpG island searcher: a new WWW resource. In Silico Biol 2003;3:325–40.
**35.** Capo-chichi CD, Roland IH, Vanderveer L, et al. Anomalous expression of epithelial differentiation—determining GATA factors in ovarian tumorigenesis. Cancer Res 2003;63:4967–77.
**36.** Murakami Y, Yasuda T, Saigo K, et al. Comprehensive analysis of microRNA expression patterns in hepatocellular carcinoma and non-tumorous tissues. Oncogene 2006;25:2537–45.
**37.** Roldo C, Missaglia E, Hagan JP, et al. MicroRNA expression abnormalities in pancreatic endocrine and acinar tumors are associated with distinctive pathologic features and clinical behavior. J Clin Oncol 2006;24:4677–84.
**38.** Volinia S, Calin GA, Liu CG, et al. A microRNA expression signature of human solid tumors defines cancer gene targets. Proc Natl Acad Sci U S A 2006;103:2257–61.
**39.** Chan JA, Krichevsky AM, Kosik KS. MicroRNA-21 is an antiapoptotic factor in human glioblastoma cells. Cancer Res 2005;65:6029–33.
**40.** Zhu S, Si ML, Wu H, Mo YY. MicroRNA-21 targets the tumor suppressor gene tropomyosin 1 (TPM1). J Biol Chem 2007;282:14328–36.
**41.** Felli N, Fontana L, Pelosi E, et al. MicroRNAs 221 and 222 inhibit normal erythropoiesis and erythroleukemic cell growth via kit receptor downmodulation. Proc Natl Acad Sci U S A 2005;102:18081–6.
**42.** He H, Jazdzewski K, Li W, et al. The role of microRNA genes in papillary thyroid carcinoma. Proc Natl Acad Sci U S A 2005;102:19075–80.
**43.** Pallante P, Visone R, Ferracin M, et al. MicroRNA deregulation in human thyroid papillary carcinomas. Endocr Relat Cancer 2006;13:497–508.
**44.** Lee EJ, Gusev Y, Jiang J, et al. Expression profiling identifies microRNA signature in pancreatic cancer. Int J Cancer 2007;120:1046–54.
**45.** Marsit CJ, Eddy K, Kelsey KT. MicroRNA responses to cellular stress. Cancer Res 2006;66:10843–8.
**46.** Marquez RT, Baggerly KA, Patterson AP, et al. Patterns of gene expression in different histotypes of epithelial ovarian cancer correlate with those in normal fallopian tube, endometrium, and colon. Clin Cancer Res 2005;11:6116–26.
**47.** Shedden KA, Kshirsagar MP, Schwartz DR, et al. Histologic type, organ of origin, and Wnt pathway status: effect on gene expression in ovarian and uterine carcinomas. Clin Cancer Res 2005;11:2123–31.
**48.** Thrall M, Gallion HH, Kryshio R, et al. BRCA1 expression in a large series of sporadic ovarian carcinomas: a Gynecologic Oncology Group study. Int J Gynecol Cancer 2006;16 Suppl 1:166–71.
**49.** Lin YW, Sheu JC, Liu LY, et al. Loss of heterozygosity at chromosome 13q in hepatocellular carcinoma: identification of three independent regions. Eur J Cancer 1999;35:1730–4.